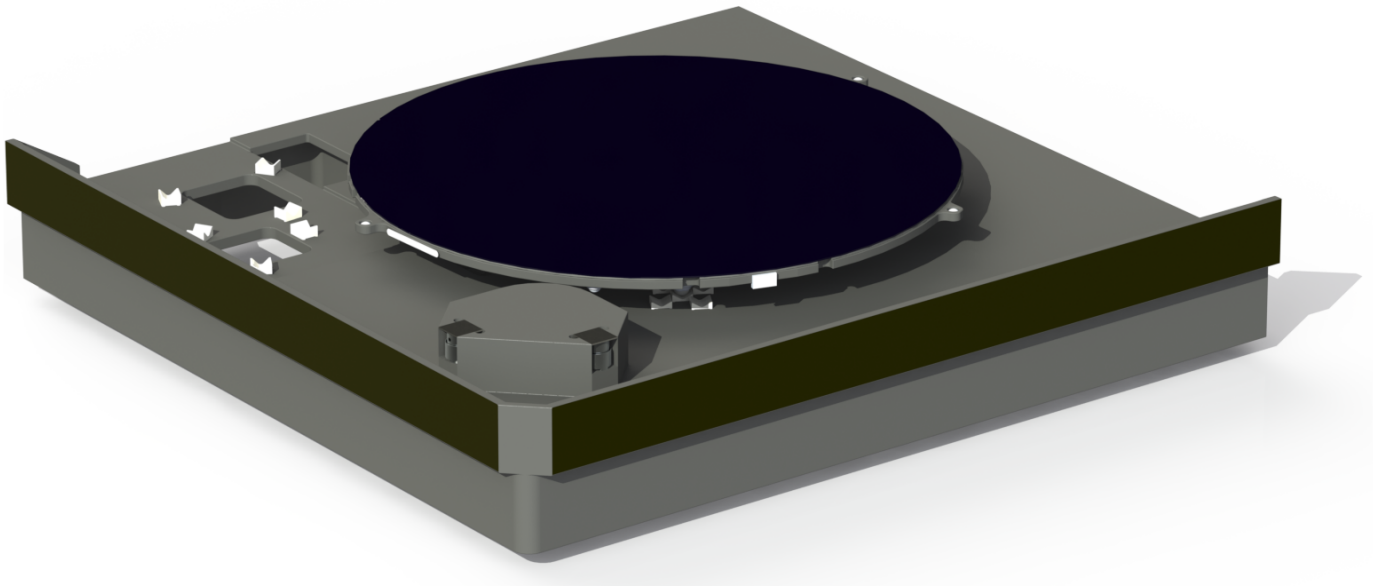

The design of a ceramic chuck with integrated mirrors

Improving the positioning accuracy of a wafer

M. Hulsebos

TU Delft

The design of a ceramic chuck with integrated mirrors

Improving the positioning accuracy of a wafer

by

M. Hulsebos

To obtain the degree of Master of Science
at the Delft University of Technology,
department of precision and microsystems engineering (PME).
To be defended publicly on 13 January 2017.

Report number:	MSD 2017.011	
Student number:	1517945	
Project duration:	March , 2016 – December, 2016	
Specialisation:	'Engineering mechanics' and 'Micro and nano engineering'	
Thesis committee:	Prof. dr. ir. J. L. Herder,	TU Delft, PME, Mechatronic system design
	Ir. P. IJ. Scheffers,	Mapper Lithography
	Dr. M. K. Ghatkesar,	TU Delft, PME, Micro and nano engineering
	Ir. J. W. Spronck,	TU Delft, PME, Mechatronic system design

This thesis is confidential and cannot be made public until December 31, 2021.

TU Delft Delft University of Technology

Abstract

With electron beam lithography, a cutting edge technology has been developed that might introduce new possibilities in the design of chips. The word "might" has been used here because e-beam lithography is not yet available for the mass production market. One of the bottlenecks in the development of e-beam lithography is the positioning uncertainty of wafers with respect to the electron beams. A wafer positioning system is used to position wafers. The accuracy of the system is highly determined by a component, that mechanically couples the wafer with the position actuators and the mirrors that are used by the interferometers. This component is called the chuck.

Topic of this project is the redesign of the chuck. The aim of this redesign is to reduce the position uncertainty caused by the chuck. In order to get to this result, a problem analysis has been performed that summarizes the bottlenecks in the positioning accuracy of a chuck. With respect to these bottlenecks, the performance of the present chuck has been analysed. The most critical bottlenecks in the present chuck turns out to be the optical quality and dynamic behaviour. This gives rise to the redesign of the chuck
In the concept development phase, 9 concepts have been created that promise to have a better overall performance. The most promising concept is a monolithic ceramic chuck with mirrors polished into 2 edges. Next to a great overall score on the estimated performance, the chuck design becomes simple which is a big benefit.

A wafer table is mounted to the chuck with a kinematic mount. Expectations arise that stick slip might occur on the interface of the kinematic mount due to expansion if the grooves are integrated in the ceramic. An analytic model has been derived that theoretically assists the expectation. Two experiments have been performed, both suffer from measurement disturbances. Although these measurements were subject to errors, the data seems to confirm stick slip behaviour. Because of this, a third experiment is proposed.

As a verification method, a set-up has been proposed to measure the actual performance of the present chuck and that of a ceramic chuck. This makes it possible to do a comparison of both concepts and select the best option.

Preface

In the final episode of my life as a student mechanical engineering at the Delft University of Technology, I was dedicated to a 9 month graduation project of which this thesis is the result. During the study I became interested in the cutting edge technology called lithography. This interest was the foundation of my graduation project at Mapper Lithography in Delft. Mapper initially challenged me to investigate the possibility of mounting glass mirrors to the chuck. As it turned out, the fundament of this challenge was the desire to have a chuck with ultra low surface roughness mirrors. This perspective slightly changed the initial research objective.

The work described in this thesis might be interesting to those that are interested in wafer positioning, metrology engineering and tribology. For Mapper, this thesis can be seen as a case study of the concept of a ceramic chuck.

My gratitude goes out to: Paul Scheffers who was my daily supervisor, the various discussions that we had were mind opening. My supervisor of the university, Just Herder who has been a great source of inspiration to get going again after running into dead end paths. Ron van Ostayen for his thoughts on the stick slip model that I derived. Joost Kortleve for making his set-up available to me and helping me out on this. The colleagues of Mapper with whom I had meetings with to get to know the system. And last but certainly not least, my family and friends. Without them I would never have managed to get this far. Enjoy the reading!

Marc Hulsebos
Delft, December 2016

List of Figures

List of Tables

Contents

1 Introduction

1.1. Progress in lithography

In 1965 Gordon Moore described the increasing number of transistors on a chip. The law states that each two years the number of transistors on a chip are doubled. Doubling the number of transistors on a chip means that the size of the details have to become smaller. The size of the details and therefore the transistor size is limited. The fundament of this limitation is found in the lithography process. Conventional lithography (see figure 1.1) makes use of ultra violet light. The ultra violet light passes through a mask in which the pattern of an electric layer is captured. After the mask the light passes a set of lenses to decrease the size of the light pattern. The lenses focus the light pattern onto a silicon wafer that is coated with a light sensitive layer. The pattern is transferred by the light into the light sensitive layer of the wafer. The pattern on the wafer will be processed in several steps in order to get the desired electrical properties of the pattern. A chip consists of many of these layers so multiple exposures need to be done to complete a single wafer.

The details of the light pattern on the wafer is size limited by the wavelength of the light that is used. A smaller wavelength can be used to make smaller details but the use of a wavelengths smaller than extreme ultra violet light (EUV) is not possible. The resolution in electron beam lithography (figure 1.2) is not limited by the wavelength of light. In this process the patterns are transferred to the wafer by bombing the wafer with electrons. The use of electrons has the advantage that the size of the patterns created becomes much smaller than the limited size produced by EUV lithography. An other advantage is that the process does not need a mask to transfer the pattern to the wafer. This makes it possible to create unique chips on the same wafer without changing masks. This advantage might be beneficial in for instance the development of new mechanically secured chips and large size chips.

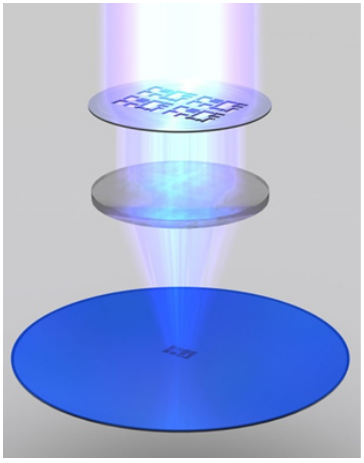

Figure 1.1: UV lithography

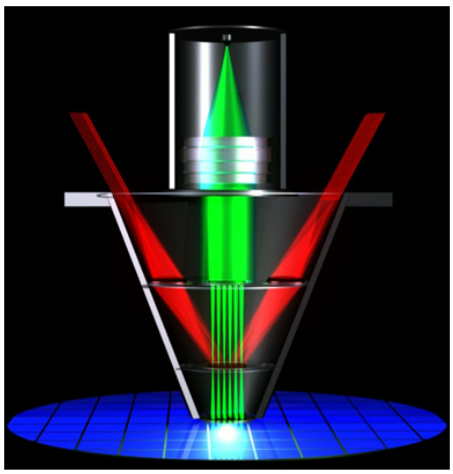

Figure 1.2: Electron beam lithography (the green beams represent the electron beams).

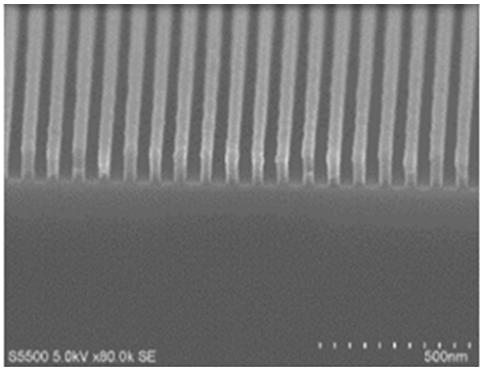

Figure 1.3: SEM picture of lines written on top of a silicon wafer by using e-beam lithography.

The use of electrons makes it necessary to use different components than in UV based lithography. The electron beam lithography machine (figure 1.4) can be divided into two systems: The electron beams system and the wafer positioning system:

1. **Electron beams system:** figure 1.2 shows the main components in the electron beams system. At the top, electron beams are created by an electron source. The beams are made parallel by a collimator and condenser lens after which the electrons pass a blanker chip. The blanker chip is a grid of very small holes, it switches beams on and off via deflection. Deflected beams collide with a beam stop, the non deflected beams pass through the blanker chip and will be deflected by a projection lens, this lens focuses the electrons onto the wafer.

2. **Wafer positioning system:** This system is used to match the desired collision position with the incoming electron beams with a high accuracy and precision. The wafer is mounted on a wafer table which is mounted on a chuck (figure 1.6). The chuck holds two mirrors that are used by interferometers to measure the position of the chuck. The chuck is also used to connect the wafer table and mirrors to the wafer stage. The stage is able to move the chuck in six degrees of freedom (dof's). A control system uses the interferometers and the stage to control the chuck.

1.2. Problem description

A challenging topic in the development of a lithography machine is overlay. Overlay is a term that is used to describe with which precision and accuracy the machine is able to write lines on top of- and next to each other. Connecting lines is essential in electron beam lithography. If lines are not connected with each other, there might be no electric connection in the developed circuit. This might be the cause of a malfunctioning chip. The overlay of the system could be improved by improving the stage stability and the accuracy of the system. Accuracy is defined by the "International Vocabulary of General Terms in Metrology" as "The closeness of the agreement between the result of a measurement and the (conventional) true value of the measurand" [11]. A critical sub module in the wafer positioning system that influences the accuracy is the chuck. A critical factor in the positioning accuracy of the chuck is the quality of the mirrors. The position and orientation of the chuck are determined by an interferometer system that measures the position of the mirrors. The shape of the mirrors determine how accurate the measurement of the mirror position actually is. It turns out that the measurements of the position of the chuck suffer from a bad quality of the present mirrors. An other critical factor in the accuracy of the position and orientation measurement of the wafer is the non collocated measurement. The position and orientation of the wafer are determined by measuring the position and orientation of the chuck. This is what is called a non collocated measurement. The environment introduces thermal and dynamic disturbances that change the shape of the chuck. These shape changes cause the wafer to be at a different location than expected. This change can not be measured and therefore it transfers directly to a measurement error. Figure 1.5 shows a simple sketch of this effect.

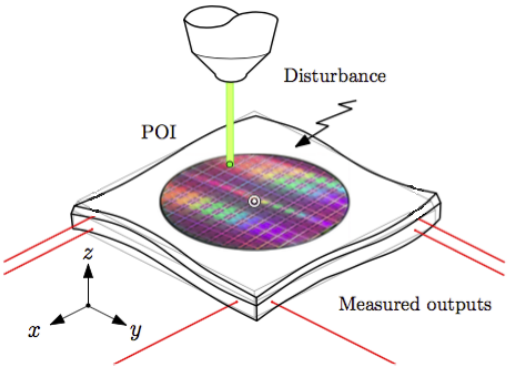

Figure 1.4: Changes of the shape of the chuck cause non collocated measurement errors. (Source of figure: www.toomen.eu)

1.3. Research objective

The accuracy of the chuck is determined by the optical quality of the mirrors and by the stability of the non collocated position measurement of the wafer. The expectation is that in the present chuck, improvements could be made on both aspects. The objective of this project is to design a new chuck and integrate improved solutions on these aspects.

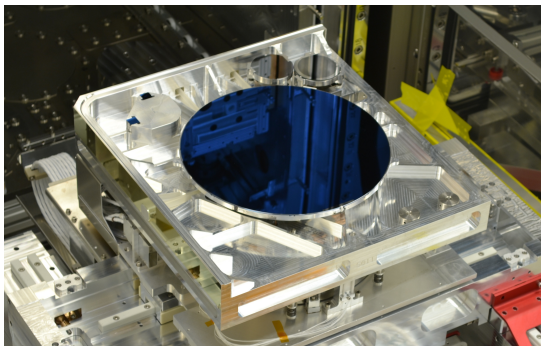

Figure 1.5: A wafer on a wafer table mounted to the present chuck.

1.4. Thesis structure

The second chapter provides an in depth analysis of the accuracy of the chuck. Bottlenecks are designated that all influence the chuck accuracy. These are used as a backbone throughout this thesis. In the last section of chapter 2, bottlenecks are considered of the total system that also influence the accuracy.

The third chapter starts by designating the functionalities a chuck should have. Solutions for each of these functionalities are analysed for their expected performance. A solution for each of the functions can be combined to form concepts. Nine concepts have been evaluated with respect to the expected performance on the accuracy bottlenecks of the second chapter. The most promising concept is topic of the detailed design.

The detailed design is the topic of the fourth chapter. As an approach, the detailed design has been performed by optimizing the performance of the chuck on each of the bottlenecks designated in chapter two.

Chapter five provides an in depth analysis of stick slip on kinematic mounts. This analysis should give an answer to the question if a stick slip mechanism should be integrated into a new design.

Chapter six is dedicated to the verification of requirements on a chuck. The verification can be used to evaluate the performance of the chuck with respect to the present chuck and the requirements on the chuck.

Chapter seven, eight and nine provide respectively a discussion, conclusion and recommendation.

2

Problem analysis

This chapter starts with an explanation of why the e-beam lithography process demands for nanometer accuracy. The way that wafers are positioned in the system is explained in the second section. The third section gives the requirements,constraints and conditions that are posed to the chuck. In the last section, the bottlenecks are summarized that influence the accuracy of the wafer positioning system. These bottlenecks form the backbone of the conceptual and detailed design phases.

2.1. Accuracy in e-beam lithography

In electron beam lithography, electrons should collide with a silicon wafer at a specified position. This position is sometimes referred to as the point of interest (POI). By moving the wafer underneath the electron beams and by turning beams on and off (an exposure), patterns can be made in a layer on the wafer. These patterns are not made at once but by connecting line segments made in multiple exposures. Critical in the performance of the final product (the chip) is that after all exposures, the lines are continuously. Overlay is the term that is used to describe with what maximum error two patterns should be on top of each other. In order to have enough overlay, a rule of thumb is that the overlay should be 25 percent of the node size that is aimed for with the technology. The present target on node size (similar to resolution) is 22nm. This means that the machine should be able to be accurate enough to place patterns within 5 nm on top of each other. In other words: The position uncertainty of the system should be smaller than 5 nm.

2.2. Wafer positioning

Positioning of the wafer is done by the wafer positioning system (WPS). This module actuates and guides the chuck on which the wafer table with a clamped wafer is mounted. A different module in the system is used to measure the position of the chuck relative to the projection lens. This module is called the metrology module. It consists of an orthogonal frame that contains two interferometer heads. Each interferometer head contains 3 bundles that are reflected on a different mirror on the chuck. Each pair of 3 bundles is used to measure the rotation about the z axis, the out of plane translations and the rotation about the horizontal in plane axis. Together they measure 5 degrees of freedom of the chuck of which the rotation about the z axis is measured twice. The translation in the z direction is measured by a capacitive sensor relative to the projection lens.
In order to position the chuck relative to the projection lens (differential measurement), each interferometer head also contains three bundles that are reflected on the projection lens to measure all degrees of freedom except the translation in z direction. A controller is used to close the feedback loop in order to keep the chuck at a specified position relative to the projection lens. The WPS consists of a long stroke which is used for actuation over large motions and a short stroke which is used to correct position errors. The long stroke consists out of two large stepper motors which actuate a platform in the y direction via a rod mechanism. The long stroke is guided by linear guides. On top of this platform, piezo steppers are mounted that actuate another platform in the x direction that is also guided by linear guides. On top of this platform, the short stroke is mounted. The short stroke is a zero stiffness stage. The only contact the top of the short stroke makes with the rest of the short stroke is via a gravity compensating spring. Actuation of the short stroke is done by 6 Lorentz actuators which can actuate all the 6 degrees of freedom. On top of the short stroke, the chuck is mounted with 3 flexures blocks. Mounting the chuck with these flexure blocks allows for thermal expansion.

The chuck contains a zero expansion platform. The shape of this platform will remain constant under thermal variations. v-grooves are mounted on top of this platform. Underneath the wafer table three balls have been mounted at the same locations as the grooves. By positioning the wafer table onto the v-grooves, the wafer table is kinematically mounted. On top of the wafer table the wafer is clamped. The low expansion platform is also connected with two mirrors that are made in two orthogonal faces on the chuck. These are used by the interferometers to determine the position of the chuck. The function of the platform is to keep the position of the wafer table constant with respect to the mirrors under thermal disturbances. The interferometer system measures the position of the wafer table by measuring the position of the chuck mirrors, this is called a non collocated measurement. Since non collocated measurement errors are a direct result of disturbances of the chuck, the chuck is a critical part in the accuracy performance of the WPS module.

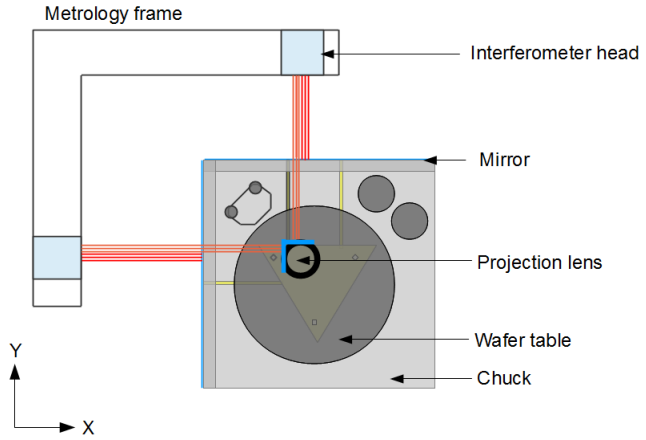

Figure 2.1: Schematic overview of the non collocated (differential) measurement. Note: the bundles that measure the position of the chuck and the bundles that measure the position of the projection lens are not located next the chuck beams (as drawn) but on top of them.

2.3. Disturbances

The chuck is subject to disturbances, these disturbances are of thermal and dynamic nature. The disturbances acting on the chuck are the cause of deformations of the chuck as mentioned in the introduction. The working temperature of the chuck is 294.5 K this condition might vary with +/- 0.5 K. The motion of the chuck is limited by maximum accelerations of 0.5 m/s2.

2.4. Bottlenecks in the position accuracy of the chuck

Disturbances and undesired variations of the geometry of the chuck can cause direct measurement errors of the wafer position. A positional measurement error reduces the accuracy of the chuck and therefore reduces the accuracy of the system. Seven bottlenecks can be designated in the chuck that influence the accuracy of the wafer position measurement. These are: Material selection, Thermal expansion, Optical quality, Alignment, Long term stability, Dynamic behaviour and the Interface connections. This section is used to elaborate on each of these bottlenecks. Each sub section provides a description of the mentioned bottleneck and gives reason why it is a bottleneck. Then the critical requirements on the bottleneck are addressed. The last part of each sub section provides a description of the present situation including the performance on the requirements.

2.4.1. Material selection

Selecting a material in an optic assembly is a complicated task because it influences many aspects in a design. Especially dynamic and thermal behaviour are critical aspects that are determined by the material choice. In the past, materials have been created that exhibit good thermal and dynamic properties in nanometre precision optics. Next to thermal and dynamic properties: - it might be obvious but very important - for the mirrors, materials should be used on which high quality reflective surfaces can be made. It is questionable if material selection on it's own is a real bottleneck. However, it has been accepted as one because the material selection influences all of the other bottlenecks and is therefore critical in the design of the chuck.

Requirements: Since the chuck is used in a vacuum environment, the out gassing of particles should be minimal. Since the process is based on e-beam lithography, no use should be made of magnetic materials. This could disturb the electron beams.

Present situation: the present body of the chuck is composed out of aluminium the function of the body is to gain dynamic stability. Thermal stability of the position of the kinematic mount with respect to the mirrors is gained by using Zerodur - which is a low CTE material - components that connect the kinematic mount to the mirrors. The optical planes are made into the aluminium by fly cutting the surfaces.

2.4.2. Thermal expansion

The temperature inside the machine is varying slightly. When a temperature difference between components exist, heat will be transferred between the components. This causes the temperature of the chuck to vary in time. Since the machine operates in a vacuum, heat can only be transferred via:

- **Conduction:** heat is conducted from the voice coils in the short stroke via the flexures into the chuck. Thermal conduction is described by Fourier in formula 2.1. Here k is the thermal conductivity, T the spatial temperature, q_0 is the heat flux.

$$-k\frac{dT}{dx} = q_0 = \text{constant} \tag{2.1}$$

- **Radiation:** Heat is radiated from the surroundings of the chuck. Radiated heat can be calculated using the Stefan-Boltzman equation given by equation 2.2. In this equation ϵ represents the emissivity, σ the Boltzman constant, A the radiating surface area and T the temperature.

$$Q = \epsilon\sigma AT^4 \tag{2.2}$$

Variation of temperature is the cause of thermal expansion (δ) of parts in the chuck. Expansion of materials can change the position of the thermal center of the kinematic mount with respect to the mirror planes. Since the thermal center of the wafer table coincides with the thermal centre of the kinematic mount, the position of the wafer will also change. This effect is called thermal drift (see figure 2.4). Thermal expansion is described by equation 2.3. α represents the coefficient of thermal expansion (CTE), L_0 the length of material subject to expansion, $T_1 - T2$ the temperature difference of the material over time.

$$\delta = \alpha L_0(T_1 - T_2) \tag{2.3}$$

Another cause of a positioning error due to thermal expansion is when the material between the kinematic grooves changes in distance too much. This happens when the grooves are mounted in a material with a high CTE. The expansion causes micro slip on the interface balls of the wafer table. The friction between the balls and v grooves can resist some expansion but at a certain expansion, the friction force is too low to hold the elastic deformation of the contact. The balls will slip to an other position.

Requirement: The position of the wafer is calibrated before each 30 second line exposure. This is done by reading line marks on the wafer. The error budget for thermal drift is 0.5nm. Because of the recalibration the thermal drift should only be less than 0.5nm within the exposure time. Therefore the requirement is that thermal drift should be less than 0.5nm in 30 seconds.

Present situation: To control thermal drift in the present chuck, use have been made of parts made out of Zerodur. Zerodur is a material with a very low CTE (in the order of 0.01 μm/mK). The low expansion platform mentioned previous, is made out of Zerodur. It is connected with three Zerodur struts to the mirror planes to constrain the z rotation and the x and y translations. In figure 2.3 the platform containing the v grooves and struts can be seen. By connecting the platform to the chuck body with three vertical rods, the other dof's are constrained. The chuck body is made out of aluminium which has a CTE of 24 μm/mK. This a relatively large CTE and therefore a temperature variation will cause a relatively large expansion. The expansion of the aluminium body of the chuck might introduce deflection of the rods underneath the low expansion platform which might cause stretching of the platform and rods. This stretch is a direct measurement error. A benefit of this solution is that only a small amount of Zerodur has to be used (Zerodur is expensive). A disadvantage is that expansion of other parts with a high CTE might still influence the kinematic thermal center - mirror distance. Stick slip is not present since the grooves are mounted on Zerodur.
A drift figure of the wafer table can be found in figure 2.6. In the present machine the drift of the thermal centre is 0.1nm/30s. This is way below the required 0.5nm/30s. Thermal expansion of the mirrors however cause the shape of the mirror to change. This also effects the long term stability.

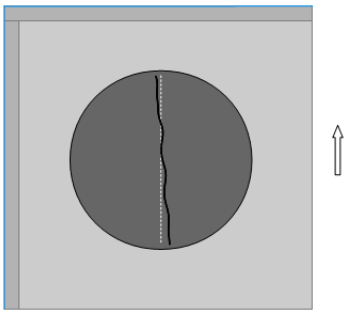

Figure 2.2: Dramatizations of the effect of thermal expansion on writing a straight line on a wafer.

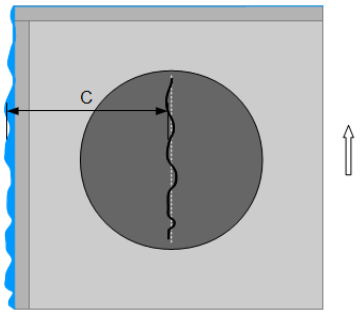

Figure 2.3: Effect of a non flat mirror surface on writing a straight line.

2.4.3. Optical quality

The interferometers use the mirrors on the chuck to measure their positions. Ideally these mirrors are perfectly flat but in reality the surface will deviate from a perfect flat plane. Deviations of the mirror surface from a perfect flat plane can be directly transfered to motion by the control system. This can be the cause of an error effect as can be seen in figure 2.5. Surface variations can be categorized in 3 spatial frequencies:

- Form, $f_s \geq 10$mm
- Waviness, $0.1\text{mm} \geq f_s \leq 10\text{mm}$
- Roughness, $f_s \leq 0.1$mm

Next to these static variations in surface height, the mirrors can be subject to thermal, dynamic and gravitational loads. These loads can cause stresses in the mirror causing deformation of the surface. The mirror shape and deformations of the mirror determine the accuracy of the measurement of the position of the mirrors.

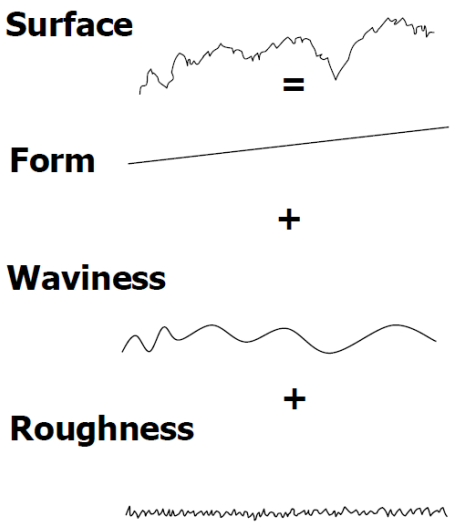

Figure 2.4: Surface deviation divided in three ranges. [25]

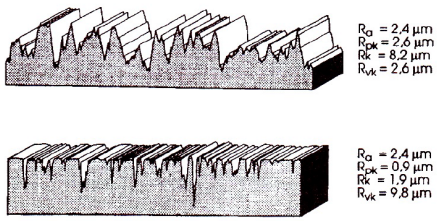

Figure 2.5: Two surfaces with the same arithmetic roughness but with a complete different surface topology.[25]

- **Mirror flatness:** The flatness of the mirror refers to the first two spatial ranges of surface variations: the form and the waviness of the mirror. The machine can compensate for un flatness by making a mirror map. In the mirror map, the system measures the height of the mirror surface at points that are 0.5mm off from each other. By interpolating between these points, the height between the points is estimated. Since use is made of interpolation, abrupt changes might be overseen (see figure 2.11). Therefore the mirrors are subject to strict requirements on flatness. These requirements are on the maximum first and second derivatives of the surface. In other words the maximum angle of the surface and the curvature.

- **Mirror roughness:** Surface roughness can be divided into many parameters that together define the roughness. The mainly used parameters for surface roughness are the arithmetic mean (R_a), the peak to peak and the rout mean square of the height (R_q). Roughness parameters should be used carefully because for instance two surfaces with the same R_a can differ a lot in surface roughness. (figure 2.8)

  Interferometry uses the change in phase and intensity of the interfering beams to measure the position of the moving mirror. When the mirrors have an insufficient surface roughness, the light will be scattered a lot. This is called speckle. Speckle is mainly caused by surface roughness and defects of the surface. Figure 2.9 shows a dramatization of this effect. The scattering will reduce the optical contrast of interference pattern at the light sensitive sensor of the interferometer causing inaccuracy of the measurement.

- **Mirror deformation** Deformations of the mirror plane give rise to measurement errors: if the mirror shape is different from the expected shape of the mirror, the difference between expected position and actual position is the measurement error. Mirror deformations come in two flavours: static deformation and non static deformations. The static deformation is caused by the gravity of the earth. The deformation this causes will be constant since gravity is (about) constant. This deformation can be compensated for in the mirror mapping if the deformations are within the flatness requirements of the mirror shape. Non static deformations however are the deformations that occur due to dynamic or thermal variations or can happen randomly.These non static deformations are caused by:

  - Bi material bending
  - Local thermal deformations

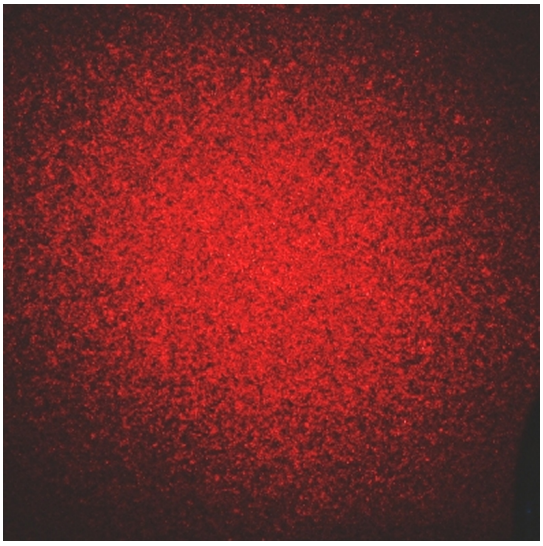

Figure 2.6: Speckle of a reflected laser beam on a rough mirror and visualized on a plane.

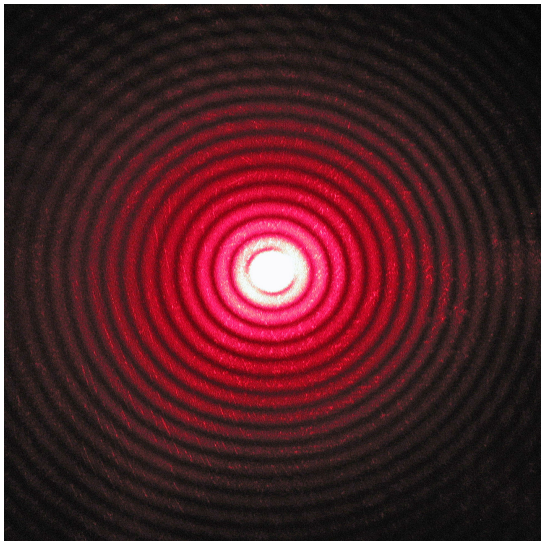

Figure 2.7: Interference pattern of a laser beam. From this the phase changes can be determined via a computer and light sensor.

  - Vibrations
  - Random stress releases

Requirements: The following requirements have been set in order to define the desired optical quality:

- In order to reduce measurement errors that are caused by scatter and speckle, the mirror should have a Ra surface roughness of 1nm or less.
- The flatness and form variations of the mirrors are restricted by the mirror mapping procedure: The variations that occur in between the mapped points can not be compensated for. The requirements on the form and waviness of the mirrors are:
  - The first derivative (or slope) of the mirror surface shall be lower than 25μrad in horizontal and vertical direction
  - The second derivative (or curvature) of the mirror surface shall be lower than 0.01m^{-1} in horizontal and vertical direction
  - Mirror form variation lower than 0.5μm.

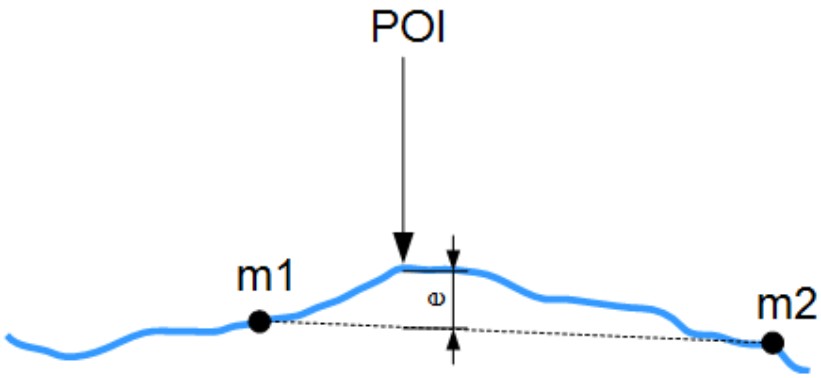

Figure 2.8: The blue line represents the mirror surface. m1 and m2 are the mapped points on the mirror and the dashed line is the interpolation line. Clearly a measurement error (e) can be observed when the mirror surface does not coincide with the interpolation line.

Present situation: In the present machine the mirrors are made in a process called fly cutting. In fly cutting a diamond edge is rotated over the aluminium surface of an edge of the chuck with a pitch of several tens of micrometers. Comparison of the fly cut aluminium chuck mirrors with Pyrex (glass) mirrors in a position measurement shows that the inaccuracy is much larger with the aluminium mirrors. This is suspected to be a combination of mirror surface roughness causing speckle and mirror un flatness at a too high spatial frequency. Because of this the interpolations between the measured points of the mirror map are subject to a large error. Figure 2.12 shows the a sample of the surface topography of the present mirrors. As can be seen, the RMS roughness is about 9nm over the line as drawn at the top left picture. The line used to determine the roughness over seems to be the most optimal line. A bit lower on the surface, the surface looks rougher. This might result in even a worse Ra and RMS roughness. Next to these figures, some spots can be seen on the surface. These are the high spatial artefacts mentioned previously. These artefacts are expected to be caused by the fly cutting process.

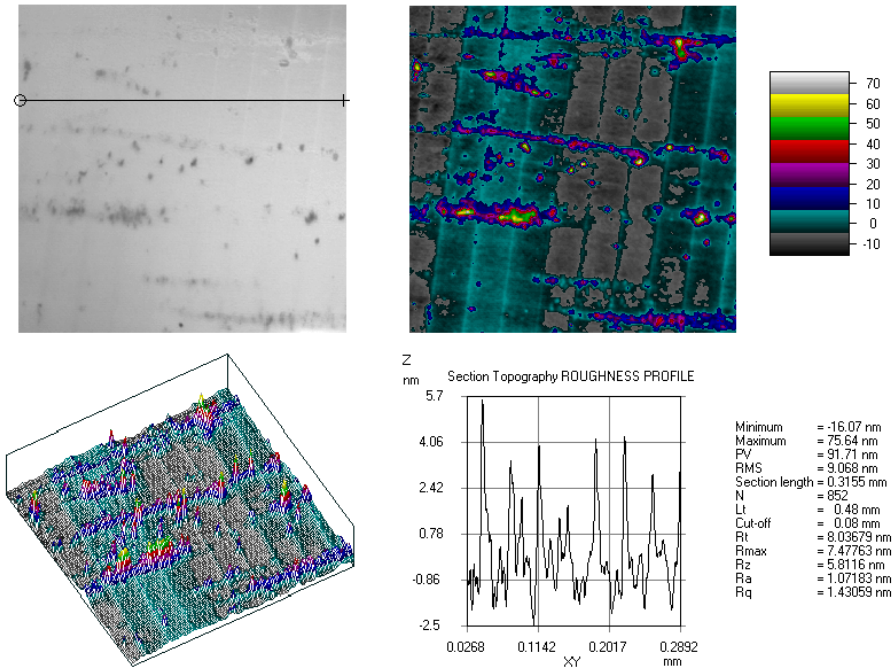

Figure 2.9: Surface topology of a mirror made by fly cutting an aluminium surface.

2.4.4. Alignment

Since the wafer position measurement is a non collocated one, the orientation of the wafer relative to the mirrors is critical. Three factors have to be taken into account:

- **Mirror orthogonality:** The mirrors on the chuck are mounted orthogonal to each other. This is done in order to measure the x and y translations and the Rx and Ry rotations independently from each other. When the mirrors however are not perfectly orthogonal, the measurements are not completely independent. This means that when the chuck for instance moves only in the x direction the y direction will also change as can be seen in figure 2.13. The feedback system wants to keep the distance in the y direction constant so the chuck is moved in y direction. This is an undesired effect.

- **Abbe error:** Due to the fact that the measurement is non collocated, rotations in the Rx and Ry direction can cause an Abbe error as can be seen in figure 2.14. This effect is minimized when the laser beam from the interferometer is reflected on a point at the same height as the wafer surface.

- **Internal alignment:** The wafer plane should be at a very small distance from the projection lens (about 100 μm). Therefore movements in the horizontal plane preferably don't introduce movements in the z direction (independent positioning). For this reason, the chuck should hold the wafer plane in a perfect orthogonal position with respect to the mirror plane.

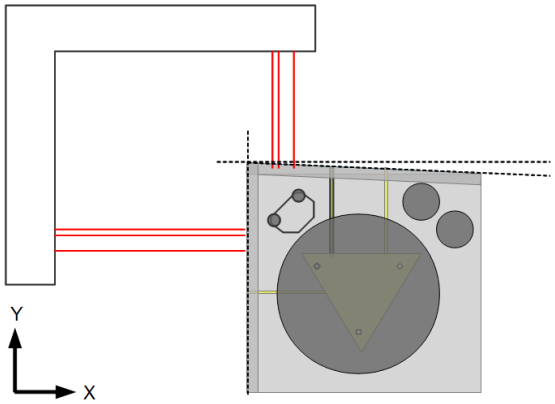

Figure 2.10: Orthogonal error of the mirror planes can cause dependant positioning.

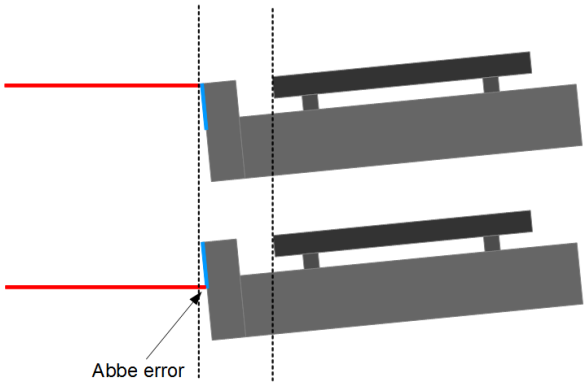

Figure 2.11: Top: correct way of measuring the plane positions. Bottom: measurement with a large Abbe error.

Requirement: The orthogonal error between the mirrors should be smaller than 50 µrad.

Present situation: The fly cutting process determines the orthogonality of the mirrors. The angular error between the mirrors on the present chuck is 10 μrad. The orthogonality of the mirrors made by this process fall within the requirements. The Abbe error is dealt with by deflecting the beams of the interferometers at the top of the mirrors at the height of the wafer surface. This does not result in an Abbe error. The internal alignment is dealt with by using adjustment screws for the low expansion platform. These are used as a first orthogonality approach. Shims (thin plates) are used to approach the desired orientation of the v grooves, and with this the desired orientation of the wafer. Alignment is not an issue in the present chuck.

2.4.5. Long term stability

In order to have a good overlay with the system, the shape of the mirrors and the alignment should be constant. Mirror shape changes can not be accounted for by mirror mapping since this is only done once in a period. Instability of the mirror shape can occur due to random stress releases in the mirrors and chuck body and due to thermal variations. These stresses are introduced in the production process of the chuck. Because changes of the mirror shape cause a direct error, it is crucial that the mirror shape will be stable for a long term. This is what is referred to as long term stability.

Requirement: Long term stability of the chuck less than 1nm in 1 month.

Present situation: Measurements show that the mirrors shape is unstable. Figure 2.15 shows the change of mirror shape for both mirrors on the chuck. The change of shape can be found on the vertical axis and the position of the measurement along the mirror on the horizontal axis. In this measurement the shape has been measure several times before and after exposures. It is hard to conclude if these variations are caused by thermal effects in the mirror or deformation of the mirror due to thermal effects elsewhere in the chuck. Although this is hard to evaluate, it can be seen that the changes are in the order of tens of nanometers. With these kind of variations an overlay of 5nm can not be met. Figure 2.16 shows the shape changes without exposures over 10 hours. The temperature varied with 0.3K and the effect is that the shape changes to a maximum of 7nm. The conclusion drawn here is that in order for the mirrors to be stable within 1nm, the chuck should stabilize for the first 10 hours in the machine.

2.4.6. Dynamic behaviour

Vibrations of the chuck are the cause of shape changes of the mirrors and changes of the orientation of the wafer table interface with respect to te mirrors. These changes cannot be measured by the interferometer causing inaccuracy. The higher the frequency of the first mode, the smaller the changes in shape are. Next to this, the vibrations have an effect on the accuracy of the control of the system. The control performance is related to the bandwidth. The bandwidth is the frequency range up to the first natural frequency of the chuck. By increasing the frequency of the first mode of the chuck, the controller will be able to control disturbances

at higher frequencies which makes it possible to move more accurate. Because of these two effect, the aim is to design for a high natural frequency.

Requirement: The natural frequency of the chuck should be higher than 400 Hz.

Present situation: The struts mount the low expansion platform to the mirrors. These components have a finite stiffness and therefore can be stretched, compressed or deflected when under influence of a dynamic load. This is referred to as the internal dynamics and causes the wafer orientation to change relative to the mirrors. Internal dynamics can be reduced by adding damping, adding stiffness and/or making parts lighter. The first mode of the open back chuck is at 300Hz. The closed back has a first mode at a frequency that is little less than 400Hz.

2.4.7. Interface connections

The chuck has interfaces with different modules in the system. Interfaces between different modules can give rise to accuracy problems when not designed properly. Therefore it is crucial to investigate these interface connections. The relevant interface connections of the chuck are:

- The chuck mounted via flexures to the short stroke.
- The wafer table mounted on the chuck via a kinematic mount.
- The initialization plates mounted on the chuck.
- The metrology frame (the interferometer beams) with the mirrors of the chuck.
- The beam measurement plates mounted on the chuck.

Interfaces between different modules can give rise to accuracy problems when not designed properly.

Requirements: The most relevant requirements on the interface connections are:

- Natural frequency of the assembled short stroke module should be higher than 400Hz.
- Interface connections should maintain position stability of the chuck.
- The chuck size is constrained by a volume claim. The volume claim should prevent collisions with other components in the machine and should position several components of the chuck assembly at the right position with the right orientation.

Present situation: The chuck is mounted to the short stroke via flexures (see figure 2.17 and 2.18). These flexures are designed to allow for thermal expansion. The flexures over constrain certain directions but under constrain others as will be explained in the chapter on detailed design.
The kinematic mount is used to reproduce the position of the wafer table and mount the wafer table exactly constraint. The kinematic mount that is used is called a Maxwell clamp(see figure C.1). Three balls are mounted underneath the wafer table. These coincide with v grooves that are mounted on a low expansion plate on the chuck. With this clamp, expansion of the wafer table will keep the wafer table centred at the kinematic centre. This is a proven method to mount the wafer table to the chuck. No stick slip effects can be seen but the thermal centre is not in the centre of the wafer. Next to this, the natural frequency of an infinitely stiff chuck mounted on the flexures is 360Hz. Better than 360Hz could therefore never be achieved with the present coupling of the chuck to the short stroke.

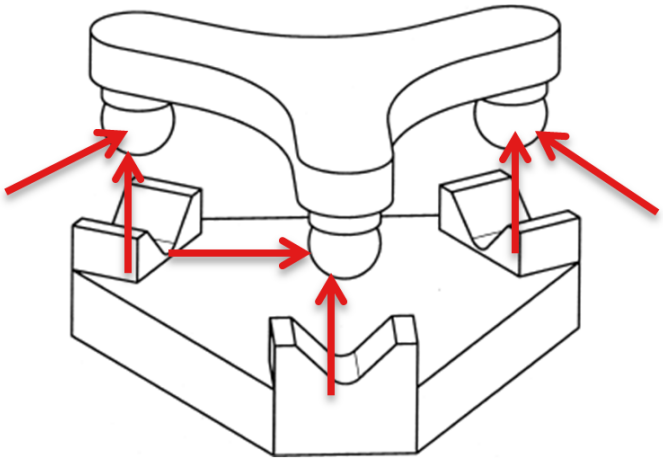

Figure 2.12: A Maxwell clamp is used to mount the wafer table to the chuck. Each groove constrains two direction (red arrows).

2.5. Manufacturability

A new design of the chuck should be manufacturable. The ability to machine, polish and assemble the chuck are some of the factors that need to be taken into account when considering a new concept.

Present situation: The chuck body is made out of aluminium, since many production companies over the world can machine aluminium components it is easy to get it manufactured. The chuck consists of many components that all have to be aligned accurately. Because of this, it takes a long time to assemble the chuck.

2.6. Performance

For concept comparison it is beneficial to rate the performance of the chuck. This is done by evaluating the performance of the bottlenecks with respect to their related requirement. The rating ranges in 5 steps from -2 to +2. Table 2.1 shows the representation of each grade. The reference '0'rating is assigned when the concept is expected to meet the specific requirement.

Rating	Representation
-2	Will never meet the requirement
-1	Will not meet the requirement but with a lot of effort it might
0	Expected just to meet the requirement
1	Will meet the requirement when disturbance becomes slightly larger
2	Will easily meet the requirement

Table 2.1: Range of rating concepts.

Table 2.2 shows the performance rating of the present chuck. From this evaluation it can be concluded that the optical quality is the most critical bottleneck. This is due to the high roughness and the artefacts on the surface. Next to the optical quality, the dynamical behaviour of the chuck is insufficient, the first mode of the open back chuck is near 300Hz by mounting a plate underneath the chuck (closed back) the natural frequency rises up to 360Hz which is still lower than the desired 400Hz. The present chuck is an assembly of components that all need to be aligned very accurately. This makes it a very complex design. So next to better optical performance and dynamic behaviour, the chuck should become less complex. The low rated bottlenecks are a good reason to make a redesign of the chuck.

Bottleneck	Rating	Comment
Thermal expansion	0	Use of Zerodur is good but the aluminium is not
Optical quality	-2	Fly cut mirror shape not good enough
Alignment	0	Works but many components have to be aligned
Long term stability	-1	Mirror shape is not stable during exposures
Dynamic behaviour	-1	Low first natural frequency
Interface connections	-1	Short stroke flexures reduce the natural frequency of total system
Manufacturability	-1	Cheap aluminium body with short lead time. Zerodur has long lead time and is expansive, only select group of manufacturers.

Table 2.2: Rating the performance of the present chuck. It is rated with a total score of '-6'.

2.7. System considerations

The position uncertainty is not only determined by the chuck. The system and disturbances from the outside of the machine can introduce position uncertainty as well. This section considers other uncertainty contributors in the system. This section is included to be complete. The aim of this section is not to give a thorough analysis of all the uncertainty contributors.

2.7.1. Feedback noise

The positioning accuracy is limited by feedback noise. Feedback noise gives rise to a minimum effective resolution. Feedback noise is mainly caused by the following aspects:

- Electronic noise caused by the electronic components used in the control system. This can be suppressed by using electronic filters.
- Mechanical vibrations of the surroundings can be reduced by vibration isolation of the wafer positioning system.
- Control loop position stability, can be reduced by accurately tuning the controller.

2.7.2. Interferometer instability

The interference pattern that is measured by the optical sensors of the interferometers when the chuck moves is periodic. Each period is a interference loop. Each interference loop reoccurs when the mirrors are moved a distance equal to the wavelength of the light that is used. By intensity measurements, the number of loops can be determined. By multiplication of the number of loops with the wavelength, the traveled distance can be determined. When the wavelength changes to a longer wavelength, the same interference loop now relates to a larger travel distance. Since changes in the wavelength are not measured, variations of the wavelength introduce a measurement error. This is what is referred to as interferometer instability. This is a cause of positioning inaccuracy.

2.7.3. Differential thermal expansion

The interferometer is mounted to some part of the machine frame and has the function to measure the position of the chuck. When temperature changes different parts of the system will heat up or cool down. With this parts of the frame expand or contract. this means that the distance between the interferometer to the chuck changes even if the chuck does not move. To control this variation, the reference is chosen to be the projection lens. The lens is also equipped with two orthogonal mirrors. On top of the interferometer that measures the chuck, there is an equal 6 beam system measuring the reference mirrors. The beam output of the second interferometer is aligned in the z planes with the interferometer output of the chuck. By doing this, the thermal expansion between the interferometers outputs is zero. Figure 2.20 shows a side view of the metrology system with both interferometers and the wafer positioning system. With both measurements it is possible to determine the distance or movement between chuck and lens by subtracting both measurements. This is called a differential measurement. By doing this, differential expansion is not an issue anymore, it is compensated for.

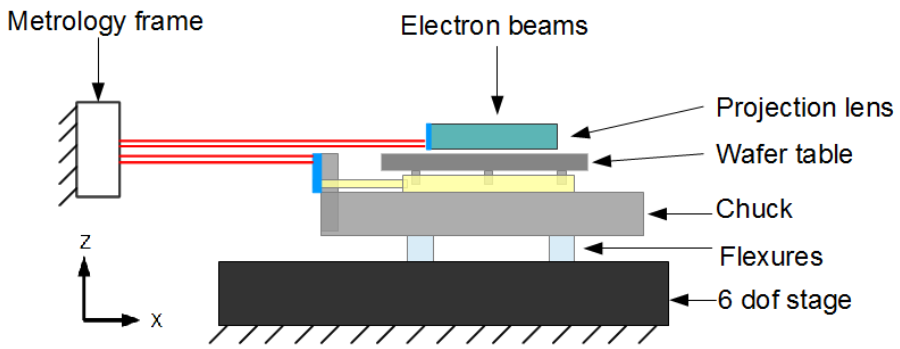

Figure 2.13: Side view of the complete motion system including the differential measurement and the projection lens.

3

Concept design

3.1. Functions of the chuck

The main function of the chuck within the wafer positioning system is that it should hold the wafer and mirrors in a well known position and orientation with respect to each other and the short stroke. In order to fulfil this function the chuck has several functional requirements :

- Mount the mirrors
- Align the mirrors
- Maintain distance and orientation between mirrors and kinematic mount

Since the focus in this project is on smooth mirrors and the position and orientation of the mirrors with respect to each other and to the kinematic mount, the functional requirement on the coupling with the short stroke is left out. The new design should be mounted onto the same flexures of the short stroke interface as the present chuck. However left out in the concept design, the coupling is analyzed in the detailed design.The remaining three functions are topic of the first part of this chapter. For each of these functions, strategies have been found that give direction to a solution for the function. For each function a number of critical aspects have been addressed. The solutions found are evaluated on these critical aspects to select promising solutions. The combination of solutions for the functional requirements lead to concepts. The expected performance of each concept is evaluated. This will induce a promising concept which is topic of the detailed design. The design feedback path, can be found in figure 3.1. The top blue boxes show the functional requirements and the yellow boxes show the bottlenecks. The dashed path is the design path. Each bottleneck interacts with the design.

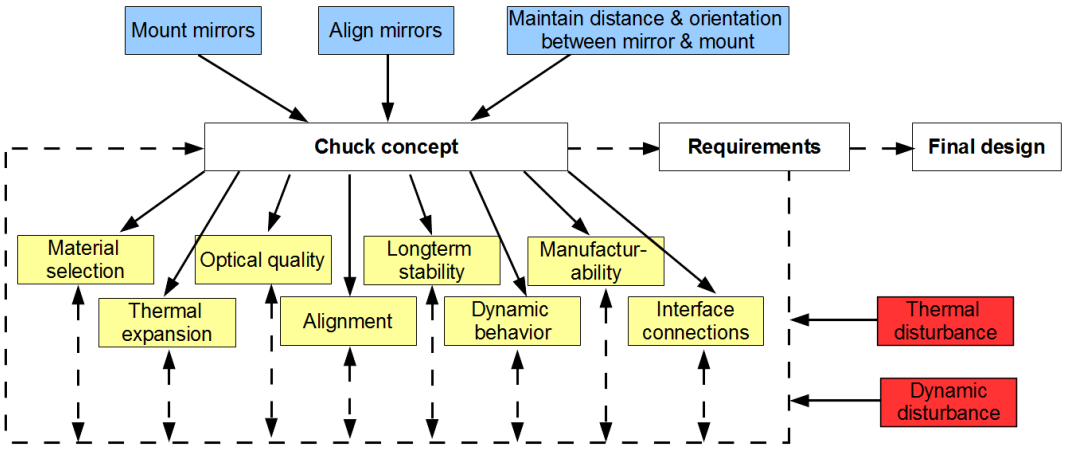

Figure 3.1: Visualization of the feedback path of the design process.

3.2. Assessment of solutions

The upcoming three sections provide a number of solutions for each of the functional requirements that have been addressed. In order to evaluate these solutions effectively, the solutions are rated for each criteria. This is done by using a scale ranging from -2 to +2 in 5 steps. Table 3.9 shows the representation of each rating. As a reference for the rating the satisfactory result is used. For each criterion, this reference '0' rating is explained. The '-1'rating is assigned when the reference is not met but might just be met with a lot of effort. The '-2' rating is assigned when the reference will never be met. The '1' rating is assigned when the reference is met and will still be met when the environmental disturbances are slightly increased. The '2' rating is assigned when the criterion easily meets the reference.

Rating	Representation
-2	Greatly inferior to the criterion
-1	Somewhat inferior
0	Satisfactory
1	Somewhat superior
2	Greatly superior

Table 3.1: Assigned ratings

3.3. Mount the mirrors

High quality mirrors should be mounted in such a way that they maintain their shape under the disturbance acting on the chuck.

3.3.1. Critical aspects

Critical aspects in mounting of mirrors are:

- **Assembly deformations:** When mirrors have to be mounted on the chuck, stresses can be introduced by the assembly which might cause undesirable deformations of the mirror.
  '0' rating: The mirrors do deform but are just within the requirements on maximum angle and curvature when assembled.
- **Dynamic deformations:** Vibrations of the mirrors cause a direct measurement error, therefore the mirror surface should be supported by a stiff enough substrate in order to suppress vibrations.
  '0' rating: The mirrors do vibrate but are just within the requirements on maximum angle, curvature and long term stability.
- **Thermal deformations:** Thermal variations in the mirror can be the cause of position changes of mapped points on the mirror due to thermal expansion.
  '0' rating: The out of plane thermal deformations of the mirror stay within the expansion requirement. Furthermore, points on the mirror have not been moved in such a way that the mirror map of the height of the surface is off with 0.5nm.
- **Mirror smoothness:** The quality of the mirror surface of the solution.
  '0' rating: The Ra mirror roughness achieved is 1nm.
- **Simplicity:** The simplicity of the solution in terms of production.
  '0' rating: The mirrors have a leas time of 6 weeks.

3.3.2. Solution strategies

With the critical aspects in mind, 3 strategy topics can be found for mounting the mirrors to the chuck:

- **Connection type:** Direct or indirect (via other components)
- **Duration of mounting:** Permanent or temporarily
- **Constraint type:** Static determined, over constrained or under constrained

The 3 topics are independent of each other and can be combined. Visualization of the position of the solutions in the strategy space will give a 2x3x2 solution matrix. Since it is hard to visualize this, solutions are visualized in two 3x2 matrices in table 3.2 and 3.3. The numbers in the table refer to the solutions that have been found using the corresponding sub strategies. These numbers will be used consequent throughout this section.

Direct	Permanent	Temporarily
Static determined	2	
Over constrained		
Under constrained	3,4	

Table 3.2: Direct mirror mounting vs other strategy topics, the numbers refer to the solutions below.

Indirect	Permanent	Temporarily
Static determined		5,6
Over constrained		1
Under constrained		

Table 3.3: Indirect mirror mounting vs other strategy topics, the numbers refer to the solutions below.

3.3.3. Solutions

The combination of strategies resulted in six solutions. The evaluation of the solutions with respect to the critical aspects can be found in table 3.4. The enumeration below provides for an explanation of each of the solutions found.

1. Two thick glass mirror bars bolted onto an aluminium chuck, the thickness of the bars will absorb the deformations that are caused by the over constrained mounting on the back of the bars. The thickness and over constrained way of mounting of the bars to the chuck will give high stiffness to the mirror surface.
2. Coating mirrors onto a chuck making it a monolith. Dynamic, thermal and optical properties can become very good when the right material is chosen.
3. A thin glass mirror connected to an aluminium chuck via an elastic layer (or bed of springs). The difference in thermal expansion between the glass and aluminium of the chuck is absorbed by the glue layer. This minimizes in plane deformations due to thermal expansion.
4. Glass mirror strips glued onto an aluminium chuck by a thin layer of glue.
5. Glass mirror bars connected via flexures to an aluminium chuck. The flexures mount the mirror bars statically determined to the chuck.
6. A glass mirror L shaped bar mounted on an aluminium chuck via a kinematic mount (3 v grooves on the chuck and 3 balls under the mirror).

3.3.4. Conclusion

The evaluation shows that a monolithic chuck is favourable above other solutions. When the mirrors are integrated as in a monolith, the assembly becomes a single part. Effects of deformations due to expansion become very small because the CTE is homogeneous throughout the complete chuck. The assembly deformations are not present since no loose parts have to be assembled. Depending on the material, the mirror smoothness and dynamic behaviour of the chuck are good too. Kinematic mounting could also be used but involves more assembly steps which makes the solution less simple. Also static bending of mirror bars due to gravity might drive problems.

	Solution	Assembly deformations	Dynamic deformations	Thermal deformations	Mirror smoothness	Simplicity	Overall score
1.	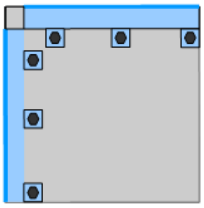	-1	1	0	1	0	1
2.		2	2	2	2	1	9
3.		-1	1	-1	1	-1	-1
4.		-2	1	-1	1	0	-1
5.		1	1	1	1	0	4
6.	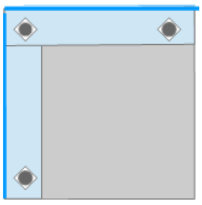	1	1	1	1	0	4

Table 3.4: Evaluation of mirror mounting solutions

3.4. Align the mirrors

The mirror alignment is used to align the mirrors in the right orientation with respect to the short stroke and the interferometers and with respect to each other (orthogonal).

3.4.1. Critical aspects

The critical aspects in the alignment of the mirrors are:

- **Precision of alignment:** What is the expected alignment precision of the mirrors.
  '0' rating: The resolution of the alignment is equal to the requirement on the offset of the mirrors and the wafer.
- **Alignment deformations:** Deformations of the mirror caused by the alignment solution.
  '0' rating: The alignment process possesses deformations of the mirror plane that are equal to the requirements on angle and curvature.
- **Alignment controllability :** The ability to control the alignment during the assembly of the mirror.
  '0' rating: Angular errors of 25urad can be compensated for.
- **Simplicity:** How simple is the solution in terms of fabrication, assembly and alignment.
  '0' rating: Lead time: 6 weeks, The alignment and assembly of the mirrors will take 2.5 days.

3.4.2. Solution strategies

Two strategy topics can be devised in which solutions can be found. The topics contain 5 strategies:

- **Position of alignment:** On chuck edge or not on chuck edge
- **Alignment type:** Self alignment, aligned when mounted or adjustable alignment

The two topics can be found on the axis of table 3.5. The location of the solutions in the strategy space have been marked with the numbers of each solution.

	On chuck edge	Not on chuck edge
Self alignment	4	
Aligned when mounted	1,5	2
Adjustable alignment	3	6

Table 3.5: Direct mirror mounting vs other strategies, the numbers refer to the solutions below.

3.4.3. Solutions

1. The mirrors are coated onto the edges of the chuck. The orientation of the mirrors with respect to the kinematic mount is therefore determined by the orientation of the edges of the chuck. The edges should therefore machined precisely to get the correct alignment of the mirrors. The mirrors can be polished to get the right surface roughness.
2. A tool is used with a flat reference face on which the mirror is mounted non rigidly. The tool can be adjustable or not but will determine the orientation of the mirror. The tool is pushed onto the chuck edges leaving the mirrors at the right orientation. This can be used in for instance a glued situation.
3. Mirror bars that are mounted non rigidly are adjusted by using three adjustment screws for each bar. The use of three screws makes it exactly possible to align the mirrors orthogonal to the laser beam of the interferometer.
4. The mirrors are pushed onto the eges of the chuck with small balls in between. The small balls are made of a hard material. The mirrors can be glued onto the chuck, the glue will be spread between the balls. The balls transfer the shape of the edges to the mirror and the glue does not effect the mirrors when it cures in this way. The flatness of the mirror is determined by the flatness and orientation of the chuck.

5. Mirrors are mounted onto the chuck. The orientation is polished into the mirror. In contrast to the first solution, since the orientation had to be polished into the mirror, this solution will take much more polishing.

6. An orthogonal mirror bar is mounted on the chuck, the kinematic mount will be aligned with respect to the mirrors in order to get the right orientation. The alignment of the kinematic mount is done by mounting shims (thin plates) of a known thickness under the v-grooves.

3.4.4. Conclusion

The choice of alignment principle is combination depending. For instance, a monolithic chuck does not need a precision screw alignment set. A accurate way of aligning the wafer to the mirrors is to use shims. This is a proven method of alignment. Polishing seems to be a good method to align mirrors by forming the shape of the alignment into the mirror. This is due to the fact that these polishing processes are computer controlled. This gives more control over the alignment process.

	Solution	Precision align.	Align. deform.	Align. control.	Simplicity	Overall score
1.	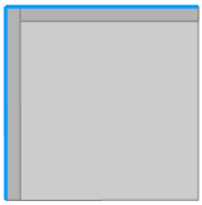	2	2	1	0	5
2.	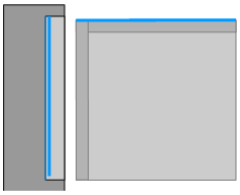	0	1	-1	0	0
3.	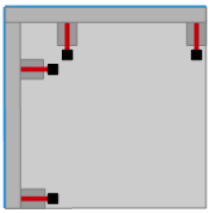	1	0	2	0	3
4.	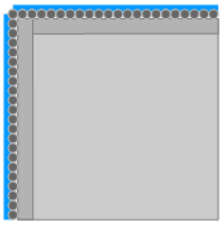	0	0	-2	0	-2
5.	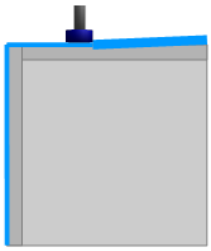	2	1	1	-2	2
6.	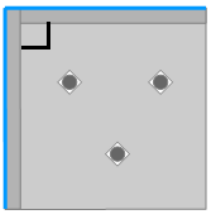	2	2	2	2	8

Table 3.6: Evaluation of mirror mounting solutions

3.5. Maintain distance and orientation between mirrors and kinematic mount

This function of the chuck deals with the distance between the thermal centre of the kinematic mount and the mirror planes and the orientation of the kinematic mount with respect to the mirrors under thermal variations. This function is important because the distance and orientations are not measurable by the interferometers and therefore have to be stable.

3.5.1. Critical aspects

The critical aspects in the maintenance of the distance and orientation between mirrors and kinematic mount are:

- **Position stability:** The drift of the thermal center (TC) of the kinematic mount with respect to the mirrors.
  '0' rating: The thermal centre of the kinematic mount drifts with 0.5nm/30s.
- **Orientation stability:** The rotation of the kinematic mount under thermal variations.
  '0' rating: The wafer rotates with 25urad/30s.
- **Dynamic behavior:** The dynamics of the mechanism or structure used to maintain the distance and orientation between mirrors and kinematic mount.
  '0' rating: First mode at 400Hz.
- **Stick slip:** Is stick slip of the wafer expected when mounted on the kinematic mount.
  '0' rating: Stick slip is present but does not cause larger jumps than 0.5nm
- **Simplicity:** How simple is it to manufacture and assemble the mechanism or structure by different companies and how much will it take to assemble.
  '0' rating: Lead time: 6 weeks, Assembly time: 1 week

3.5.2. Solution strategies

	Low CTE material chuck	Hybrid CTE material chuck
Mirror face at deterministic reference	1,5,6	4
Strut connected		2,3
Counter acting expansion		

Table 3.7: Direct mirror mounting vs other strategies, the numbers refer to the solutions below.

3.5.3. Solutions

1. The complete chuck is made out of a low CTE material, the material between the mirrors and kinematic mount will hold the position and orientation change due to thermal effects within limits. The dynamics can be controlled by making the chuck lightweight. No internal dynamics are present since this solution is a rigid body. Stick slip might be an issue when low but not zero CTE materials are used ($\gg 10^{-7}$).

2. Zerodur struts are mounted on the back of Zerodur mirror bars and connected to a zero expansion platform which is mounted via rods to an aluminum body. By making the complete mirror bars of Zerodur, the struts can be connected to the back since the mirrors will not expand under thermal load. The function of the aluminum body is to add stiffness to the chuck.

3. Zerodur struts are connected to the mirrors via caps. These caps should be engineered in a way that the ends of the struts are in plane of the mirror surface. The struts are connected to a zero expansion platform on rods. Again the aluminum body offers the desired stiffness of the chuck.

4. A Zerodur platform with mirrors and kinematic mount integrated is connected to an aluminum body via a bed op rods. The rods allow for the thermal expansion of the chuck leaving the platform undeformed. The springs should be tuned in order to gain enough stiffness and not deform the body under thermal variations.

5. The mirrors and chuck body are matched with CTE's. Pyrex and Silicon Carbide for instance nearly have the same CTE. The drift of the SiC might be small enough to stay within limits. A changing temperature will not be the cause of orientation changes of the mirror sice the matched CTE will not cause relative displacements that might cause stresses and therewith deformations.

6. A glass mirror is pushed to a reference point made in low CTE material, The distance variation under thermal variation between reference point and the TC of the kinematic mount is kept within limits due to the low CTE.

3.5.4. Conclusion

A monolithic low CTE chuck is in terms of position stability very favourable as can be seen in table 3.8. This is due to the fact that assemblies often have a lower dynamic performance and are prone to deformations due to CTE differences. Furthermore a monolithic body is a simple solution.

	Solution	Position stab.	Orientation stab.	Dynamic behavior	Stick slip	Simplicity	Overall score
1.	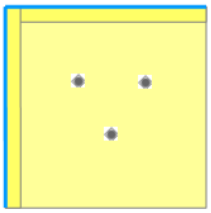	2	2	2	0	2	8
2.	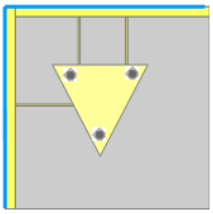	1	1	0	2	-2	2
3.	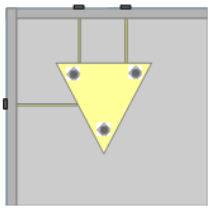	0	0	0	2	-2	0
4.	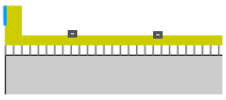	2	2	-1	2	-2	3
5.		-2	0	1	0	0	-1
6.		1	1	0	0	0	2

Table 3.8: Evaluation of mirror mounting solutions

3.6. Concepts

By combining solutions of the previous sections, concepts have been created. In this section these concepts can be found. First, each working principle is explained. In table 3.10 the concepts and their evaluation can be found.

1. Thick glass mirrors glued onto an aluminium chuck, thickness of the mirrors should keep the optical surface flat under small expansion of the chuck. A platform (triangle) which is made out of Zerodur and contains the v-grooves, is connected with rods to the mirror surface to keep position of the wafer table constant relative to mirror surface.

2. Monolithic zero CTE material chuck (Zerodur). The chuck will not deform due to thermal effects. A light-weighted body should obtain an natural frequency of 400Hz. The v-grooves are integrated in the chuck.

3. A monolithic chuck made of a low CTE (but not zero) material. Silicon carbide or Pyrex are options. The low CTE material keeps the TC-mirror distance within limits. The v-grooves are integrated in the chuck. Stick slip might occur on the v-grooves due to the small but changing distance between the grooves and TC. This should be prevented.

4. Zerodur top with mirrors coated on the edges. Wafer table grooves are integrated into the Zerodur top. Rods connect the relative thin and non stiff zerodur top to a stiff aluminium base to obtain a high natural frequency. Rod connection reduces the deformation of the top by expansion of the aluminium. The reasoning behind this solution is that the amount of Zerodur in the concept can be minimized which will minimize cost.

5. Same as concept 3 but in this concept the v grooves of the kinematic coupling of the chuck and wafer table are mounted on a zerodur platform (triangle). The zerodur platform will be at a marginally stable position relative to the mirrors. The distance between the grooves is constant due to the zerodur, therefore: no stick slip occurs.

6. L shaped glass mirror bar mounted with v grooves and balls to a Silicon Carbide chuck, the grooves should be integrated in the SiC chuck.

7. Present chuck but in this concept the mirrors are not made by flycutting the aluminium. The edges in this concept are coated with a Nickelphosphorus layer. The layer is than polished to get the right mirror surface roughness.

8. Present chuck with thin mirrors glued onto the edges. The thin mirrors allow for small deformations in axial direction. The tangential deformations are assumed to be small. (Concept of Mapper under test)

9. Low CTE chuck with L shaped mirror bar pushed to reference points on low CTE chuck by springs on the back of the L bar.

3.7. Assessment of concepts

The concepts are evaluated in the same way as the present chuck is evaluated in chapter 2. The rating scale that is used is given by table 2.1. As mentioned before, the '0' rating is assigned when the concept is expected to just meet the requirement of the specific bottleneck. For reasons of clarity, the requirements given in chapter 2 (that are used as a reference in the evaluation) are summarized below.

Bottleneck	Related requirement
Thermal expansion	Thermal drift in 30 seconds within 0.5 nm
Optical quality	Ra of 1nm or less
	Mirror slope less than 25 μrad
	Curvature less than 0.01 m^-1
	Mirror form variation lower than 0.5μm
Alignment	Orthogonal error less than 50 μrad between mirrors and wafer plane
Long term stability	Less than 1nm variation of mirror surface in 1 month
Dynamic behaviour	First mode should at least be 400Hz
Interface connections	First dynamic mode of assembly should at least be 400Hz
	Interfaces should not interfere with position stability of wafer with respect to mirrors
Manufacturability	Lead time maximum of 6 weeks, assembly time maximum of 3 weeks

Table 3.9: Bottlenecks and their related requirements. The rating of '0' has been assigned when the concept just meets the requirement.

3.8. Final concept

The found concepts were evaluated on their expected performance on each of the bottlenecks in the previous section. From this evaluation it can be concluded that the most promising concepts are concept 3 and concept 5. Both concepts are based on a monolithic chuck made out of a low CTE material. The difference between these concepts is the way that the v-grooves are integrated in the chuck. In concept 3 the v-grooves are directly integrated in the low CTE material. A critical thought on this concept is that stick slip might occur when the wafer table is mounted on the grooves and the temperature of the chuck changes slightly. There are multiple ways to solve this but one way to do this is given by concept 5. In this concept the v-grooves are mounted on a Zerodur platform which is mounted to the chuck. The platform does not expand under variation of temperature since it is made out of Zerodur (CTE « 10^{-7}). Adding a platform to the chuck involves aligning the platform and the need for more parts that have to be manufactured. This will drive the cost and time to assemble the chuck which is undesired. Because of this concept 3 is more favourable but it should be investigated if stick slip actually occurs in order to say whether or not concept 3 is feasible.
The next chapter is on the detailed design of concept 3. Chapter 5 investigates if a stick slip cancelling module should be integrated or not. Note that concept 5 is already a solution to the expected stick slip problem. There exist more ways to get rid of stick slip effects.

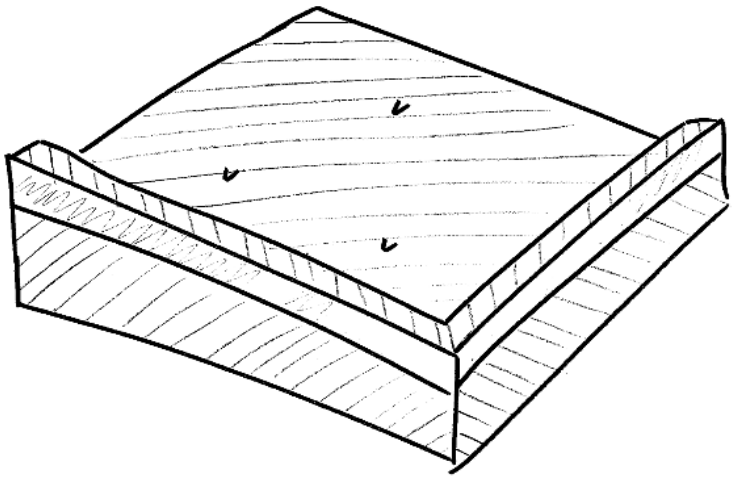

Figure 3.2: A promising concept: a chuck made out of Silicon Carbide.

	Solution	Thermal expansion	Optical quality	Alignment	Long term stability	Dynamic behavior	Interface connections	Manufacturability	Overall score
1.	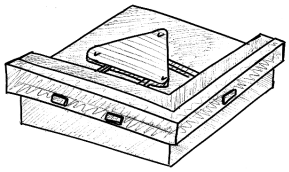	0	1	-2	-1	-1	1	-2	-4
2.	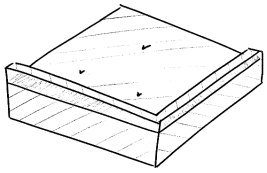	2	2	1	2	-1	1	-1	6
3.	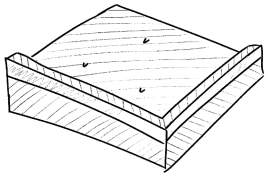	1	2	2	2	2	0	2	11
4.	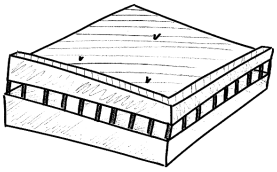	2	2	-1	2	0	1	-1	5
5.	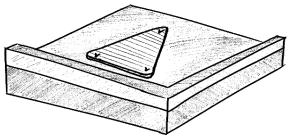	1	2	2	2	2	2	0	11
6.	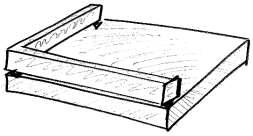	1	1	0	2	1	0	1	6
7.	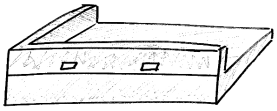	0	0	-1	-1	-1	1	1	-1
8.	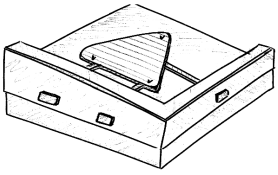	-1	0	-1	-2	-1	1	1	-3
9.	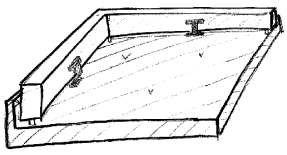	1	1	0	1	1	0	2	6

Table 3.10: Evaluation of filtered concepts

4

Detailed design

Topic of this chapter is the detailed design of the most promising concept - the low CTE chuck - from the previous chapter. The first part is on the design of the chuck with respect to the bottlenecks that have been addressed in the problem analysis. The chapter ends with detailed dimensions of the chuck.

4.1. Material selection

Selecting a material in an optic assembly is a complicated task because it influences many aspects of the design. Especially dynamic and thermal behavior of a material are critical. In the past, materials have been created that exhibit good properties in nanometer precision optics. In this section, an optimal material is selected. This selection is based upon performance numbers of materials which are called figures of Merit.

4.1.1. Material properties

Table 4.1 shows the material properties of a selection of materials. These materials are commonly used in optic-mechanical systems. Some materials - for instance Zerodur - are specifically used in optical components whereas other materials - such as SiC - are used in both optical components as in the mounting structure [29]. Since the chuck is a monolithic part, the mounting structure and the optical part are made out of the same material.

Material	E (Gpa)	$\alpha \cdot 10^{-6}$ m/(m·K)	ρ (g/cm^3)	$\frac{E}{\rho} \cdot 10^6$ (m^2/s^2)	k (W/m·K)	c (J/kg·K)	$\frac{€}{\text{kg}}$[1]
ZPF-N	150	0.0	2.50	60.0	5	?	376
Zerodur cl.0	90.6	0±0.02	2.53	35.8	1.5	800	
cl.1	90.6	0±0.05	2.53	35.8	1.5	800	
cl.2	90.6	0±0.1	2.53	35.8	1.5	800	612
ULE 7972	67.6	0±0.03	2.21	30.6	1.31	767	
Astro Sitall	92	0±0.15	2.46	37.4	2	920	199
Fused silica	73.0	0.58	2.21	33.0	1.4	670	
Invar	141	1.3	8.05	17.5	15	525	
CESiC	350	2.3	2.96	118	145	710	300
UltraSiC	410	2.1	3.15	130	175	665	
NT-SiC	360	2.5	3.03	119	130	680	
Silicon	131	2.6	2.33	56.2	149	700	
Pyrex	63	3.25	2.23	28.3	1	753	
Titanium gr.3	105	8.6	4.5	23.3	19	523	
Glass[2]	70	9	2.5	28.0	0.8	800	
Al 6061	68.2	24	2.68	25.5	170	896	2.3

Table 4.1: Material properties of a selection of materials.

4.1.2. Figures of merit

A way to find an optimal material for the chuck body is to use figures of Merit. Figures of Merit are numbers that reflect on the performance of a material on specific physical properties. For instance the specific stiffness which is the ratio of the Young's modulus and the density. Materials with a high specific stiffness give a lot of stiffness to a design with a relative low mass. Both of these properties influence the natural frequency of the chuck. Therefore it is desired to have a high specific stiffness. Another important figure of Merit is the steady state distortion. It gives the ratio between the thermal conduction and the expansion coefficient. For homogeneous expansion it is desired to have a high thermal conductivity. Thermal expansion should be small in order to maintain position stability so the steady state distortion should be high. Next to these figures of Merit, several others can be found in table 4.2.

Figures of Merit	Desired	Si	Si/ SiC	CVD SiC	C/ SiC	Zerodor	ULE	Be I-220	Al 6061-T6
Specific Stiffness, E/rho	High	59	99	145	89	36	30	164	25
Transient Response, k/rho c	High	0.25	0.27	0.32	0.28	0.003	0.003	0.21	0.24
Steady State Distortion, Ek/alpha	High	7700	19840	38750	12200	2950	2900	31900	513
Dynamic Distortion, Ek/alpha c	High	10.7	29.6	55.4	18.5	3.9	4.1	17.5	0.5
Steady State Distortion, k/alpha	High	56	64	83	52	33	43	105	7.4
Dynamic Distortion, k/alpha c	High	0.08	0.1	0.12	0.08	0.04	0.06	0.06	0.01

Table 4.2: Table with figures of Merit of selected materials. Table copied from [10]

The best options referring to the figures of Merit seem to be SiC and Beryllium. Since beryllium is toxic and magnetic, using this material is not an option. Therefore SiC is the material of choice for the monolithic chuck concept.

4.1.3. Silicon carbide

Silicon carbide (SiC) is a material with a low CTE ($\approx 2.7 \cdot \mu m/m \cdot K$). Next to the fact that the CTE of SiC is low, SiC has a high thermal conductivity (≈180J/m·K) and a high Youngs Modulus (≈ 400GPa) . Both of these properties can be beneficial. SiC exists in about 250 crystalline forms but only two are mostly used in optics engineering: α-SiC and β-SiC. The two types differ slightly from each other in their material properties. The form of the SiC is defined by the method used to produce the Silicon carbide. Basically there are four ways to produce SiC [29]:

- **Sintered:** SiC powder is mixed with a sinter aid (e.g. a phenolic resin). The mixture is formed under high pressure into a "green phase" block. The green phase block can be machined easily because the powder is only held together by the resin and therefore the component is not very hard yet (see figure 4.1). Machining can be done after which the block goes into a oven at 2000 °C. The sinter aid is burned out and the SiC sintered together. An advantage of this method is that large monolithic components of SiC can be produced with complex geometry. A disadvantage can be that the machined block can shrink up to 20 percent. For this reason, the sintered block needs to be post machined in order to achieve the required tolerances. A sintered body of SiC is hard, the hardness forces the use of diamond cutting tools which will often brake. Because of this the post machining is an expensive process.

- **Chemical vapour deposited:** The hardest and purest kind of SiC. The gas methyltrichlorosilane is decomposed into SiC and hydrochloric acid. This decomposition is done under presence of hydrogen and silicon at high temperature and low pressure. The deposited vapour leaves the SiC at the surface of a substrate which is mostly a SiC body formed in a different process. The SiC layer that is left can be polished to a mirror having a surface roughness in the order of angstroms.

- **Reaction bonded:** In this process, SiC particles are mixed with Carbon particles and flocculants. The mixture is put into a negative mold of a desired component and is dried leaving a porous green phase body. After the body is dried, it is machined and heated in an oven at 2000 degrees. Liquid Silicon is added to infiltrate in the porous green phase body and react with the carbon to form SiC. This way of SiC production is less prone to shrinkage but a drawback is that the properties of the material of the final component are not homogeneously throughout the body. This is due to the fact that SiC particles already present in the green phase and the reaction formed SiC have different properties.

[2] Approximate costs are depending on a lot of factors, the prices mentioned were calculated from the prize of a rough block of material of the size of the present chuck. Information is gathered from optical component manufacturers.

[2] Average properties for float glass

- **Converted:** Carbon fibres are mixed with phenolic resin and formed under high pressure in a mold. The blank of carbon fibres and resin are put in an oven to let the phenol react to form carbon matrices around the fibres. This leaves a solid green phase body. The green phase body can be machined after which the body is turned in a high temperature oven again. Liquid Silicon is added to the body to infiltrate into the carbon body and form SiC. The main withdraw of this method is that the infiltration depth is about several millimetres. Because of this it is impossible to make a big block of monolithic SiC with this process.

Each of these processes has it's advantages and disadvantages. CVD is mostly used to create dense thin surfaces. The other methods can be used to create structures. In collaboration with Mapper, Zygo has been selected as a manufacturing company since they can produce optical SiC components and have the technology to create very smooth surfaces. Zygo makes use of the conversion method to produce SiC parts. The conversion method of producing SiC has some limitations that should be taken into account in the detailed geometrical design of the chuck:

1. The infiltration depth of Silicon is about 5mm. Therefore the maximum thickness used in the design should be 5mm.
2. Shrinkage of the green body when sintered makes it necessary to over size the chuck and perform a post sinter machining step.

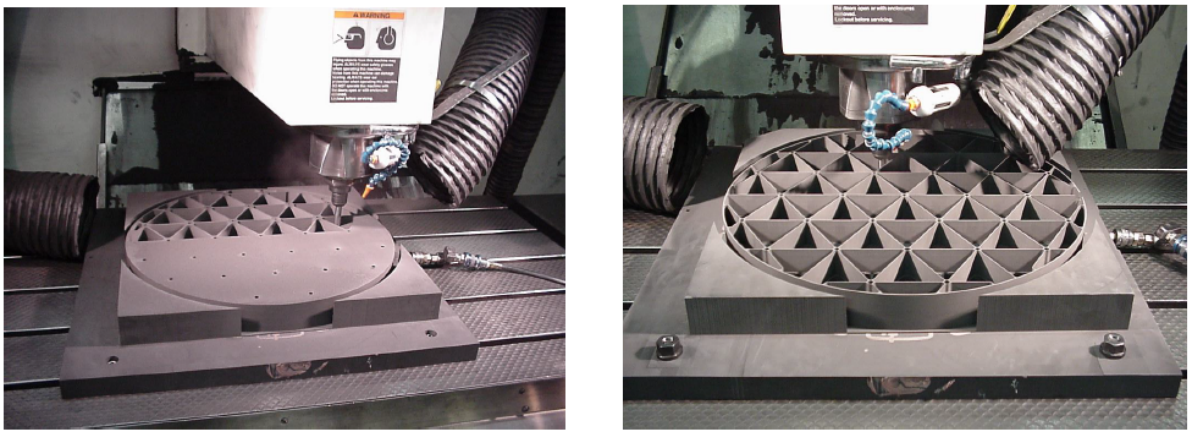

Figure 4.1: Green phase machining of a mirror blank before sintering. After the part has been sintered, post machining has to be done. (source: www.poco.com)

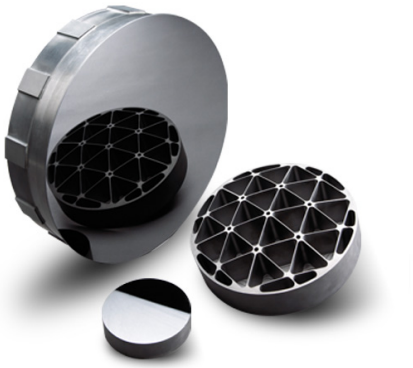

Figure 4.2: Lightweight CVD coated SiC mirrors (source: www.coorstek.com)

4.2. Thermal expansion

The requirement on drift due to expansion of the chuck is that the thermal center of the wafer relative to the mirror should be kept within 0.5nm during one lane exposure (30 seconds). In the SiC chuck concept, the kinematic v-grooves are integrated in such a way that the thermal center is in the middle of the grooves. The thermal centre of the chuck coincides with the thermal centre of the kinematic mount due to the radial symmetric way that the 3 flexures mount the chuck to the short stroke. The flexures allow for some thermal expansion. The question arises if the thermal center of the chuck which is also the thermal center of the wafer table moves less than 0.5nm in 30 seconds under a maximum temperature difference of 1K relative to the mirrors.

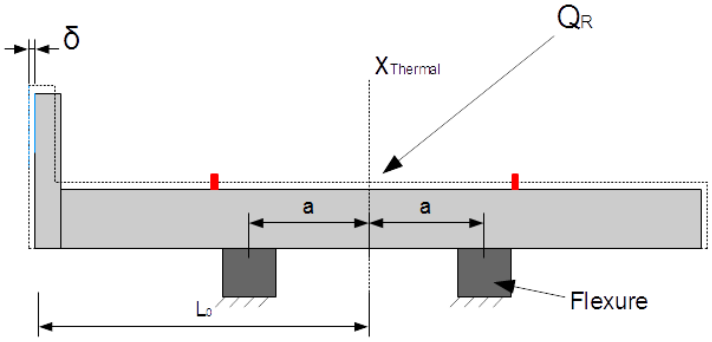

Figure 4.3: Simple side view representation of a monolithic chuck with integrated wafer table interface grooves (red blocks). Mounted on the flexures that connect the chuck to the stage. Radiative heat from the surrounding heats up the chuck which is the cause of thermal expansion. Thermal expansion will lead to a direct measurement error of the size of δ

To determine the expansion of the chuck over 30 seconds, first the temperature change of the chuck should be calculated. The change in temperature is caused by a difference in temperature of the surroundings. Heat from the surroundings will be transfered to the chuck by radiation. Since the chuck is operating in a vacuum, no heat will flow due to convection. Next to this, the only mechanical contact is made with the flexures of the short stroke. Since the short stroke is thermally conditioned, it is assumed that conduction via the flexures is also negligible.
Furthermore in the model it is assumed that the temperature is equal throughout the entire chuck. This assumption can be made because of the very high thermal conductivity of Silicon Carbide.

The heat flow due to radiation can be calculated by using the Stefan-Boltzman equation (4.1).

$$\dot{Q} = \epsilon \sigma A (T_1^4 - T_2^4) \tag{4.1}$$

Where d$\dot{Q}$ is the heat flow between the surroundings and the chuck due to radiation, ϵ is the emissivity, σ is the Stefan-Boltzman constant ($= 5,67 \cdot 10^{-8}$), A the total surface area of the chuck, T_1 is the averaged temperature of the surroundings and T_2 is the temperature of the chuck.

The heat flow causes the temperature of the chuck to change. Next to the heat flow, the change in temperature is related to the mass of the chuck (m) and the heat capacity (c) of Silicon Carbide. The relation that describes the temperature in the chuck by a total heat flow can be derived by rewriting the equation for heat capacity (equation 4.2) as follows:

$$Q = mc\Delta T \tag{4.2}$$

$$\dot{Q} = \frac{\mathrm{d}Q}{\mathrm{d}t} = \frac{\mathrm{d}}{\mathrm{d}t}(mc\Delta T) = mc\frac{\mathrm{d}T}{\mathrm{d}t} \tag{4.3}$$

$$\dot{Q}\mathrm{d}t = mc\mathrm{d}T \tag{4.4}$$

To check if the requirement on thermal drift is met by the chuck, it is necessary to calculate the temperature difference over 30 seconds. Since the time interval of interest and the heat flow are both small, the relation between temperature and time due to heat flow can be assumed linear. Because of this, integration of equation 4.4 leads to the linear relation of equation 4.5. With this equation the temperature difference can easily be calculated.

$$\dot{Q}\Delta t = mc\Delta T \tag{4.5}$$

With the relation for the temperature difference over a time period found, the expansion of the chuck can easily be found. Expansion due to heat flowing into a system can be described by equation 4.6.

$$\delta = \alpha L_0 \Delta T \tag{4.6}$$

With α the coefficient of thermal expansion and L_0 the distance between thermal center and the mirror. Combining equation 4.1, equation 4.5 and equation 4.6 in equation 4.7 gives the desired model. With this equation the requirement (a maximum drift of 0.5nm over 30 seconds) can be checked under the specified thermal condition (maximum temperature difference of 1K).

$$\delta = \frac{\alpha \epsilon \sigma A (T_1^4 - T_2^4) L_0 \Delta t}{mc} \tag{4.7}$$

The parameters in the previous model have been analyzed with the properties of SiC, the geometrical properties of the chuck and a total mass of the chuck of 10kg. The results can be found in table 4.3. From the calculation it can be concluded that the expansion of the chuck is within the requirements when the temperature difference of the surroundings is at the maximum condition of 1K.

Parameter	**Result**
Heat flow ($\dot{Q}$)	0.232 W
Temperature difference chuck over 30s (ΔT)	$1 \cdot 10^{-3}$ K
Expansion in 30s (δ)	$4.5 \cdot 10^{-10}$ m

Table 4.3: Calculated intermediate results of the model used to derive the maximum expansion of the chuck in 30 seconds.

4.3. Optical quality

A major benefit of the concept is that the mirrors are integrated in the body of the chuck. Integration of the mirrors can be done by using chemical vapor deposition(CVD). CVD is a method used to deposit a thin layer of material on a substrate. After deposition the surface is polished to get the desired mirror specifications.

4.3.1. Chemical vapour deposition

The crystal orientation of the SiC particles of the substrate are random. The random orientation of the substrate makes the surface properties inhomogeneous. Polishing a surface with inhomogeneous properties is hard because some parts may be easy to remove whereas others are hard to remove due to orientation depending hardness. In order to get more homogeneous material properties, a siC layer should be deposited with a high purity. The high purity makes the properties of the layer homogeneous. In the CVD process the material methyltrichlorosilane is decomposed into SiC and hydrochloric acid. A cloud of SiC particles is pushed towards the target surface accompanied by a hydrogen flow. At the surface the SiC particles will bind onto the surface. The SiC deposited on the substrate (the chuck) has a high purity and the thickness of the CVD layer is typically about 100 μm.

4.3.2. Mirror polishing

Mirror polishing is done by rotating a polishing pad over the mirror surface with a polishing slurry between the surface and the pad as can be seen in figure 4.5. The slurry consists of a fluid with particles. Changing the parameters (grain size, hardness etc.) of the used particles changes the quality of the surface. There exists a combination of parameters for which the surface roughness is the optimal. The rate at which material is removed is given by equation 4.8 (according to [17]).

$$\frac{dz}{dt} = KVP \tag{4.8}$$

In this equation K is a proportional parameter that combines all polishing parameters. P is the pressure of the polishing pad on the mirror and V is the relative velocity. The removal function of the polish pad is given by equation 4.9. The removal function together with a time function give the predicted amount of material that is removed.

$$R(x,y) = \lim_{T \to \infty} \left(\frac{1}{T} \int_0^T \Delta Z_r(x,y,t)\, dt\right) \tag{4.9}$$

A common method of using the previous conventional polishing method to get a sub nanometre surface finish (according to many papers for instance [10],[14],[17]) is by using computer controlled optical surfacing (CCOS). A schematic overview of this method can be found in 4.4. In this method the shape of the surface is measured by an interferometer or profilometer. A removal function is determined based on the polishing tool that is used. The process control software calculates a predicted error and a time function that relates the time the polishing pad should be above certain area's. A cnc code is produced by the software and the mirror is polished. The surface shape is measured again and the same process will take place again when the requirements have not been met yet. With this iterative process surface roughness of up to angstroms (10^{-10}m) can be achieved.

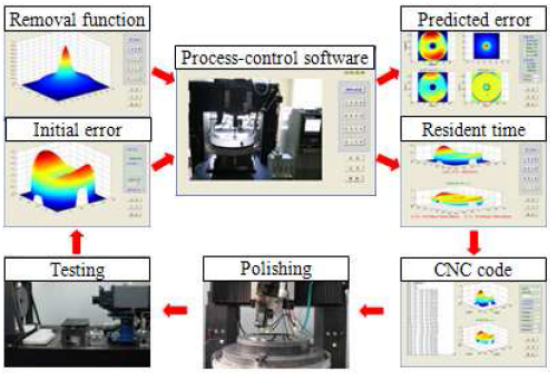

Figure 4.4: CCOS polishing process (source:[17])

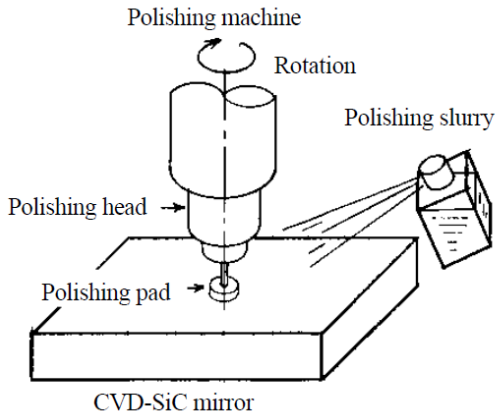

Figure 4.5: Polishing to ultra low surface roughness. (source:[14])

The interaction between mirror surface and polishing tool is the basis for "Print through" of structures behind the mirror (see **??**). This is an undesired error effect. The structure behind the mirror causes a locally higher stiffness to the mirror plane. Because the polishing pressure stays the same, the mirror will have a smaller deformation when there is some structural part mounted on the back side. This will give a larger deviation from the desired form of the mirror.

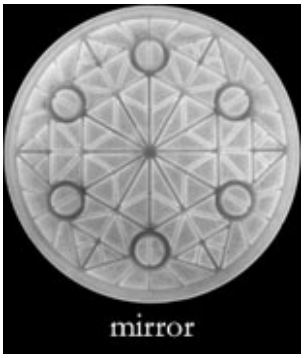

Figure 4.6: Picture of the bottom of a mirror body.

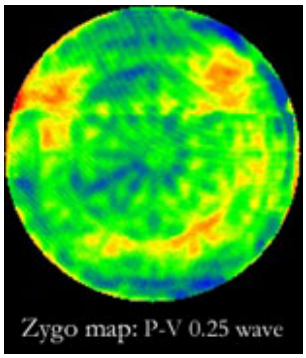

Figure 4.7: Surface profile of a mirror. Print through can clearly be observed. (source:[1])

The print through effect is prevented by not using a lightweight pattern behind the mirrors. The mirror should be thick enough to not overly deflect under the load of the polishing tool. If the mirror without backbone support is thick enough is depending on the polishing process used by the manufacturer. This information is not yet accessible. The requirement on the manufacturability of parts in SiC by Zygo is that the maximum thickness of any part should be 5mm. Therefore the maximum thickness has been chosen for the thickness of the mirror planes as can be seen in figure 4.8.

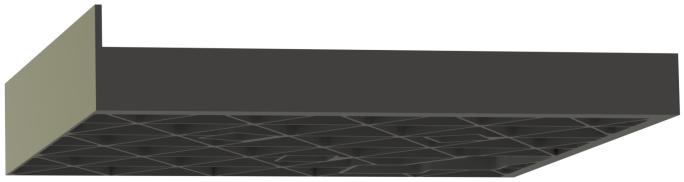

Figure 4.8: Side view of the chuck concept, the left side plane is a complete mirror. the thickness of the mirror is 5mm.

4.3.3. Mirror deformation

As mentioned in the problem analysis, deformation of the mirror plane is a bottleneck in the wafer positioning accuracy. Therefore the new design should be analyzed on possible undesired deformations. All the mirror deformations together result in the total mirror deformation error. The resulting error should be in agreement with the requirements.

Gravity

A finite element analysis on the static deformation due to gravity can be seen in figures4.9-4.11. The figures show the deformations of the concept in respectively x,y and z direction.

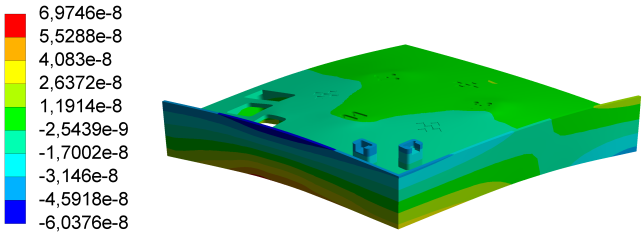

Figure 4.9: Deformation of the mirror planes in x direction

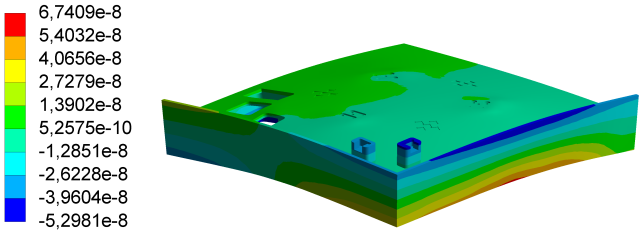

Figure 4.10: Deformation of the mirror planes in y direction

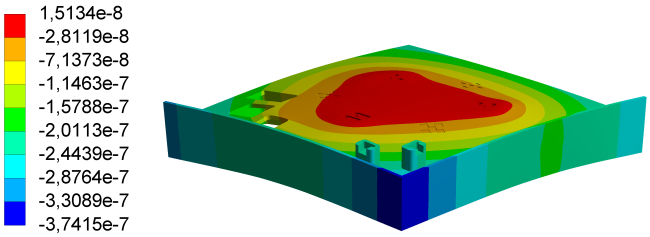

Figure 4.11: Deformation of the mirror planes in z direction

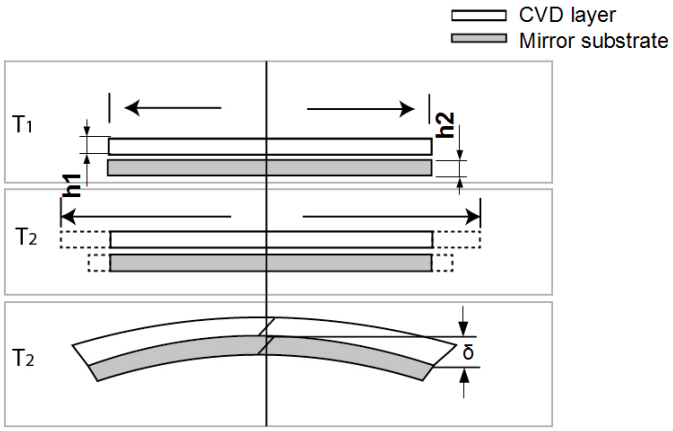

Figure 4.12: Bi material bending due to the difference in CTE.[16]

	Converted SiC layer	CVD SiC layer
α ($\cdot 10^{-}6$m/mK)	2.0	2.2
E (Gpa)	410	465
t (mm)	5	0.1
b (mm)	75	75

Table 4.4: Properties and parameters of the CVD and substrate layers

Since the deformations are small, the first order derivative for the y-z plane mirror can be calculated with the linearised equation:

$$\tan\phi = \frac{\Delta x}{\Delta y} \tag{4.10}$$

The FEM analysis of the deformations in x and y direction have been used to calculate the slope of the mirror surface. The y-z plane mirror has a slope of 0.054 μrad in the y direction. The slope in the z direction is 1.73 μrad. For the mirror in the x-z plane the slope in x direction is 0.056 μrad. in z direction the slope is 1.61μrad. As mentioned earlier, the static deformation can - when within it's limits - be compensated for by mapping the surface. Figure 4.11 shows that the mirrors deflect in the z direction in the order of a tenth of a micrometer. Since this position will be constant this is not influencing the position of the mapped points.

Bi material bending

The mirrors are polished in the CVD layer on the mirror substrate. The SiC that is deposited in the CVD process has slightly different material properties as the SiC substrate. The difference in CTE between both layers gives rise to the bi material bending effect. The effect is schematically represented in figure 4.12. The difference in CTE is the cause of different thermal expansion of both layers. Since the layers are connected to each other, shear stress will be presented at the interface this causes bending of the surface. The curvature under which the surfaces will bend under a variation in temperature can be calculated according to [16] with equation 4.11. ΔT_{ref} is the difference between the temperature and the reference temperature of the zero stress condition at which the cvd layer is deposited. Furthermore, α is the CTE, t is the thickness,b the width and E the Youngs modulus of the respective layer.

$$\kappa = \frac{6b_1b_2E_1E_2t_1t_2(t_1+t_2)(\alpha_1-\alpha_2)\Delta T_{\text{ref}}}{(b_1E_1t_1^2)^2+(b_2E_2t_2^2)^2+2b_1b_2E_1E_2t_1t_2(2t_1^2+3t_1t_2+2t_2^2)} \tag{4.11}$$

The curvature is related to the radius of curvature as $\kappa = 1/R$. Table 4.4 shows the properties and parameters of interest of both layers. In combination with equation 4.11 the curvature can be calculated. It is assumed that the "no stress" situation is at 1000K. At room temperature the curvature becomes $\kappa = 0.005\text{m}^{-1}$. The radius of curvature that belongs to this curvature is $R = 1.96 \cdot 10^5$. Since the operating temperature varies within $\Delta T_{\text{operate}}$ =1K, the mapped surface and the actual surface can differ due to a deflection relative to a maximum $\Delta T_{\text{operate}}$ = of 1K. The deflection of the mirror is revered to as δ in figure 4.12. The change in

deflection is related to the change in curvature by the trigonometric relation given by equation 4.12. ΔR can be calculated by determining $\Delta\kappa$ which can be found by changing ΔT_{ref} with $\Delta T_{\text{operate}}$ in equation 4.11.

$$\delta = \Delta R - \sqrt{\Delta R^2 - (L/2)^2} \tag{4.12}$$

In which L is the length of the mirror. With 1K variation in temperature, according to equation 4.12: the maximum deflection of the mirror plane is $\delta = 0.16\mu$m.

Local thermal deformations
Local thermal deformations arise when the temperature is not equal over the entire mirror. In other words, thermal gradients are present in the mirror. In this situation, some area's are expanded more than other area's of the mirror. This causes mapped points on the mirror to move, therefore the mirror map becomes less valid. However this effect is very small in the plane of the mirror.
The out of plane effect might be more critical. To estimate the order of magnitude of the error that will be made, let's assume that the local temperature of some part of the mirror is 0.1K higher than the surrounding. With a mirror thickness od 5mm, the local out of plane thermal expansion of the mirror becomes:$\delta = \alpha t \Delta T = 2.2 \cdot 10^{-6} \cdot 0.005 \cdot 0.1 = 1$nm. Since the mirror is free in both directions, the error will be half of the expansion: 0.5nm.
The cause of a non homogeneous temperature spread can be due to heat transferred via the short stroke, radiation of heat from the surrounding or local heating due to the laser. The last effect is called photo thermal expansion. This happens when the laser beam heats the mirror locally causing an expansion of the mirror. Since the reflectivity of the mirror is 90 percent, the heat that is dissipated in the mirror is 10 percent. The energy of the beam is several several milliwatts. The beam is only for a short period on the same spot, therefore it is assumed that the effect is negligible.

Vibrations
When the mirror plane starts to vibrate, the position of the mirror changes relative to the wafer. The change of position is relative to the energy of the disturbance that is introduced and the eigenmode of the chuck. The higher the eigenmode of the chuck, the lower the displacements of the mirror are. This is due to the fact that the same amount of energy needs to move the mirror at a higher frequency with the conservation of energy, the displacements should become lower. The relative displacements can be evaluated with the Rayleigh-Ritz method. Because of this effect, it is desired to get design for a high stiffness. Since the exact conditions in the machine are not available, no calculation of the displacements can be done. The displacements that the mirror plane makes should be measured.

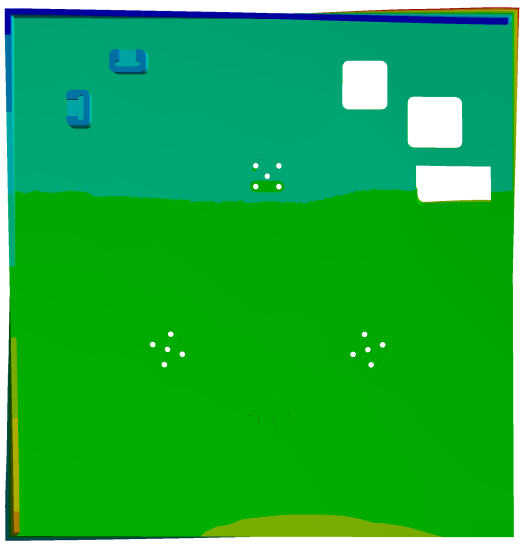

Figure 4.13: Top view of the first mode of the chuck, note the deformation of the mirror surface due to vibrations.

Total deformation
Table 4.5 shows the factors that sum up to the total deformation with the calculated results. Because the mirror deformations due to thermal effects and vibrations can not be calculated exactly, the total deformation can not be calculated. The table is shown for completeness.

	Deflection (nm)	Slope (μrad)	Curvature (m^{-1})
Gravity	60	0.056	
Bi material bending	160	1.3	0.005
Local thermal deformations	1	-	-
Vibrations	-	-	-

Table 4.5: Maximum out of plane deformations in the translating direction (x or y)

4.4. Alignment
The alignment refers to the alignment of the mirrors with respect to each other and with respect to the kinematic mount. The chuck is a monolithic part. The accuracy of the alignment of the mirrors with respect to each other is therefore a direct result of the machining accuracy of the chuck. Zygo makes SiC parts by converting a Carbon green phase body. A disadvantage of this method is that it causes parts to shrink. Since shrinkage can be inhomogeneous, the final alignment of the mirrors should therefore be made into the chuck by a fine post machining step. Zygo is capable to machine the alignment way below the requirements opposed to the chuck.

The alignment of the mirrors with respect to the kinematic mount can be done by using shims. Shims are thin plates that are available with a thickness of 1+x mm. With x steps of 1 micrometer, steps of 10 micrometer and steps of 100 micrometer. The shims are placed underneath the v-grooves which can therefore be adapted in relative height by steps of 1 micrometer. This is a proven method of alignment to align the kinematic mount with the mirrors.

4.5. Long term stability
Only little information is available on the long term stability of SiC mirrors and structural parts. The long term stability should therefore be tested in a validation set-up. Chapter 6 shows how this could be tested.

4.6. Dynamic behaviour
Since the SiC chuck is a monolithic part, the dynamics involved are the Eigen modes of the chuck. The requirement on the first Eigen mode is that the chuck has a frequency of at least 400 Hz. The higher the Eigen mode, the lower the measurement error due to vibrations of the chuck. A semi optimization has been performed in order to choose the size and shape of the pockets used for light-weighting. The most commonly used shapes in lightweight components are hexagonal and triangular pockets. In Solidworks a rough design has been made of a monolithic chuck that includes most of the interfaces with the different modules (wafer table, short stroke etc.) see figure4.14. The lightweight pattern of this rough design has been adapted several times. Each design has been analysed with Ansys (Finite element software) for it's Eigen modes. The semi optimization has been performed on three variables: shape, height of the pattern and typical diameter of the pocket. Figure 4.15 shows the patterns that have been analysed. The optimal shape has been found by using the same typical diameter and height for hexagonal pockets and triangular pockets.

From the table it can be seen that the pocket size is a significant parameter for the stiffness of the chuck. Looking at the performance figures of the shapes $\frac{f_1}{m}$ (figures given in the last column of the table), it can be seen that the triangular pocket size of 50mm with a height of 40mm has the highest hertz/kg ratio. This performance figure is exactly two times larger than the hexagonal pockets of size 50mm and height 40mm, which is remarkable. The result of this semi optimization is that triangular 50mm pockets with a height of 40mm is the optimal solution from the selected shapes. Because of this, the final design of the chuck will have this pocket shape.

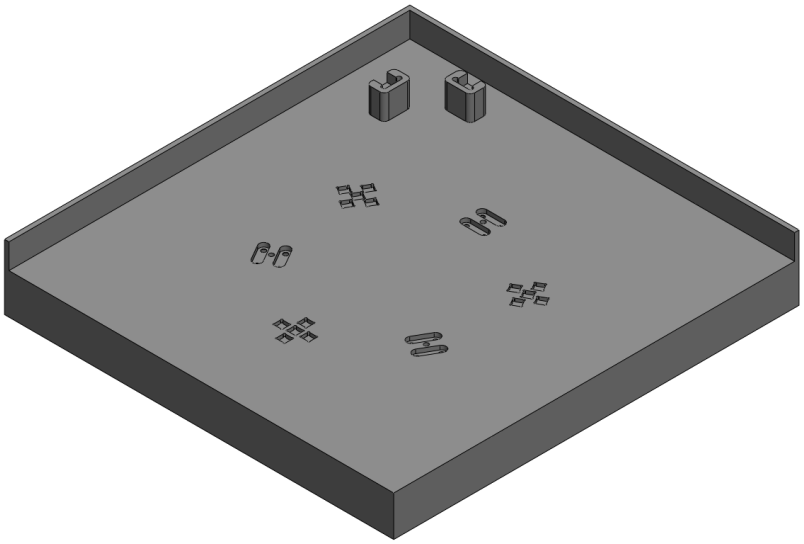

Figure 4.14: Top view of the rough design used in the semi optimization of the pocket shape.

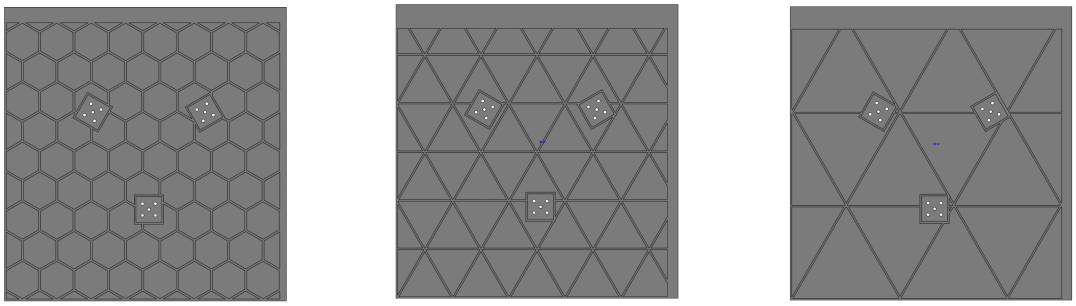

(a) (b) (c)

Figure 4.15: Various pocket shapes used in the semi optimization of the lightweight pattern.

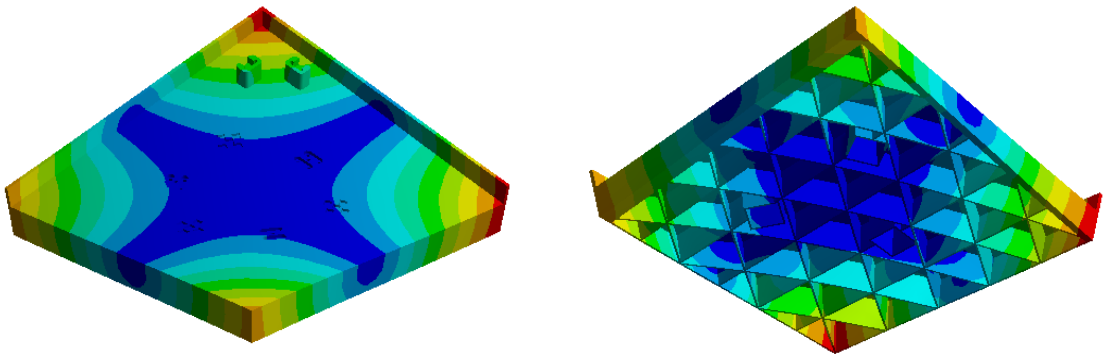

(a) Top view (b) Bottom view

Figure 4.16: Visualization of the first vibration mode.

Pocket shape	D(mm)	h(mm)	m(kg)	f_1(Hz)	$\frac{f_1}{m}$(Hz/kg)
Hexagonal	50	20	6.13	360	58.7
Hexagonal	50	40	7.80	443	56.8
Triangular	50	20	5.80	460	79.3
Triangular	50	40	7.30	823	112.7
Triangular	100	20	5.24	392	74.8
Triangular	100	40	6.12	652	106.5
Present chuck Alu.		40	9.25	420	45.4
Present chuck SiC		40	9.88	930	94.1

Table 4.6: Comparison of natural frequencies with variation of pocket size and shape of the lightweight pattern. The last two rows show the natural frequency of the present chuck in Aluminium and in SiC

4.7. Interface connections

4.7.1. Connection to the short stroke

Short stroke flexures

The chuck is connected to the short stroke via so called flexures. A figure of these flexures mounted on the short stroke can be found in figure 4.17. The flexures are designed to allow for manufacturing tolerances and thermal expansion of the chuck. By mounting the flexures under an angle of 120 degrees the displacements become deterministic under expansion and will create a thermal centre. The combination of the flexures should constrain the chuck exact in order not to induce stresses in the chuck that cause deformations. Each of the degrees of freedom (dof) should be stiffly constrained because low stiffness constraints can be excited causing low Eigen modes of the assembly.

Constraint analysis

The flexures consist out of a fixed body and 3 intermediate body's connected to each other by three notches. A free body has six degrees of freedom and a notch constrains one rotation. Notch 1 and notch 3 are relatively thin (0.7mm) compared to notch 2 (2mm). This means that the stiffness of some of the constraint directions of notch 1 and notch 3 are much lower than those of notch 3. Figure 4.19 shows the intuitive constraint analysis of notch 1 and 3. Figure 4.20 shows the analysis of notch 2. Due to the difference in stiffness of the constraints, 3 gradations can be assigned in the constraint analysis. The constraints can be divided into soft (green), medium (orange) and hard constraints (red). The soft constraint normally represents the degree of freedom. The hard constraint represents the constrained degree. The medium constraint is the constraint with relative low stiffness. Notch 2 is just a normal notch, it releases 1 dof and hard constrains the other 5 dofs. As can be seen in figure 4.19, due to the thin notch of 1 and 3 the y direction and z rotation become medium constraints. The result is that the hard constraints of this notch are equal to the hard constraints of a leaf spring.

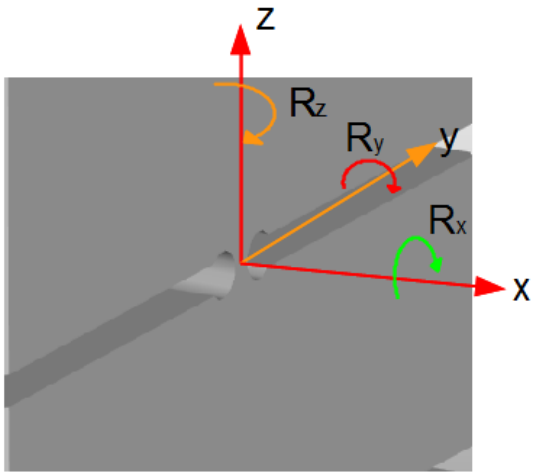

Figure 4.17: Constraint analysis notch 1 and 3

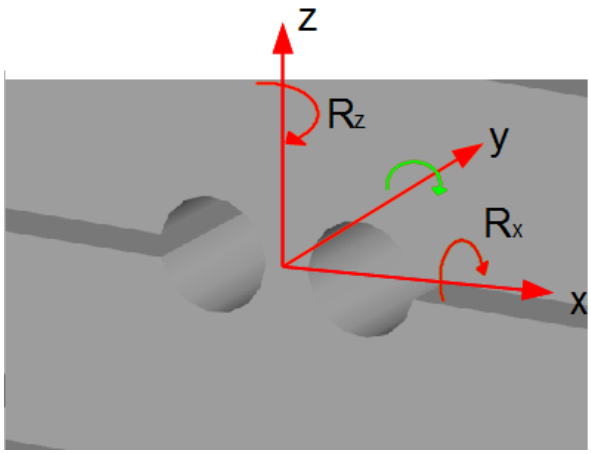

Figure 4.18: Constraint analysis notch 2

Figure 4.21 shows the constraint analysis of a full flexure. As can be seen in the figure, the degrees of freedom that are released in body 1 are the released degrees of the thin notch. Body 2 has an extra released degree due to the perpendicular notch on top of body2. Notch 1 does not release any more degrees. It only reduces the stiffness of the constraints. Wrapping up, the total flexure constrains 2 translations: x and z. The rotation about z and the translation in y are medium constraints and the rotations about x and y are free degrees.

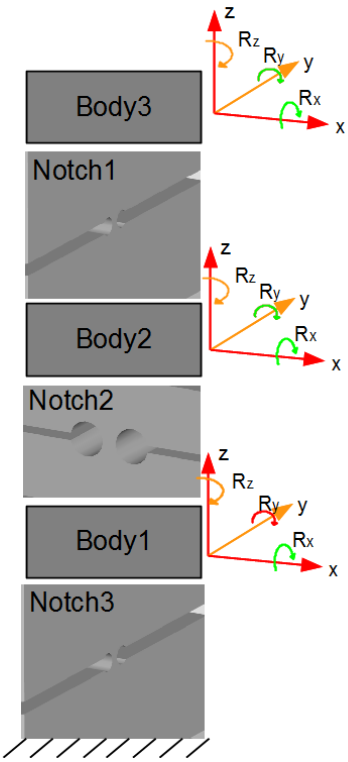

Figure 4.19: Intuitive constraint analysis of a flexure.

Figure 4.22 shows the positions of the flexures with the constraints that act on the chuck due to the flexures. As it can be seen from the figure, each flexure constrains the z translation of the chuck with a hard constraint. Because the flexures are not mounted in line, they also constrain the rotations about the x and y axis of the chuck. Furthermore, each flexure constrains a direction in the x-y plane with a hard constrain. This is the same kind of constraint in a kinematic mount, the constraints act perpendicular to the radial line through the centre and flexures. Because of this, the flexures constrain the rotation about the z axis and the translations in x and y direction. Considering the hard constraints, the chuck is exactly constrained. However, the medium constraints cause the chuck to be slightly over constrained. The medium stiffness can induce stresses in the chuck. The six medium constraints acting on the chuck over constrain the chuck by 6 times. A modal analysis can be performed on the chuck mounted on the flexures. The figures in figure 4.23 show the first three eigen modes of the chuck when it is mounted on the flexures. Since only the modes due to the flexures are of interest, the chuck has been modelled with an infinite stiffness. By doing this, the visible modes are only caused by the stiffness of the flexures. The first eigen mode can be found at f_1 =340Hz. It can clearly be seen that this mode is the rotational mode about the z axis. The second and third modes are the translational modes in the x and y direction, since the stiffness in both directions is equal (due to symmetry), the modes are at the same frequency: $f_2 = f_3 = 470Hz$.
The natural frequency of the rotational mode is relatively low. This low frequency implies a low stiffness of the constraints that should constrain the rotational motion of the chuck. This low stiffness can be addressed to notch 2. The notch should constrain the perpendicular translation (in figure 4.20 the x direction). However because of the low mode, the thickness of the notch (2mm) is not enough to gain enough stiffness in this direction causing the low rotational mode of the chuck. Therefore the x constraint in notch 2 can also be grouped with the medium constraints.

When the actual chuck is mounted onto the flexures, the stiffness that couples the flexures together becomes lower due to the finite stiffness of the chuck. Because of this, the real modes becomes even lower than calculated. The requirement on the chuck is that it has a first natural frequency higher than 400 Hz. This requirement becomes worthless because the rotational mode caused by the flexures is even lower. In order to raise the natural frequency of the assembly, the connection between the short stroke and the chuck should be redesigned.

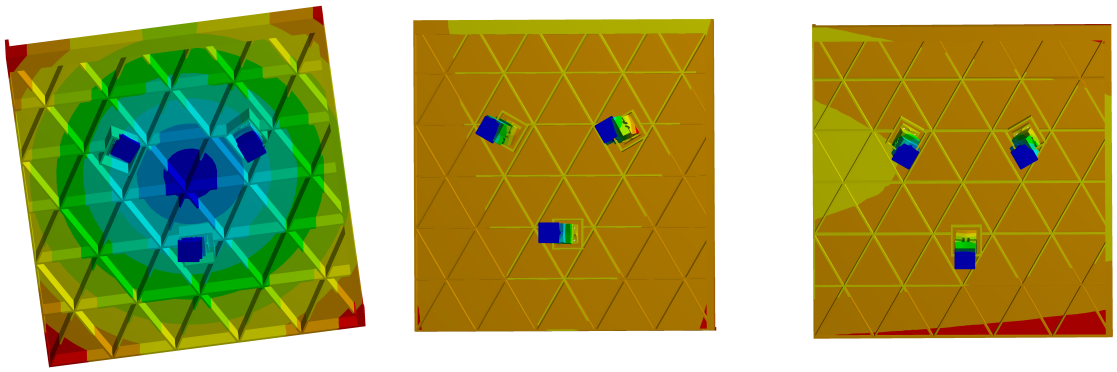

(a) Rz rotational mode @340Hz (b) X translation mode @470Hz (c) Y translation mode @470Hz

Figure 4.20: Bottom view of the first three modes of an infinitely stiff chuck mounted on the flexures.

Recommendation
A different way to mount the chuck to the short stroke is to makes use of three "bipods" as in a hexapod (figure 4.24). Each bipod consists of two rods (or flexure combinations that also constrain one dof). In this way each bipod constrains two directions. By mounting the bipods in a radial symmetric way, thermal expansion of the chuck will keep the thermal centre in the centre. By mounting the chuck with the bipods to the short stroke, the chuck will be exactly constrained relative to the short stroke.

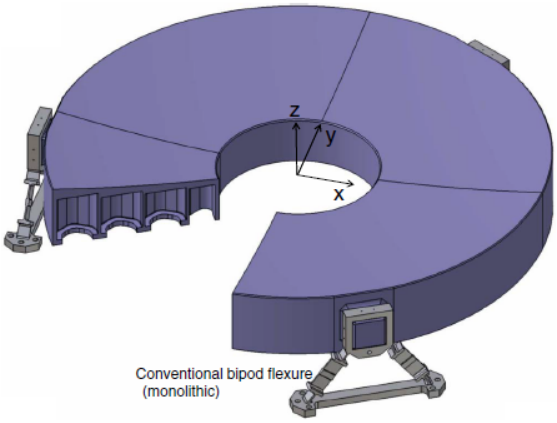

Figure 4.21: A mirror mounted with three bipod's. (source:[12])

4.7.2. Kinematic coupling of the wafer

In the design the v-groove islands of the kinematic mount are integrated in the SiC body as can be seen in figure 4.25. Temperature variations are the cause of expansion of the chuck. When the chuck expands, the position of the grooves relative to the kinematic centre changes. However the position of the balls relative to the centre of the wafer will stay at their position. Since the grooves move relative to the balls when the chuck expands, the expectation is that stick slip will occur at the interface. When stick slip occurs, the wafer table will move to a different position relative to the mirrors. Movements of the wafer table relative to the mirrors will cause a direct error in the position measurement, therefore stick slip is an undesired effect. Further investigation of the effect is necessary in order to check if the effect is present and if it is large enough to cause an error in the measurement. Stick slip will be investigated in the next chapter. The reason that this is not an issue in the present design is that the v grooves are mounted on a Zerodur platform that does not expand.

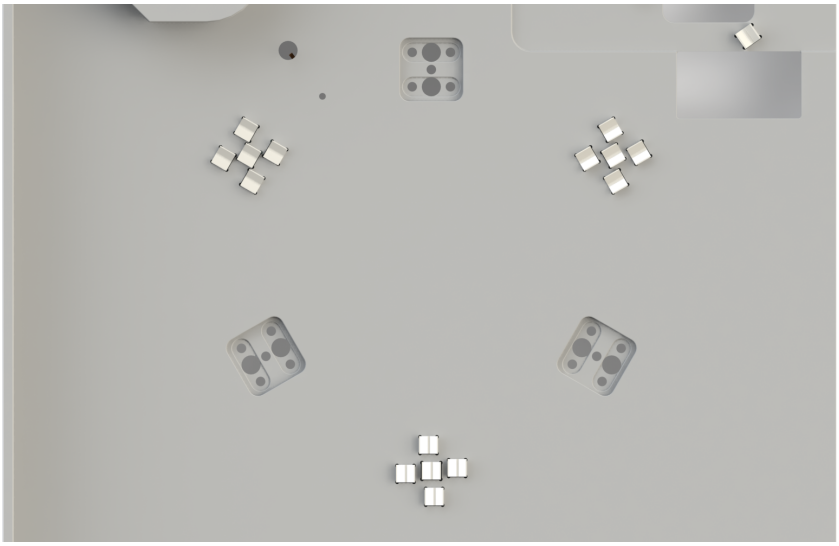

Figure 4.22: The 3 integrated v-groove islands and the 3 locations of the flexure connection.

4.8. Manufacturability

Zygo is a well known manufacturer in optical components. Conversations with Zygo showed that the requirements on the optical surfaces of the chuck could easily be met. However there are several concerns in the manufacturability of a SiC chuck that should be considered:

1. How close will the CTE of the CVD layer match the substrate? A mismatch might cause too large deflections of the mirrors.
2. How solid will the chuck be (no cracks etc.)?
3. Is the complete green phase carbon chuck converted into SiC?
4. Would post machining still be within the cost budget?
5. Is it possible to bolt components to the chuck with titanium bolts without causing defects?

These concerns should be taken into account when developing a prototype.

4.9. Final design

In the previous sections, the dimensioning of several aspects influencing the behaviour of the chuck has been performed. For instance the dimensioning of the pockets underneath the chuck. Next to the dimensioning with respect to the behaviour, a lot of the dimension requirements are on the geometrical properties of the chuck. These refer to the volume claim of the chuck, the positions of several plains with respect to the wafer plain and other special features. All features that have been dimensioned are:

1. Mirror length and height.
2. Pocket size of the lightweight pattern.
3. Holes for the flexure connections.
4. V grooves of the kinematic mount for the wafer table.
5. The volume claim.
6. The center of gravity is located at the right position. When all parts of the assembly have been mounted, the center of gravity should coincide with the center of the kinematic mount. The requirement on this is that the center of gravity of the assembly is within a maximum radius of 0.5mm from the center of the kinematic mount. Since the thickness of components made out of SiC is 5mm, the balancing have been done by adding extra ribs underneath the chuck as can be seen in figure 4.29.
7. The end of both mirrors is supported by a rib. This is done in order to prevent breakage of the mirror when something hits the back of the mirror. Breakage of SiC can occur rapidly due to the hardness of SiC.
8. The sides of the chuck have edges so that the chuck can be lifted holding the edges by a person. Otherwise the chuck could only be lifted by using the surface friction of the sides.
9. Initialization platform has been added with on top an electric conductive coating for the capacitive sensors used to measure the z position of the chuck.
10. Grounding interface for the wafer table.
11. V grooves of the Kinematic mounts for the beam measurement plate and knife edge plate.
12. Holes for the beam measurement plate, knife edge plate and Faraday cup.
13. Initialization mark interfaces.
14. A hexagon containing 6 pockets have been fitted between the flexure connections.

All correct dimensions have been brought together in the final design of the chuck. Renders of the final design can be found in figure 4.26-4.29. Some of the critical dimensions can be found in the 2D drawings in figure A.1 and A.2. The adaptations of the 'simple design' chuck as was used in the dynamic analysis result in a lower first mode. The first mode of the final design is at 613Hz which still is highly above the required 400Hz.

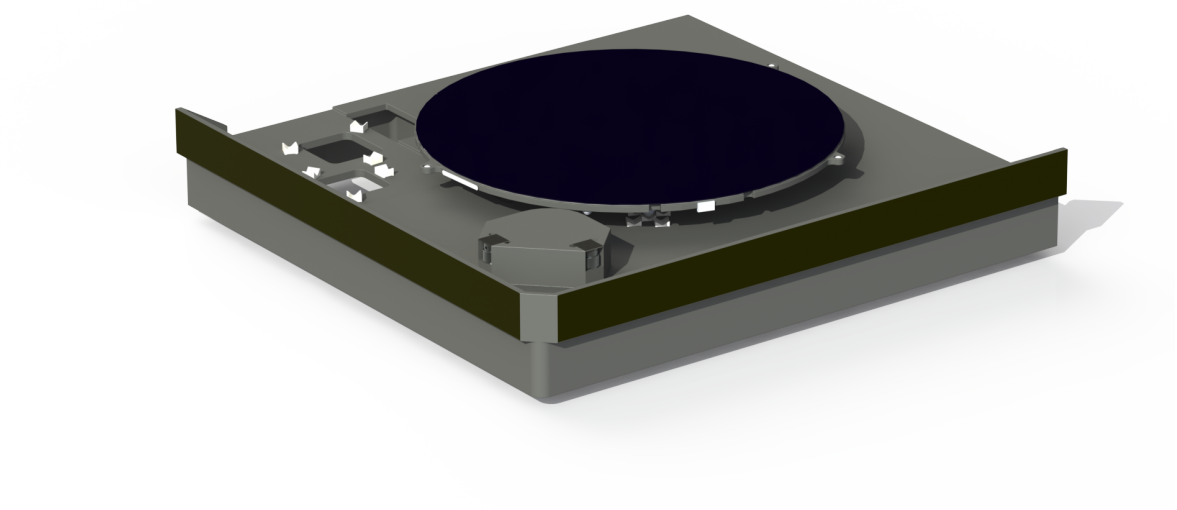

Figure 4.23: Final design of the chuck with a wafer table mounted on top of the v-grooves.

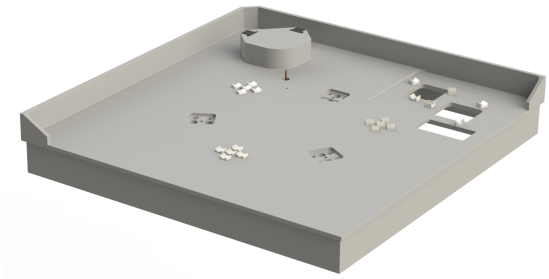

Figure 4.24: Top view from the back of the final chuck design.

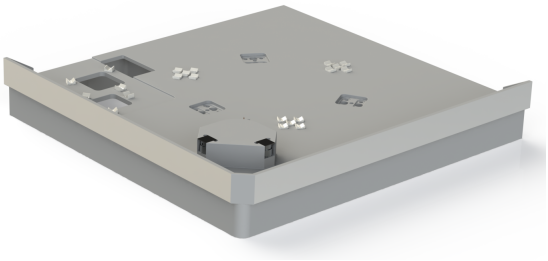

Figure 4.25: Frontal top view of the final chuck design.

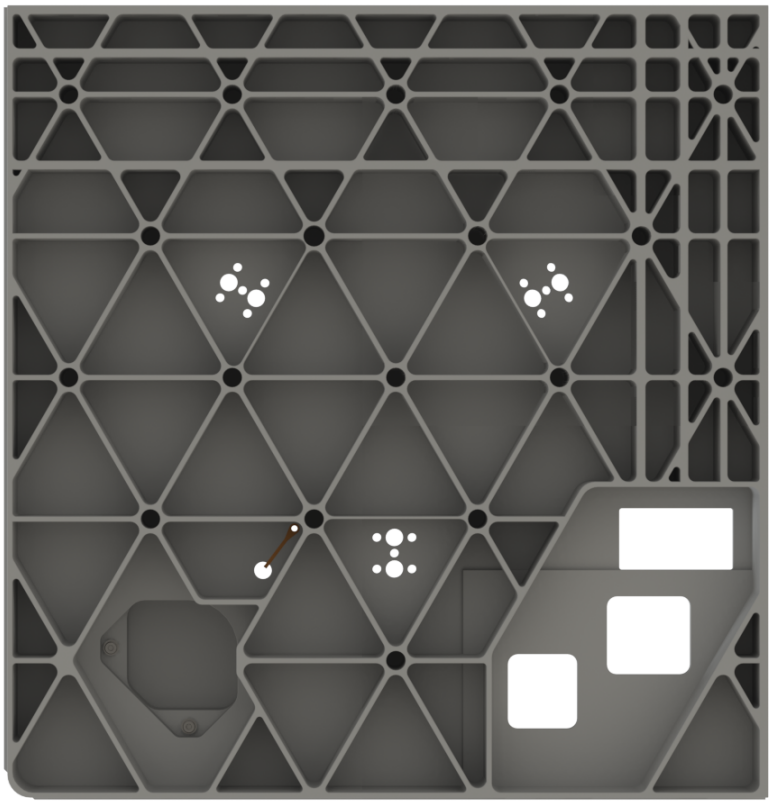

Figure 4.26: Bottom view of the lightweighted bottom of the final chuck design.

5

Stick slip

It is expected that stick slip occurs when v-grooves are integrated in the Silicon Carbide body of the chuck. The aim of this chapter is to give an answer to the question at which temperature variation this will occur. An answer to this question will be the answer to the question if an anti stick slip mechanism should be integrated or not. In the first part, an analytic model is derived to describe stick slip on kinematic mounts. The second part is dedicated to two measurements on stick slip effects. The third section provides for a recommended measurement set-up.

5.1. Analytical model

5.1.1. Stick slip behaviour

Stick slip is an effect that can occur when two parts in contact move relative to each other. A simple model that is often used to explain stick slip behaviour can be found in figure 5.1a. The square in the figure represents the ball of the kinematic coupling. The stiffness of the wafer table and the contact stiffness are represented by springs. The position of the groove changes due to thermal expansion. The change in position creates a force on the contact (loading of the contact spring in the model). Static friction is acting on the block with an equal but opposed force. As long as the static friction is below the maximum static friction, the contact force will be transfered to the body. Once the maximum static friction is reached, the contact spring will vanish and the block will slip in the direction of the static friction. While the grooves expand further, the effect will be repeated. The force displacement relation of the effect can be found in figure 5.1b.

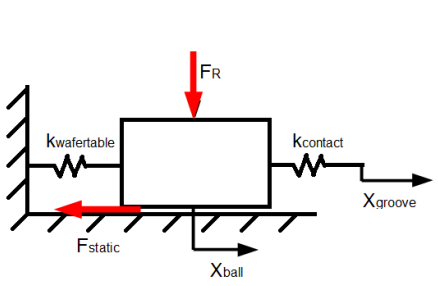

(a) Simplified stick slip model

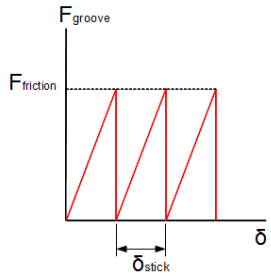

(b) Sketch of the relation between the relative displacement of the ball ($\delta = x_{\text{ball}} - x_{\text{initial}}$) and the force on the contact. The force loads the contact stiffness until a maximum force is reached, the ball will slip back and the force will drop to zero and starts loading again.

Figure 5.1: The stick slip effect

5.1.2. Stick slip on the kinematic mount of the wafer table

In a situation where the wafer table is placed on 3 v-grooves (figure 5.2), the contact stress is only due to the mass of the wafer table. It is assumed that in this situation no lateral forces (in the direction of the groove) have been build up (figure 5.3a). When heat flows into the chuck, the chuck will expand. The expansion of the chuck causes the grooves to move away from the thermal centre. The moving grooves load the elastic contacts between the balls and grooves. (figure 5.3b). At a certain expansion, the friction force of one of the grooves has been reached. At this instance the friction force cannot hold the contact force any longer and the ball will slip away (figure 5.3c). This does not happen all at once on each interface since the friction force of each groove varies slightly. The balls will find a new rest position on the groove according to the law of minimum of potential energy (5.3d). This position might be slightly different than the first position on which the wafer table was mounted on the grooves. Further heating of the chuck can make the other balls slip as well. Next to heating, cooling down of the chuck causes the same effect.

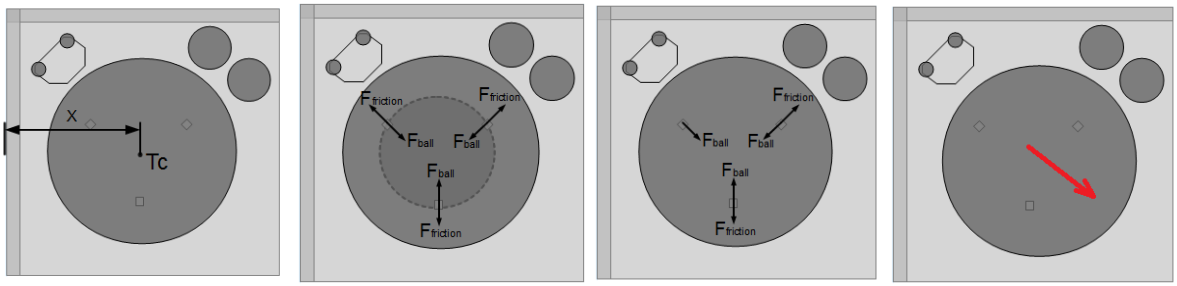

(a) Wafer table positioned on the three v grooves, there is no stress on the contact points.

(b) Heat flowing into the chuck will cause an expansion of the chuck. The circle through all grooves will grow in diameter and tension will be build up on the ball groove interface.(stick)

(c) At a certain expansion the static friction of one of the interfaces will become lower than the tension force of the interface. The energy of the interface will be released in kinetic energy and kinetic friction energy. (slip)

(d) The wafer table will move to a new position.

Figure 5.2: Stick slip on wafer table

5.1.3. Hertz contact

The linear behaviour between force and displacement of the contact force can be explained by considering the deformation of the contact. A ball placed on a flat will have a single point contact which is described by Hertz as the Hertz contact area. This is visualized in figure 5.4a. The equation that defines the hertz contact radius a on a single flat surface is given by equation 5.1 (according to [20]). When a load in the lateral x direction is applied, material will be pushed away. This is the cause of the lateral stiffness.

$$a = \left(\frac{3 F_{\mathrm{R}} R_{\mathrm{ball}}}{4 E_{\mathrm{eq.}}} \right)^{1/3} \tag{5.1}$$

With E_{eq}:

$$E_{\mathrm{eq}} = \left(\frac{1 - \upsilon^2_{\mathrm{groove}}}{E_{\mathrm{groove}}} + \frac{1 - \upsilon^2_{\mathrm{ball}}}{E_{\mathrm{ball}}} \right)^{-1} \tag{5.2}$$

5.1.4. Lateral stiffness

The lateral stiffness is related to the normal force on the wafer table via the hertz contact area. The net normal force on a single ball is simply a third of the total gravity force on the wafer table:

$$F_{\mathrm{N}} = \frac{m_{\mathrm{WT}} g}{3} \tag{5.3}$$

The resulting force on a single flat face of the v groove can be calculated with equation 5.4. φ is the angle of the v groove. The reason for the factor 6 to appear is that the normal force (which is divide over 3 balls) is

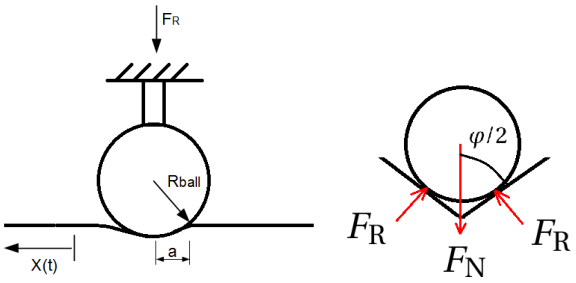

(a) Dramatization of the hertz deformation of a ball on a normal flat surface.

(b) Ball positioned on v-groove.

divided over two faces on the groove.

$$F_{\mathrm{R}} = \frac{m_{\mathrm{WT}} g}{6 sin(\varphi/2)} \tag{5.4}$$

With the resulting force, the hertz contact radius can be calculated. According to [20], the lateral stiffness can be calculated using the hertz contact radius and an equivalent shear constant (G_{eq}) with equation 5.5.

$$k_{\mathrm{lateral}} = 8 G_{\mathrm{eq.}} a \tag{5.5}$$

With G_{eq}:

$$G_{\mathrm{eq}} = \left(\frac{2 - \upsilon_{\mathrm{groove}}}{G_{\mathrm{groove}}} + \frac{2 - \upsilon_{\mathrm{ball}}}{G_{\mathrm{ball}}} \right)^{-1} \tag{5.6}$$

5.1.5. Maximum stick displacement

The relation between relative displacement between a ball and a single flat surface on the groove ($\delta = x_{\mathrm{groove}} - x_{\mathrm{ball}}$) and the force is given by equation 5.7.

$$F_{\mathrm{groove}} = k_{\mathrm{lateral}} \delta \tag{5.7}$$

The force will build up until the static friction has been reached(equation 5.8). When the static friction force has been reached, the friction will become lower (kinematic friction) and the ball will slip.

$$F_{\mathrm{friction}} = \mu F_{\mathrm{R}} \tag{5.8}$$

At the moment just before slip the following relation holds:

$$F_{\mathrm{friction}} = F_{\mathrm{groove}} = k_{\mathrm{lateral}} \delta_{\mathrm{stick}} \tag{5.9}$$

By rewriting equation 5.9, the total displacement before slip occurs can be found:

$$\delta_{\mathrm{stick}} = \frac{\mu F_{\mathrm{R}}}{k_{\mathrm{lateral}}} \tag{5.10}$$

The displacement of the groove is caused by thermal expansion of the chuck. Therefore, the maximum stick displacement can be related to temperature change of the chuck as in equation 5.11.

$$\delta_{\mathrm{stick}} = \alpha R \Delta T_{\mathrm{stick}} \tag{5.11}$$

With R the radius of the circle on which the grooves are mounted. Rewriting the previous equations gives the maximum temperature difference of the chuck related to the friction coefficient, the normal force, the thermal expansion, the radius of the kinematic mount and the lateral stiffness of the groove:

$$\Delta T_{\mathrm{stick}} = \frac{\mu F_{\mathrm{R}}}{\alpha R k_{\mathrm{lateral}}} \tag{5.12}$$

5.1.6. Analytic result

The v-grooves are made out of Zirconiumoxide and the balls are made out of Siliconnitride. The properties that belong to these materials can be found in table 5.1.The geometrical properties that belong to the interface can be found in table 5.2.

Constant	Size
E_{ball}	275 GPa
E_{groove}	200GPa
υ_{ball}	0.25
υ_{groove}	0.3
μ	0.2
α_{SiC}	$2.0 \cdot 10^{-}6$ m/mK

Table 5.1: Constants referring to the material properties of Zirconiumoxide and Siliconnitride.

Property	Size
m_{WT}	1.5 kg
φ	120°
R_{ball}	0.004 m
R_{mount}	0.11 m

Table 5.2: Properties of wafer table and kinematic interface.

With the previous parameters, the stick slip model can be used to calculate the stick displacement. The stick displacement together with other results of the analytical model can be found in table 5.3. From the results, it can be concluded that the ball will slip when the groove has been moved relative to the ball with 62nm. The temperature difference needed for such an expansion is about 0.283K. Since the temperature in the machine varies about 1K, it can be concluded from the analytical model that stick slip occurs.

Variable		Result
Resulting force on single face	F_{R}	2.831 N
Hertz contact radius	a	$4.074{\cdot}10^{-5}$
Single contact stiffness	k_{lateral}	$0.909 \cdot 10^{7}$ N/m
Friction force	F_{friction}	0.566 N
Stick displacement	δ_{stick}	$6.226 \cdot 10^{-8} m$
Maximum temperature difference	ΔTstick	0.283 K

Table 5.3: Properties of wafer table and kinematic interface.

5.2. Stick slip due to actuation of a ball on a v-groove

The analytical model showed that stick slip effects should be expected on the kinematic mount. To confirm this, an experiment can be performed to see if stick slip actually occurs on a v-groove - ball interface.

At the time writing stick slip measurements were also performed by a research group at the TU Delft. Measurements on the ball groove contact were also done on the set-up available at the TU Delft. In order to integrate the specific ball groove contact into the set-up, the set-up was slightly adjusted.

5.2.1. Method

Figure 5.4 shows the adjusted set-up. A ball is pressed into a messing ball holder and is aligned with a v groove which is glued onto the bottom of the frame. Actuation of the base is done by a voice coil and the position of the base is measured by an interferometer with a measurement error of about a nanometer. Guidance (and small alignment adjustment) is done by using ferromagnetic fluid and a magnet on a threaded rod. The ferro fluid forms a ring on the outside of the magnet and when in contact with a flat area air is trapped in the middle, this makes it a low friction guidance. To reduce over constraints to a minimum (zero is not possible due to instability) the base is guided by 5 of these ferro fluid rods.
The position of the base is controlled by a PID controller. The actuator exerts a force on the base in the free direction of the ball v groove combination. With this set-up force-displacement relations can be found which will be used to determine the maximum stick displacement, the contact stiffness and the friction force.

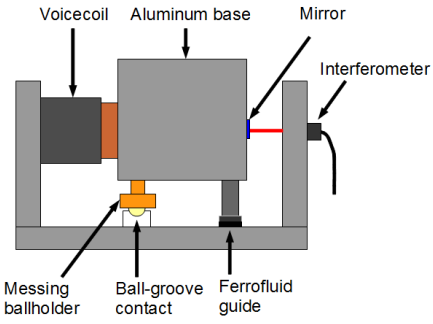

(a) Schematic overview of the retrofitted set-up

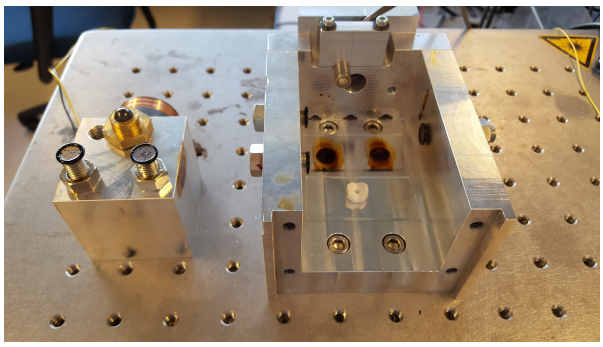

(b) Picture of the disassembled set-up as it was used in the experiment. On the left the slider block can be seen and on the right the base. Note that the front panel is removed.

Figure 5.3: Experimental setup as it was available at the TU Delft including the adjusted contacts.

A ramp force is exerted on the base. The force time ratio is kept low to reduce the effects of jerk on the ball groove interface. The force is controlled by the PID controller. The base is moved in both positive as negative direction to check if the measured effect is the same in both directions -which it should be- and no strange effects from the set-up interfere with the measurement. Measurements are performed 4 times in each direction.

5.2.2. Result

A positive direction measurement can be found in figure 5.5. The result can be divided into two sections: The first section is the part where the graph is near linear, this is when stick occurs. when the friction force has been reached, the position will strongly deviate from the linear line of the first section. In this second section, slip occurs. Multiple measurements have been performed (see Appendix). The graphs of some measurements show a less sharp transition. In these measurements slip occurs at a lower force. This might be caused by a lower friction coefficient due to for instance a contaminated surface. From the measurements, the stiffness can be calculated and the stick distance and friction force can be determined. The results are summarized in table 5.4. On average, the stick displacement is 0.8μm. This displacement relates to a temperature difference

of the chuck of 2.8K.

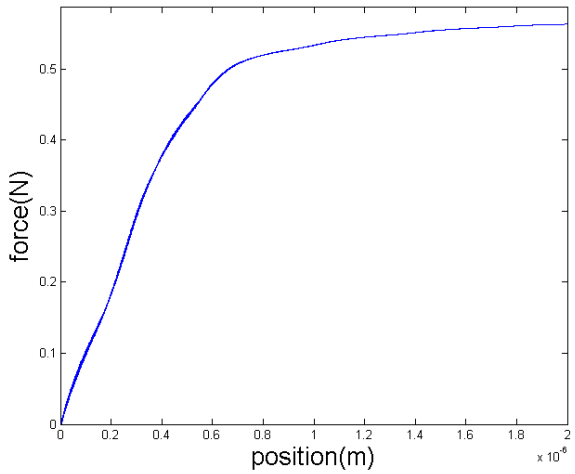

Figure 5.4: A typical measurement. The friction force is 0.5N. The force is reached after a 600nm stick traject. Further increasing the force causes slip of the ball.

Measurement	$k \cdot 10^6$ (N/m)	$x_{\text{stick}} \cdot 10^{-7}$(m)	F_{static}(N)
1	1	6	0.36
2	1.04	7	0.51
3	1.09	6	0.53
4	0.92	6	0.38
5	0.86	10	0.43
6	0.79	18	0.56
7	1.22	12	0.52
8	0.91	8	0.51
9	1.40		
10	1.40		
11	1.50		
12	1.50		
13	1.60		
14	1.60		
15	1.58		
16	1.42		

Table 5.4: Measurement 1-8 refer to stick slip measurements. Measurement 9-16 refer to the measurements of the set-up stiffness.

5.2.3. Discussion

From the results in table 5.4 a comparison can be made with the analytical model. It turns out that the measured contact stiffness is a order of 10 lower than the calculated contact stiffness. This means that slip will occur after a stick phase which is 10 times larger than calculated. The difference can be caused by three aspects:

- Wrong analytical model.
- Rotation of the base causing an Abbe error.
- The assumption that the rest off the set-up is infinitely stiff is not valid.

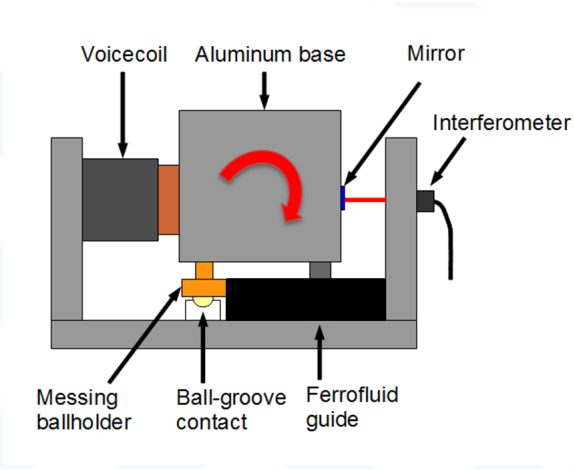

Figure 5.5: Expected parasitic motion (rotation) of the set-up.

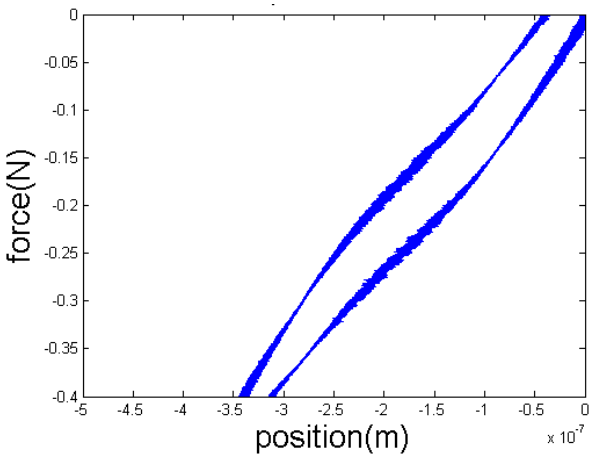

Figure 5.6: Measurement with a blocked ball. The force on the base is ramped up to 0.4N (top line in graph), therafter it is released back to zero force (bottom line). The difference in both paths is due to backlash and the sinusoidal effect is due to the non linearity of the interferometers. The undesired position variation can clearly be seen.

The set-up is considered to have infinite stiffness apart from the contact stiffness. In fact the set-up consist of parts that could not be assumed to have a infinite stiffness. The model can be found in figure 5.8. By mechanically locking the position of the ball, "parasitic stiffness" can be measured. This parasitic stiffness consists of stiffness of the guides, stiffness of the ground and stiffness of the base. The Abbe error caused by pressure on the z constraining guide rods is also covered by the parasitic stiffness. The Abbe error however is not a real stiffness itself but can be handled as if it is a stiffness.
A test have been performed in which the ball has been mechanically locked by blocking the holder as can be seen in figure 5.7. 8 measurements showed that the stiffness of the set-up measured is about $1.5 * 10^6$N/m. Using this parasitic stiffness and the measured stiffness (k_{eq}) from the stick slip measurement, the actual contact stiffness can be calculated by using equation 5.13.

Figure 5.7: Representative stiffness model of the first experimental set-up.

$$k_{\text{contact}} = \frac{k_{\text{parasitic}} k_{\text{eq}}}{k_{\text{parasitic}} - k_{\text{eq}}} \tag{5.13}$$

Using the data found in the experiments, the calculated contact stiffness is about $3 \cdot 10^6$.

5.2.4. Conclusion

In this experiment, only one single ball groove combination has been tested. In the actual situation, there are interactions between three ball groove contacts that are connected to each other via the wafer table. Performing a measurement on the real system would be favourable. Besides this, the measurement set-up does not seem to be accurate enough. A more realistic measurement should be performed.

5.3. Stick slip due to heating of a wafer table

Stick slip measurements on a single ball groove contact showed to be unreliable. Therefore it might be better to measure stick slip effects on a more realistic situation.

5.3.1. Method

In the concept, the grooves are integrated in the SiC body, heating of the chuck will cause the grooves to move. The wafer table is thermally conditioned. This means that the temperature will is kept constant and the wafer table does not expand. However, the balls might move due finite stiffness of the wafer table and the ball mount. In this experiment the function has been reversed: a SiC wafer table is mounted on the v grooves of a Zerodur platform. The Zerodur platform maintains the position of the grooves like the thermally conditioned wafer table does in the real situation. On top of the grooves of the Zerodur platform, a SiC Wafer table is mounted. In the experiment the wafer table will be heated by a lamp. This will give the same temperature/expansion ratio as in the SiC chuck. This means that the ball will move relative to the groove in the same way as in the real situation.

A lamp at a distance from the wafer table slowly heats the table up. The temperature is measured at different locations of the table using thermocouples. To measure the position of the wafer table, three clamps have been mounted on the Zerodur platform that hold three capacitive sensors. Three reference flags made out of aluminium are mounted underneath the wafer table. These are used by the capacitive sensors as the measurement positions. Each of the sensors measures in one direction of a groove, in this way the largest displacements are measured. These are the "free" directions for expansion. Since the range of the sensors is less than 2mm, the sensor and flags should be aligned carefully. The alignment has been done by making special tools (see figure 5.11 and 5.12) that consist out of a metal plate with square holes at the right locations. Pushing the sensor mount and the flags against the reference face on the tool and glueing the part to the platform will mount the flags and sensor mounts at the right position. In order to minimize the thermal expansion effects of the reference flags and the sensor mount, the locations of the glue dots are important. The flags are mounted by application of two glue dots on each of the sides of the flags. The glue dots on the reference flags compensate each other. In this way the nett displacement due to expansion of the glue dots and aluminium flag will be minimised. The glue dots on the cap mounts are applied in the plane of the sensor end. (figure 5.11). The sensors used are capacitive sensors made by Lion precision. The specific version has a rms resolution of 20 nm for a 2mm calibrated prope. Since the expected jumps are of the order of 100 nm, the resolution of the sensors should be sufficient. The capacitive sensors are connected to a driver box which is connected to the computer together with the driver for the thermocouples. A python script collects the data from the sensors. The script collects data for 0.01s at a frequency of 5Hz. Measurement frequency of the cap sensors is 500Hz. Therefore in this window of 0.01s, 5 data points of the cap sensor pass. These are averaged. Since the driver of the thermocouples is relatively slow, the frequency of 5 Hz can not be exceeded. An example of the data collection can be seen in figure 5.15. Note that the "zoomed in" data points are at a different time scale.

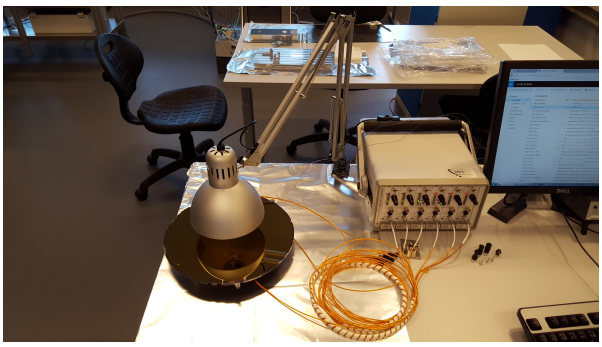

Figure 5.8: Experimental set-up overview.

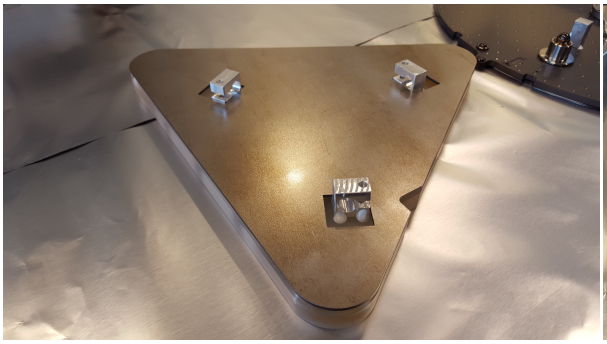

Figure 5.9: Assembly tool for the sensor mounts on top of the Zerodur platform.

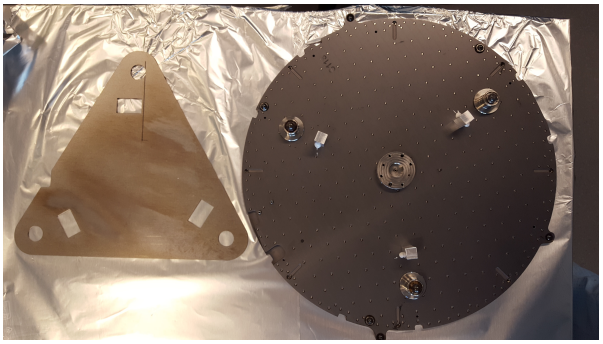

Figure 5.10: Left: Assembly tool for reference flags. Right: Wafer table with reference flags mounted for the capacitive sensors.

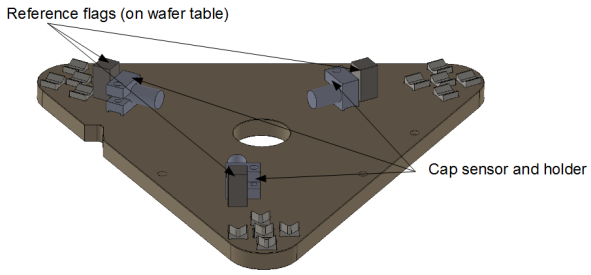

Figure 5.11: Zerodur platform with v grooves, sensor mounts and capacitive sensors.

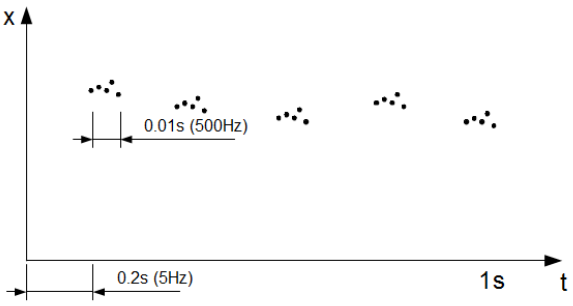

Figure 5.12: Data collection by the software used in the measurement.

5.3.2. Results

Figure 5.16 shows a typical measurement of the heating and cooling of a wafer table. The top graph of shows the position of the three reference flags under the wafer table (p1-p3). The red line is the expected position of the flags which has been calculated by using the measured temperature of the SiC at the position of the flag. The graph below gives the temperature of different locations of the setup. Temperature measurements have been performed on the aluminium reference flag, the glue dot connecting flag and wafer table and on the wafer table at the position of the flag.
A selection of special measurements can be found in appendix B.2. Some of the temperature measurements are on the temperature of the cap sensor clamp to see what the effect is on the position of the sensor. Note that the time scales vary since some measurements have been performed over a longer time period.

5.3.3. Discussion

A number of measurements have been performed (see appendix B.2). Some of these measurements indeed showed jumps. The jumps however did not occur consequently over the different measurements. In order to be able to repeat the measurements in which stick slip has been seen, many different measurements have

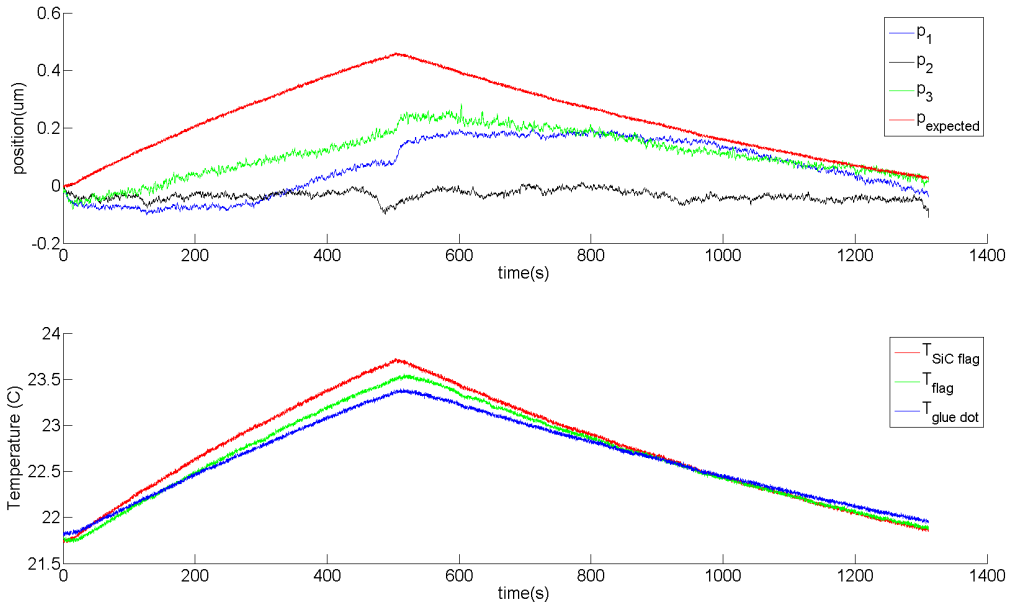

Figure 5.13: A typical measurment of the heating and cooling traject of a wafer table.

been performed in which parameters were adjusted in the hope to find the specific circumstances under which stick slip occurs. The parameters that have been varied are: Lamp-wafer table distance, grounding of reference flags, remounting the wafer table on the grooves, rotating the wafer table to make different ball groove contact, Duration of heating, starting temperature when heating. When jumps occurred none of the measurements could have been reproduced when the exact same circumstances were applied.

In the performed measurements, some remarkable effects were observed. Some of the effects can be observed in each measurement. Whereas other effects are only observed in a few measurements. The observed effects are:

- In some measurements: Jumps that occur asynchronously.
- In some measurements: Jumps that occur synchronously.
- In some measurements: Offset between positions implying a relative movement of the thermal centre.
- In each measurement: An abrupt position decrease when the lamp is turned on.
- In each measurement: An abrupt position increase when the lamp is turned off.

Jumps that occur asynchronously
Figure B.9 - B.11 shows some measurements in which jumps have been observed. The jumps occur randomly with different position changes. The graph of figure B.9 shows a single jump. In for instance the graph of figure B.10 multiple jumps can be seen whereas some measurements do not show jumps at all. No explanation have been found for this difference yet. However, calculations in the first section showed that jumps in the order of 100nm were likely to occur. It can be seen that the jumps are indeed in the 100nm. Because of this it is expected that the jumps are caused by stick slip.

Jumps that occur synchronously
Figure B.7 shows some jumps that occurred synchronously. The jumps are of the size of 100nm. Since the effect on the positions is near exact the same but opposite, the measurement is suspicious. The effect turns out to be reproducible by moving the lamp towards and from the wafer table surface. The effect that this movement has on the measurement can be found in figure 5.17. The effect is due to capacitance change measured by the sensors. This is due to the fact that initially the reference flags were ungrounded. Grounding the flags

reduced effect. This effect gives reason to conclude that in the measurements in which these jumps occurred, the lamp slightly changed position. This can be due to vibrations from the surrounding environment since the setup is not vibration isolated.

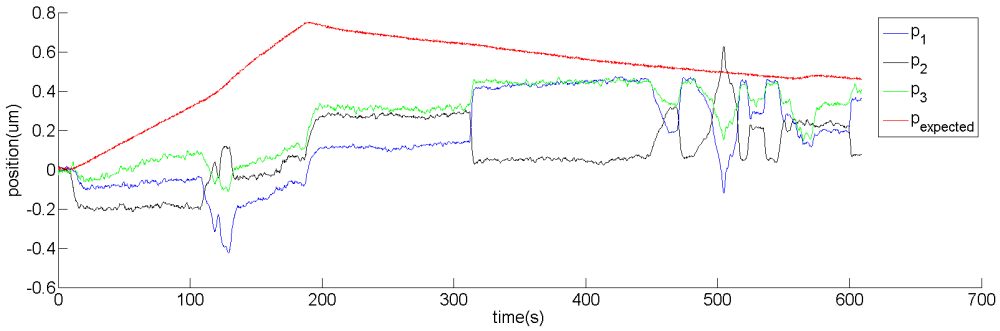

Figure 5.14: Effect of moving the lamp between 2cm and 40cm of the wafer table surface.

Offset between positions implying a relative movement of the thermal centre
Figure B.12 shows a measurement in which the chuck is heated 3K from the initial temperature and cooled back down to the initial temperature. The 3 positions do not return to their initial positions as is expected when the wafer table is cooled down to the initial temperature. This implies that the balls have been slipped over the groove.

Abrupt changes in relation to lamp on/off
Each of the measurements show the same effect when the lamp is turned on and when it is turned off. For instance at t=0s in figure B.9: The position of the flags seem to come closer to the cap sensors. Since the wafer table is heated, it should expand and therefore the flags should move away from the sensors. When the lamp is turned off at around t=180s, the reference flags quickly move away from the sensors which implies an expansion. Since the temperature change of the SiC could not account for such a large expansion where it in fact should contract, the problem might be heating and cooling of the flag and glue dot. Since both the flag and the glue dot have a high CTE of respectively 24μm/mK and 64μm/mK, the effect of thermal expansion of the glue dot and flag can not be neglected. Therefore a model has been made which can be seen in figure 5.18.

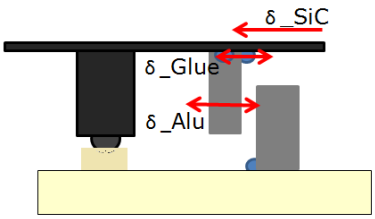

Figure 5.15: Representative expansion model of several parts of the second experimental set-up.

5.3.4. Conclusion

The advantage in this experiment is that the measurement set-up is a near one to one translation of the concept. The disadvantage in this set-up is that the relative position change between ball and groove is based on expansion of the wafer table. Heating causes undesired expansion of parts used to measure the position. Next to this, the heating is hard to control. Although the errors in the measurements, the conclusion can be drawn that stick slip effects are present. With the measurement performed however no conclusions can be made on how long the stick phase is and what the stiffness of the groove is.

5.4. Stick slip due to actuation of three v-grooves

The previous measurements seem to show stick slip effects. Unfortunately no conclusions can be made on how long the stick phase is. This information is necessary to say whether or not an anti stick slip mechanism should be integrated in the SiC chuck or not. Both measurement set-up's however did have advantages that could be used in a new measurement set-up: The advantage of the first experiment is that the movement of the ball is controlled by using a sensor, actuator and a PID controller. The advantage of the second experiment is that the measurement is performed on a real wafer table - groove set-up. Because of this, the stiffness of the set-up does not influence the effect. This section provides a recommendation on a third set-up that combines the advantages and gathered knowledge from both performed experiments.

5.4.1. Method

Figure 5.19 and 5.20 show the design of the recommended set-up. In this set-up, the grooves are mounted on a stage that has 1 dof. The stage consists out of an aluminium groove support connected by four leaf springs to a large aluminium base block. The four leaf springs over constrain the support of the v groove. The idea here is that only small movements in the order of 1 μm have to be made (see [13] for a test of this principle). The components should be made monolithic to minimize manufacturing tolerances. The position of each support is measured by a capacitive sensor which is mounted in a clamp. The sensor together with a voice coil and a PID controller are used to control the movement of the support. This could be interchanged with a piezo actuator an feed forward controller if desired. Measuring the support directly gives a very accurate measurement of the position of the groove. A wafer table is positioned on top of the grooves. Underneath the wafer table, 3 flags are mounted that are used as a reference for three different capacitive sensors that are mounted on top of the aluminium base block. These sensors are only used to measure the position of the wafer table.

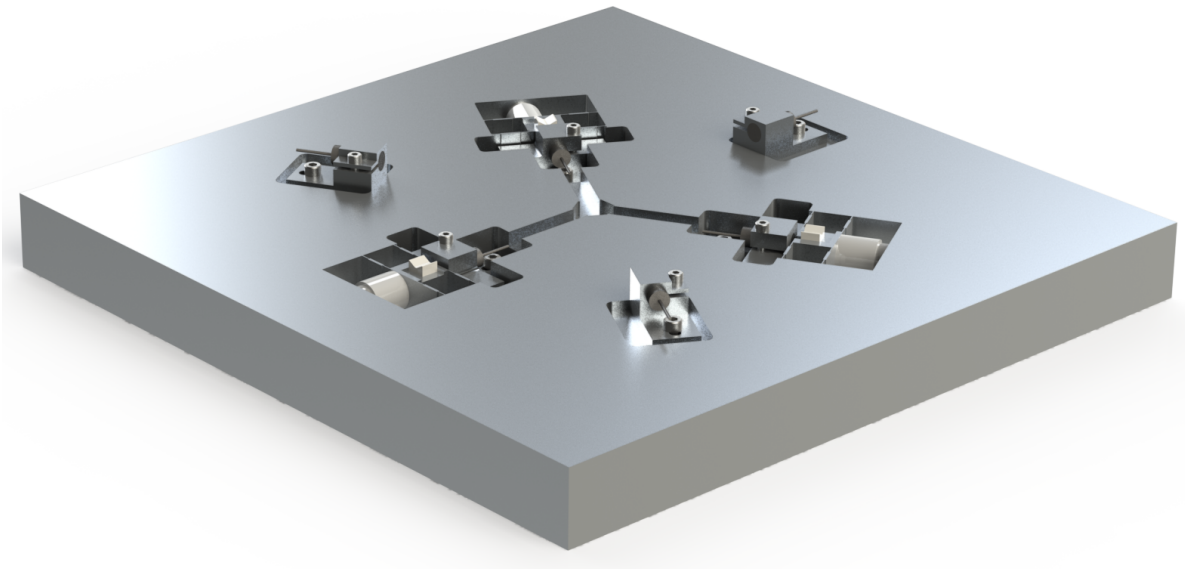

Figure 5.16: The set-up recommended for more reliable results in stick slip measurments on a kinematic mount.

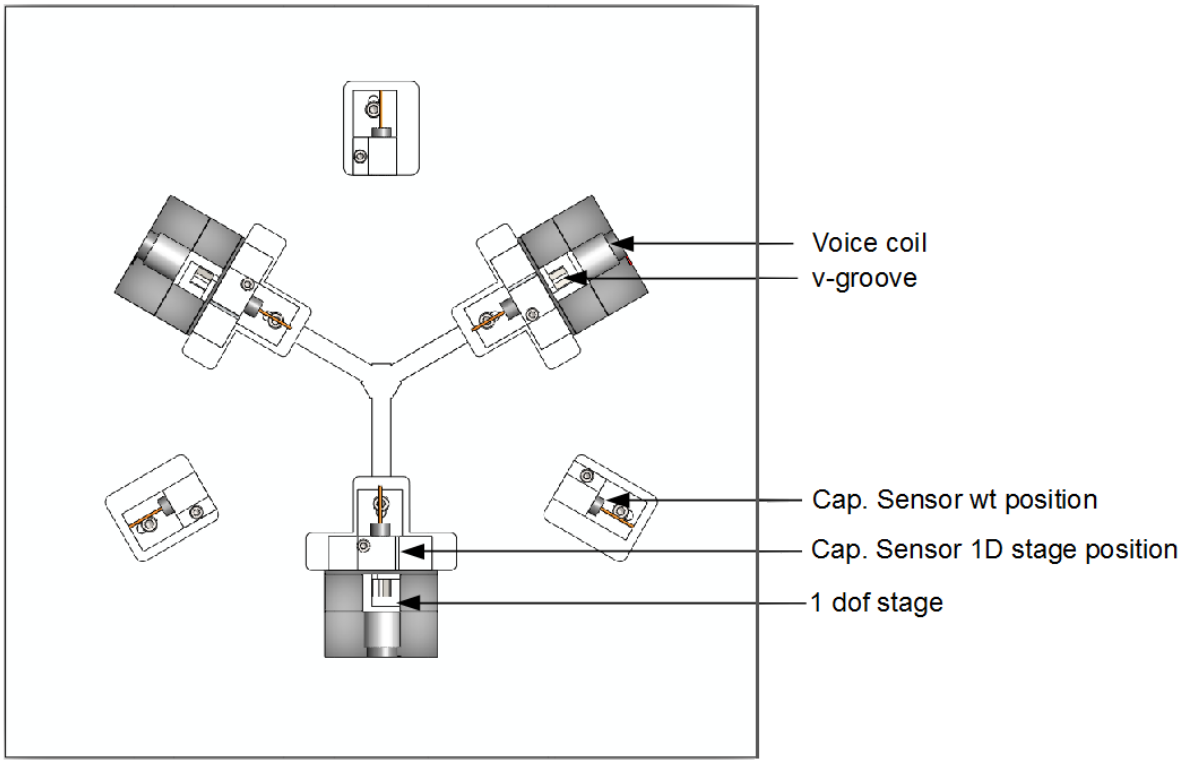

Figure 5.17: Top view of the recommended set-up

6 Verification

From calculations, simulations and manufacturer promises, one can not conclude whether or not a physical embodiment of the chuck would really meet the requirements or not. To be sure that it does, the performance of the chuck should be verified. As mentioned in chapter two, the performance of the chuck can be measured by measuring the properties of the chuck that relate to the critical requirements. The first part of this chapter is devoted to the properties that should be measured. The second part shows set-up's that are able to measure these properties.

6.1. Measurand

The properties that should be measured are called measurands. The measurands that need to be determined in order to verify the requirements are:

- Thermal expansion: The drift of the thermal centre of the wafer table relative from the mirrors of the chuck.
- Optical quality: The shape of the mirrors on a nanometre scale.
- Alignment: The angles between the mirror planes.
- Long term stability: The shape stability of the mirror planes over a long period.
- Dynamic behaviour: The natural frequency of the system and of the chuck.
- Stick slip effect: The position stability of the wafer with respect to the mirror planes under a thermal load.

6.2. Measurement set-up

The measurands of the previous section can be checked using the following three verification set-up's:

- The best way to measure the optical shape is by using a 3D optical surface profiler since they can be used to measure nanometre roughness. (See comparison of figure 6.1). In an optical profiler, the chuck is fixed onto a frame. The optical profiler travels over the surface of the chuck. Light is reflected from the surface of the mirrors on the chuck. At the profiler, an interference pattern will be created which is analysed by software. This results in a surface map of the mirror. With this map, the roughness, form and waviness of the mirrors can be determined.

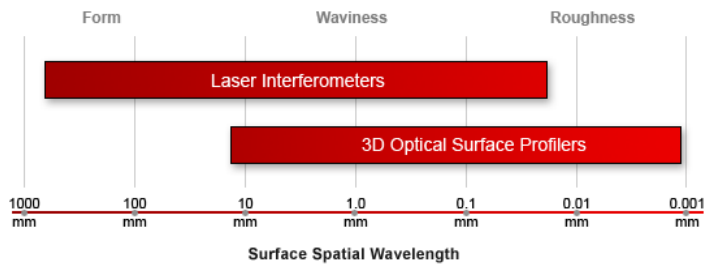

Figure 6.1: A comparison of the methods used to measure surface shape of mirrors. source: www.zygo.com

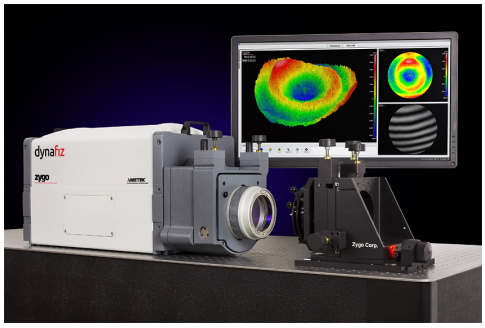

Figure 6.2: A 3D optical surface profiler.

- The dynamic behaviour of the chuck could be tested by performing an modal analysis. Accelerometers should be mounted to the chuck at different locations. An impulse should be applied to the chuck in order for the chuck to vibrate in it's natural frequency. The analysis should be performed on a chuck mounted to the flexures of the short stroke. The free vibration mode of the chuck could be determined by suspending the chuck with a cord to a frame and again performing the analysis.
- The remaining measurands could all be measured by using the interferometer system of the machine (see figure 6.4). 3 bundles are reflected on each mirror plane of the chuck. One of these surfaces together with the 3 bundles is shown in figure 6.3. With beam 1 and 2, the angle of the surface about z can be measured. 2 and 3 together can be used to measure the rotation about x. All of the bundles together are used to measure the distance in y direction between the interferometer and the mirror plane. In the machine 4 of these bundle groups are present. A wafer table with an L-bar mirror on top of it with a very well known geometry should be mounted on top of the v grooves of the chuck. By doing so, a differential measurement could be performed between chuck mirrors and wafer.

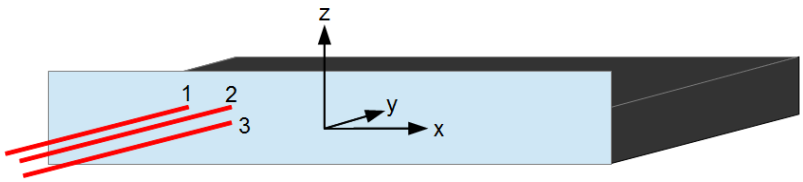

Figure 6.3: Single mirror plane with 3 interferometer bundles.

1. Thermal expansion could easily be measured by measuring the distance to the chuck and the distance to the wafer table from the interferometers. Drift will be the cause of an increase of relative distance. By using thermocouples, the temperature could also be measured. The thermal conditions (1K fluctuation) could be imitated by a heat sticker mounted onto the chuck.
2. The alignment could be measured by using the angular information of each of the bundle groups. In order to do so, the accuracy of the angle between the interferometers should also be considered.
3. Long term stability could be measured by performing a mirror map several times over a longer period.
4. Stick slip could be measured by using the information of the differential measurement of the wafer table and the chuck. Jumps in the relative position will indicate if stick slip is present.

Results of this verification should be compared with the requirements and with the properties of the present chuck. With this comparison one can evaluate the real performance of a SiC chuck using the evaluation rates of chapter 2.

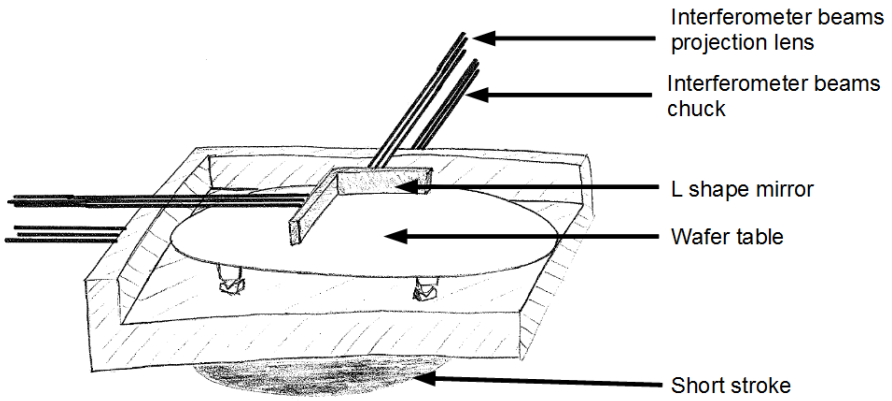

Figure 6.4: Verification set-up of four of the bottlenecks. The interferometers in this set-up are already present in the machine. The only addition is a wafer with a mirror L-bar.

7 Discussion

Analysis of the problem show that the optical performance of the present chuck is bad. In order to improve the optical performance of the chuck, Mapper wanted to find a way to mount glass mirrors to the chuck without worsening the performance of the chuck. This was the initial assignment of this thesis. In the problem analysis it became clear that Mapper did not specifically had to mount glass mirrors to the chuck. Next to the optical performance of the chuck, the dynamic behaviour and long term stability of the chuck are also below the desired performance. The new assignment was to make a new design of the chuck that should have mirrors with a lower surface roughness. In the redesign, dynamic behaviour should have been improved. Next to this, it is a desire to have a chuck that is assembled more easily.

Evaluation of the performance of the function of the chuck could be done by evaluating the performance of each of the functional requirements of the chuck. However, by evaluating the performance in this way, multiple other aspects are overlooked. Therefore the performance of the chuck is evaluated based on the performance on each of the eight bottlenecks. This section treats the reader with a discussion and the results on each of these bottlenecks for a SiC chuck.

7.1. Material selection

The selection of SiC as a material for the chuck seems to be optimal. The dynamic and thermal properties of SiC are great. Besides this, SiC CVD mirrors can obtain sub nano meter roughness.

7.2. Thermal expansion

The requirement on thermal drift is that the centre of the kinematic mount should not drift more than 0.5nm in 30 seconds away from the mirrors. If the thermal drift will stay below this figure is calculated with a simple thermal model. This model assumes that the only heat transfer is by radiation from an environmental temperature difference of 1K. The calculated drift with this simplified model is below the 0.5nm requirement. The assumption that the only heat transfer is due to radiation might however be over simplified. First of all the temperature difference is expected to be smaller than the assumed 1K. This will cause a lower temperature rate than calculated. In contrast to this, the thermally controlled short stroke might introduce a heat flow which is not negligible. This would increase the temperature rate again. A more advanced thermal model could be used to find a more accurate temperature variation of the chuck.

7.3. Optical quality

The requirements on the roughness and flatness of the mirrors of the chuck could easily be met. Critical however might be the bi-material bending of the mirrors. Calculations show that when the CTE of the CVD layer is off by 0.2μm/mK, the maximum deflection of the mirrors due to the bi-material bending effect might be in the order of 100nm for a temperature change of 1K. This is beyond the requirement on the shape change. This calculation however is simplified, the calculation has been done on a simple free floating beam. The mirrors of the chuck are connected to the body of the chuck and is supported on both ends. The actual bending might therefore be lower but notion should be taken of the fact that bi material bending will be

present if the CTE of the CVD layer does not match the CTE of the chuck body. The properties of SiC are however slightly tunable (see [18]) to the desired CTE.

7.4. Alignment

The mirror edges on the present aluminium chuck are machined within the requirements of the alignment. With this in mind, it is assumed that manufacturing companies are able to machine surfaces in SiC accurate enough. This makes it unnecessary to integrate an alignment mechanism for the mirrors. The problem with SiC however is that machining in the green phase can be done easily but machining of a sintered body becomes difficult due to the hardness of the sintered material. Since the body shrinks about 20 percent, it is expected that the surfaces should undertake a lot of post machining. This might drive the costs.

7.5. Long term stability

Little is known in literature on the long term stability of SiC mirrors. Therefore the long term stability should be measured. One can think of a measurement set-up in which a sample chuck is made containing at least a short piece of a mirror and a light weighted base. Preferably, the size of this test chuck is the same as the actual chuck. The accuracies demanded in the actual chuck that drive the costs however, are not necessary. Measuring the position of fixed points on the mirror multiple times over a long period will give the desired information on long term stability. Integrating three v grooves makes it possible to measure more than only the long term stability of the chuck.

7.6. Dynamic behaviour

Modal analysis of the present chuck have shown that the natural frequency is near 300 Hz in the open back situation. When a plate is mounted on the bottom of the chuck, the natural frequency is near 350Hz. The modal analysis on the SiC chuck showed that a natural frequency higher than 400Hz can easily be obtained, even with an open back design. The benefit of an open back design is that the assembly becomes more easy and the chuck becomes lighter. The weight of the assembly is near 8kg. This is about 4kg lighter than the present chuck which is of interest in the control of the system. A lighter chuck could be moved with a higher control accuracy.

7.7. Interface connections

7.7.1. Kinematic mount

In order to couple the wafer table to the chuck, a kinematic mount is integrated in the SiC body. It is suspected that stick slip occurs on the interface of the ball and v-groove of this mount. An analytic model showed that the position of a groove could move over about 60nm prior to slip of the ball. This coincides with a temperature rise of the chuck of 0.3K. In the first experiment performed, the ball sticks to the surface of the groove 500nm before slip occurs. It is assumed that the measurement set-up was not stiff enough and therefore a too large stick phase has been measured. In the second experiment which is more equal to the real situation, a number of strange effects have been noticed. Some of the effects seem to be due to stick slip. Since error effects also occur, a third measurement set-up has been proposed. In this experiment, the positive aspects of both measurements has been combined. The first experiment has the benefit of a controlled way to move a groove without introducing undesired expansion as was the case in the second experiment. The benefit of the second experiment is that it is more equal to the real situation because a real wafer table is used. Furthermore no angular effects that influence the measurement will occur. Although this measurement set-up seems to be more reliable, the resolution of the sensors makes it possible not to see stick slip occur. Therefore, it might be considered to measure the position with interferometers in the new set-up.

7.7.2. Coupling of the chuck to the short stroke

A modal analysis on the chuck mounted on the short stroke flexures has been performed. The analysis shows that when the chuck is modelled as an infinitely stiff component, the resulting natural frequency of the system becomes 360Hz. This results in a rotational mode on the flexures. This means that when the natural frequency of the chuck is higher than 400Hz, the system will still have a rotational mode lower than 360Hz. The flexures are a weak link within this system. In order to increase the natural frequency of the system, the coupling with the short stroke should be redesigned. preferably by 6 rods in a 3 v beam configuration.

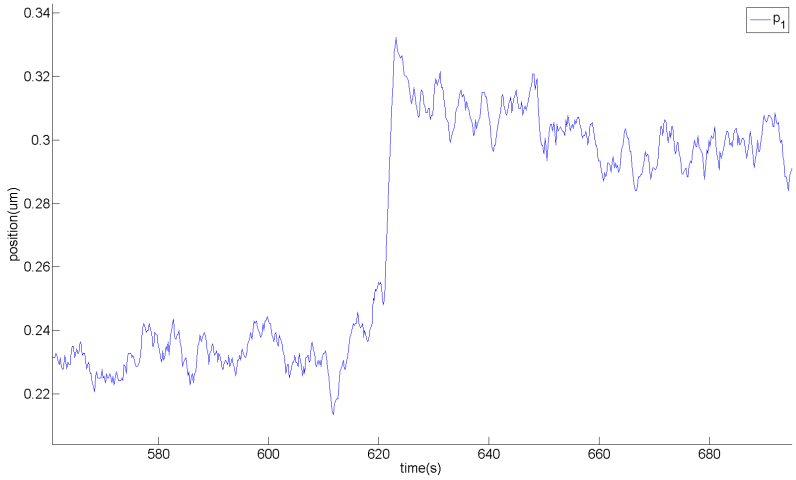

Figure 7.1: The effect of stick slip?

7.8. Manufacturability

As a manufacturing company, Zygo has been selected since they can both manufacture SiC components as they are an established manufacturer of optical surfaces. Zygo makes use of the conversion method for SiC. This means that components are constraint by a maximum thickness. Furthermore shrinkage is an issue. Because of this it might eventually be cheaper to select an other company to produce the SiC body with an other method that is not constrained by a maximum thickness and shrinkage of parts.

7.9. Other promising concept

The concept design resulted in 9 concepts. Next to the monolithic SiC chuck, glass mirror bars mounted by a kinematic mount on a SiC body seems to be a good idea as well. A benefit of glass mirrors is the low price. A disadvantage of such a solution is that the chuck involves more alignment steps and becomes more complex. Although companies do not share their prices very easily, it is expected that making CVD mirrors is expensive. When prices are available it should be considered if the simple monolithic chuck is worth the price difference with respect to the more complex glass mirror bars on a SiC body.

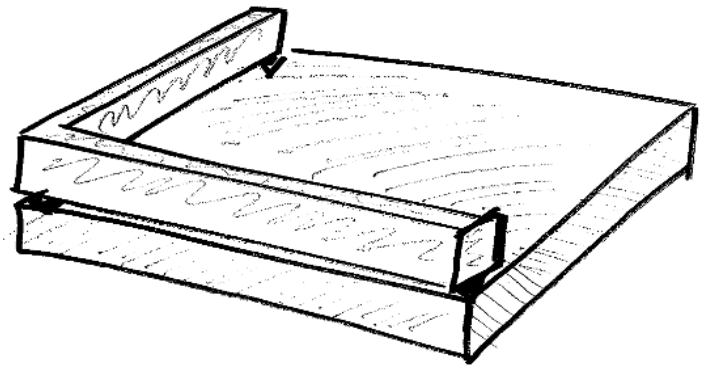

Figure 7.2: The concept of a glass L bar mounted via a kinematic mount to a SiC body might be promising as well.

8

Conclusion

This design project has been performed with the aim of improving the accuracy of the chuck. Over the course of this project the following original contributions to knowledge have been found:

1. An overview of bottlenecks causing inaccuracy in a high performance non collocated measurement system using interferometers.
2. A conceptual framework that can be used to develop concepts for measurement bases used in high performance non collocated measurements.
3. The detailed design of a high performance Silicon Carbide chuck.
4. An analytic model of stick slip behaviour on a (maxwell) kinematic mount.
5. The proposal of an improved method to measure stick slip effects on a kinematic mount.

This chapter provides the conclusions that can be drawn from the performed work. It is discussed according to the found contributions.

8.1. Inaccuracy analysis

The chapter on problem analysis provides an overview of the inaccuracy bottlenecks in a non collocated position measurement system that makes use of interferometers. This overview could be used in the inaccuracy analysis in a concept development/detailed design phase or in an actual design of a high performance measurement system. Based on each of the bottlenecks, requirements should be assigned. The idea is that all the requirements together should result in a maximum total position error that is below the desired overlay error of the system. With the presented evaluation procedure, the performance of a design could be evaluated. This results in an overview of the factors on which a design should be improved.
The presented problem analysis also provides insight in the accuracy limitations of the present chuck. The analysis showed that the optical quality of the present chuck is a main inaccuracy factor. This is the result of the relatively high surface roughness of the mirrors (>9nm) and the random artifacts on the mirror surface due to fly cutting. Another factor pushing the inaccuracy of the chuck is the low natural frequency of the chuck. The first mode of the present chuck is about 360Hz. The target on the natural frequency is above 400Hz. Next to this, the flexures turn out to be a limitation in the natural frequency of the stage. The flexures cause a first dynamic mode that is even below the 360Hz. The performance on long term stability of the chuck does not meet the target either. This is due to thermal effects in the mirror or in the rest of the system. This is another reason for a redesign of the chuck.

8.2. Conceptual design framework

The conceptual design framework consists of three paths that are combined at the end to form a concept. Each path is related to a particular functional requirement. The functional requirements of the chuck are: mount the mirrors, align the mirrors and maintain distance and orientation between mirrors and kinematic

mount. Based on the strategies that have been found for each function, solutions can be found. These solutions can be evaluated based on the given criteria. An evaluation procedure has been presented to select the most promising concept.
The most promising solution for mounting the mirrors is to coat the mirrors to a base. Due to homogeneity and the ability of use of low CTE materials, thermal deformations and assembly deformations are expected to be lower than in other solutions that are based on mounting separate mirrors. For the alignment of the mirrors a monolithic chuck seems to be optimal. Alignment by machining and polishing seems to easily meet the target. The most promising solution in maintaining the position and orientation of the wafer seems to be the use of a low CTE material body. Low CTE material is preferred prior to zero CTE material because of it's excellent dynamic properties of the material.
With the solutions, 9 concepts have been developed. The concept of a low CTE monolithic chuck with coated mirrors turns out to be the most promising solution when evaluated on it's criteria. No wonder: it is composed out of each most promising solution. However the monolithic low CTE chuck with coated mirrors seems to be optimal, two other promising concepts have been found. These concepts are based on the mounting of an L-bar mirror to a low CTE base. These concepts could be considered when the production of a monolithic coated chuck turns out to be too expensive.
Based on the criteria, it is expected that the concept of mounting glass mirrors to a aluminium chuck by using glue will reduce the performance of the chuck. This is due to the expected low long term stability, bad thermal behaviour and complexity of the concept.

8.3. Detailed design of a SiC chuck

Silicon carbide has been selected as the optimal material for a chuck because it possesses excellent figures of merit. Especially the high specific stiffness ($\frac{E}{\rho}$) and steady state thermal distortion ($\frac{k}{\alpha}$) are beneficial. This is because they will result in respectively excellent dynamic and thermal behaviour.
A thermal model has been developed in order to calculate the thermal drift of a wafer table thermal centre mounted on a SiC chuck. With the thermal model, a heat input of 0.23W has been calculated. This heat input will result in a thermal drift of 0.5nm/30s. This is within the requirements. Although this calculation is not based on a very accurate thermal model, it can be concluded that a SiC chuck is thermally feasible since the order of magnitude is near the target.
The mirrors in the concept are polished into a SiC CVD layer that is deposited on a SiC base. A theoretical study showed that sub nanometer roughness could be achieved in a SiC CVD layer. Since the target is 1nm, it could be concluded that this target will be met. Considering this concept special attention should be paid to bi-material bending. A test mirror bar with the desired geometric dimensions resulted in excessive bending in the order of 100nm. This occurs when the CTE mismatch of the CVD layer is in the order of 0.1 μm/mK. This bending effect is limited in the design by the way it is supported. However, deformations due to this effect should be expected. This can be reduced by matching the CTE of the CVD layer precisely with the CTE of the base.
A semi optimization of lightweight patterns shows that triangular pockets used to create a lightweight design will result in better dynamic properties than hexagonal pockets. More specifically, pockets in the order of 50mm width will result in a much higher stiffness than pockets with a width of 100mm. This conclusion can be drawn by inspecting the performance figure $\frac{f_1}{m}$. This figure for triangular pockets is twice as high as the figure for hexagonal pockets. FEM calculations show that the final design with 50mm triangular pockets possesses a natural frequency of 615Hz.
A constraint analysis has been performed based on the difference in stiffness of each of the constraints of a flexure. The result of the analysis is that the flexures constrain the chuck exact but the constraints that should constrain the rotation of the chuck possess a low stiffness. This is the cause of a limitation of the natural frequency of the stage assembly. The natural frequency will never exceed 360Hz due to this fact. An alternative mounting method has been proposed that should increase the natural frequency. In this method the chuck is mounted via 6 rods to the short stroke like in a hexapod.

8.4. Analytic stick slip model

An analytic model has been derived that predicts that stick slip will occur at the interface of the chuck with the wafer table. This is the interface of a kinematic mount that consists out of 3 balls and 3 v-grooves. With this model a contact stiffness of $0.9 \cdot 10^7$N/m is found. The static friction is calculated to be 0.57N. With this result it is found that the ball will stick to the groove over a displacement of 60 nm. A larger displacement will

cause the ball to slip. The calculated maximum displacement will be achieved when a SiC chuck changes by 0.3K in temperature.

8.5. Improved stick slip measurement set-up

Two experiments have been performed in order to verify the analytic results of the stick slip model. In the first experiment, measurements are performed on a single ball v-groove combination. It turns out that this set-up is subject to an angular error due to the rotation of the base. The angular error causes the observed stick distance to be longer than the actual stick displacement. The observed stick displacement is 0.6 μm. In a Silicon Carbide chuck, a groove displacement of 0.6 μm is achieved when the temperature of the chuck changes with 2.3K. Since the actual stick displacement is smaller, slip is expected to occur within this 2.3K temperature difference.
A second experiment has been performed in which a wafer table is mounted onto a kinematic mount. The temperature of the wafer table is increased in order to change the relative distance of the balls and grooves by expansion of the wafer table. The measurements show some abrupt displacements in the order of 100nm. These seem to be jumps caused by stick slip. However, the temperature increase causes undesired expansion of the reference flags used by the capacitive sensors. The undesired expansion spoils the measurements and therefore no final conclusions on stick slip can be made based on this experiment.
A third experiment is proposed. This experiment combines the advantages of the two performed experiments in order to measure the stick slip effect precisely. Thermal variations could be controlled in this set-up. Furthermore, the measurements are performed on a real -3 ball/groove- kinematic mount. This will exclude error effects caused by low stiffness of the set-up.

Recommendation

The work in this thesis still contains some open ends. Next to the open ends, some new insights have been gained that can be beneficial for Mapper Lithography.

An insight that has been gained in the performed work is the low natural frequency of the complete short stroke module. The weak link turns out to be the flexures that couples the chuck to the short stroke actuator. The natural frequency will never be higher than 340Hz due to these flexures. In order to get a higher natural frequency, the connection of the chuck with the short stroke actuator should therefore be redesigned.

Whether or not stick slip will be present in a SiC chuck under the present thermal conditions of the machine still has to be determined. This can be done by using the proposed experimental set-up of chapter 5. A control program should be written in order to control the motion of the grooves precisely. The programmed motion should simulate the expansion of a SiC chuck. The result of the measurements should give answer to if stick slip can be seen on the wafer table or not. And if so, what will be the temperature difference that will cause stick slip. With this knowledge, the question could be answered if a stick slip canceling mechanism should be integrated. Appendix C shows a rough approach to a conceptual framework for such a stick slip canceling mechanism.

The design project that has been performed shows that a SiC chuck would be a feasible solution within the requirements that have been set. If a SiC chuck will really meet these requirements, a prototype should be made. The procedure in chapter 6 should be used to measure the performance of the prototype chuck. Building a prototype would also gain insight in the costs and difficulties in the manufacturing of SiC components. With this knowledge a decision could be made if the SiC chuck is a real improvement of the present situation.

A

Measurements

A.1. Measurements of stick slip due to actuation of a ball on a v-groove

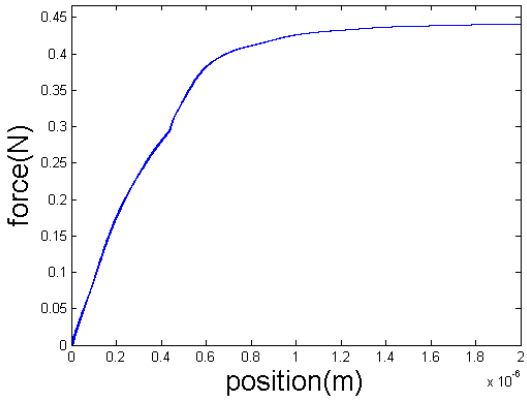

Figure A.1: Positive direction measurement

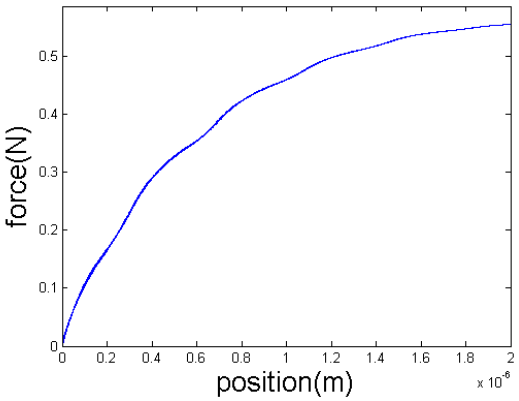

Figure A.2: Positive direction measurement

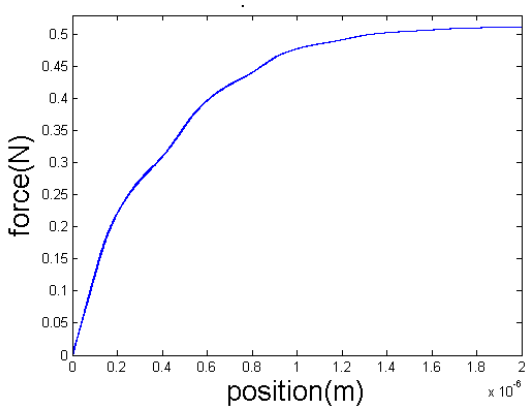

Figure A.3: Positive direction measurement

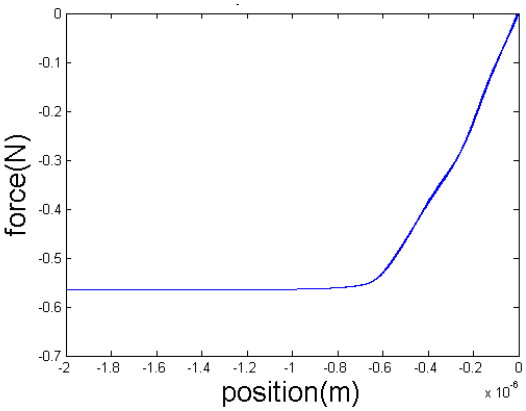

Figure A.4: Negative direction measurement

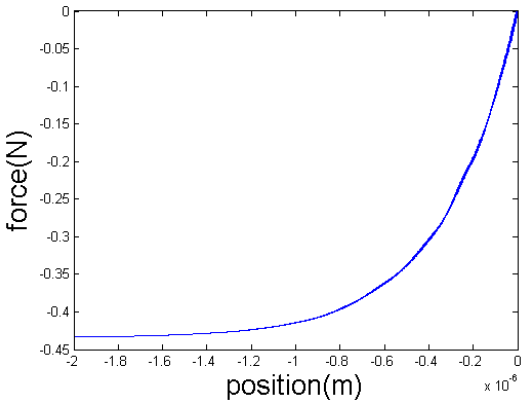

Figure A.5: Negative direction measurement

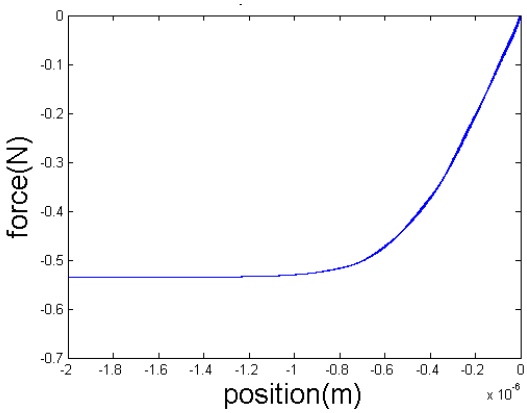

Figure A.6: Negative direction measurement

A.2. Measurements of stick slip due to heating of a wafer table

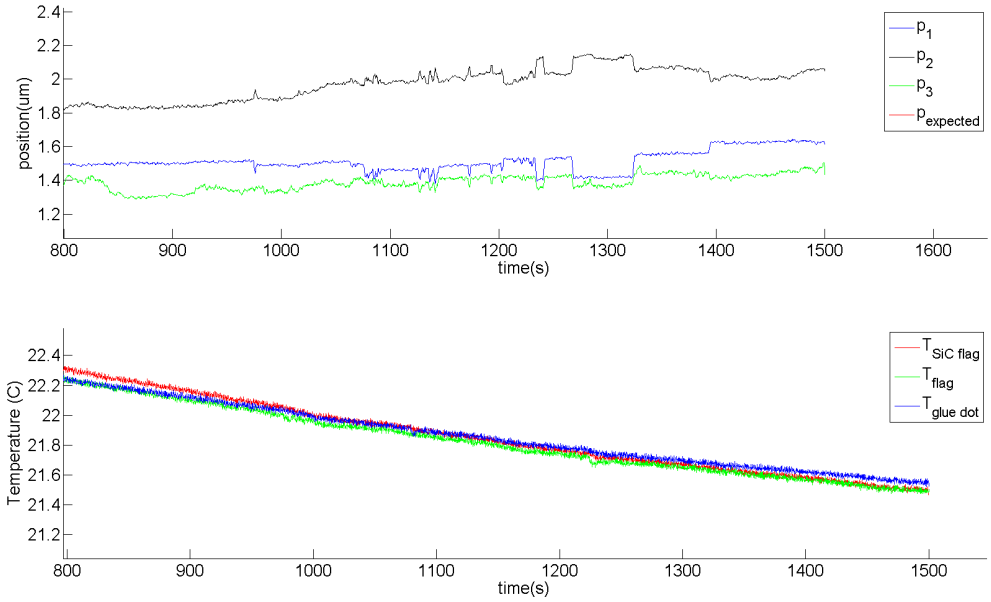

Figure A.7: Jumps occurring synchronously with the same (counter) movements.

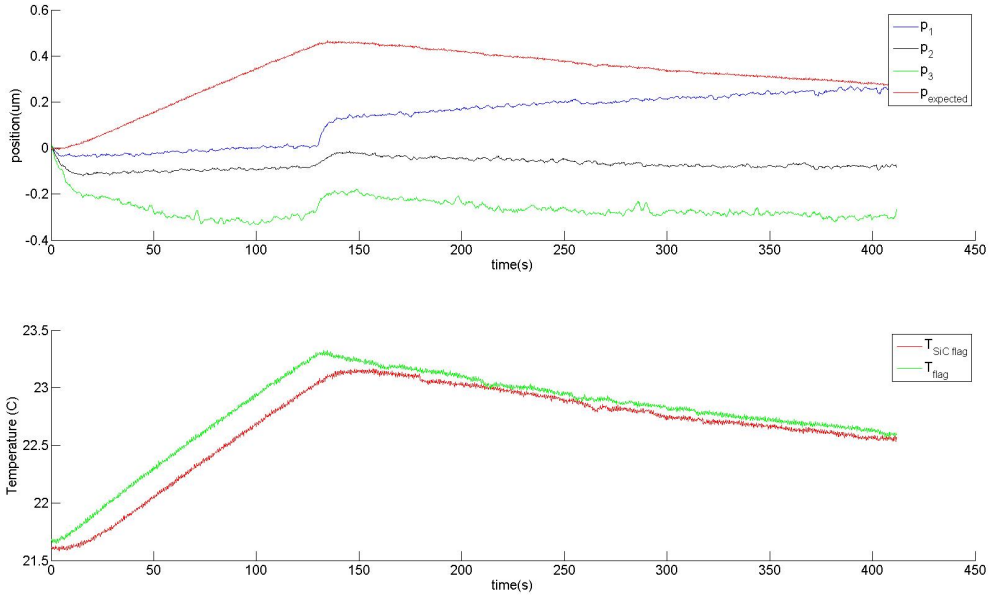

Figure A.8: Asynchronous movements p1,p2 and p3

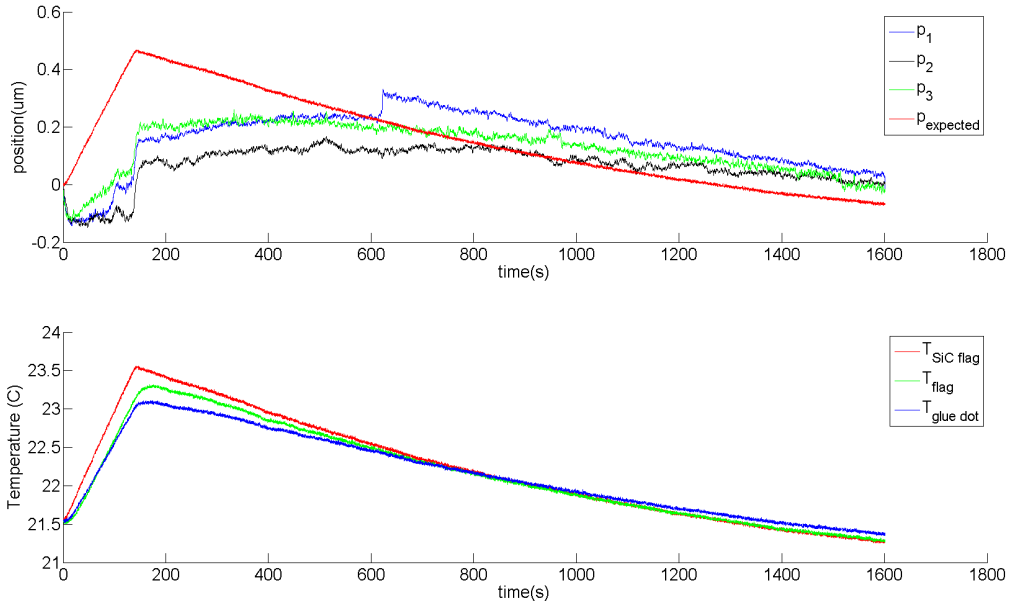

Figure A.9: Jump of p1

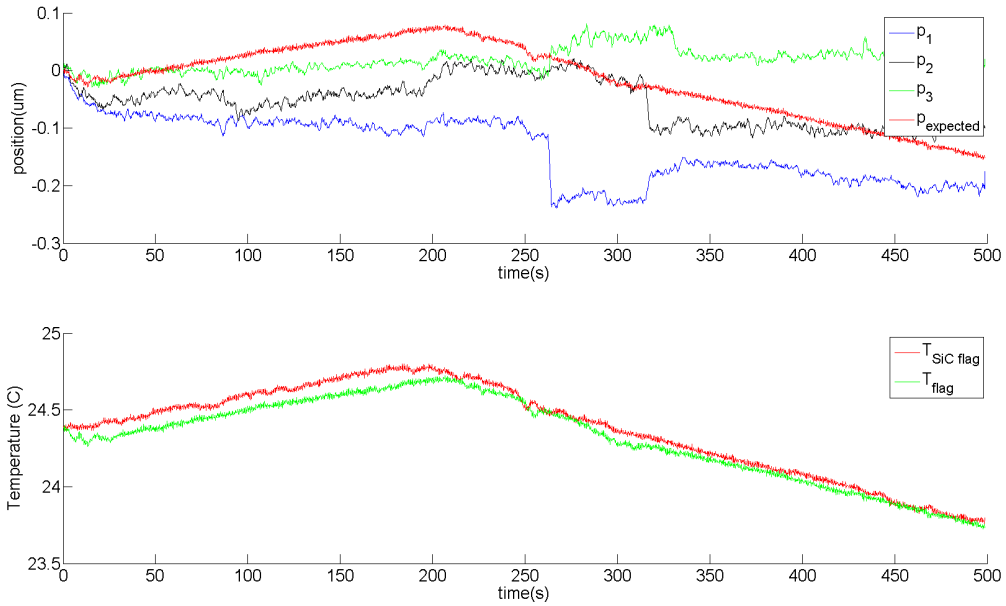

Figure A.10: Multiple jumps of each position, occurring at the same instance with non equal movements.

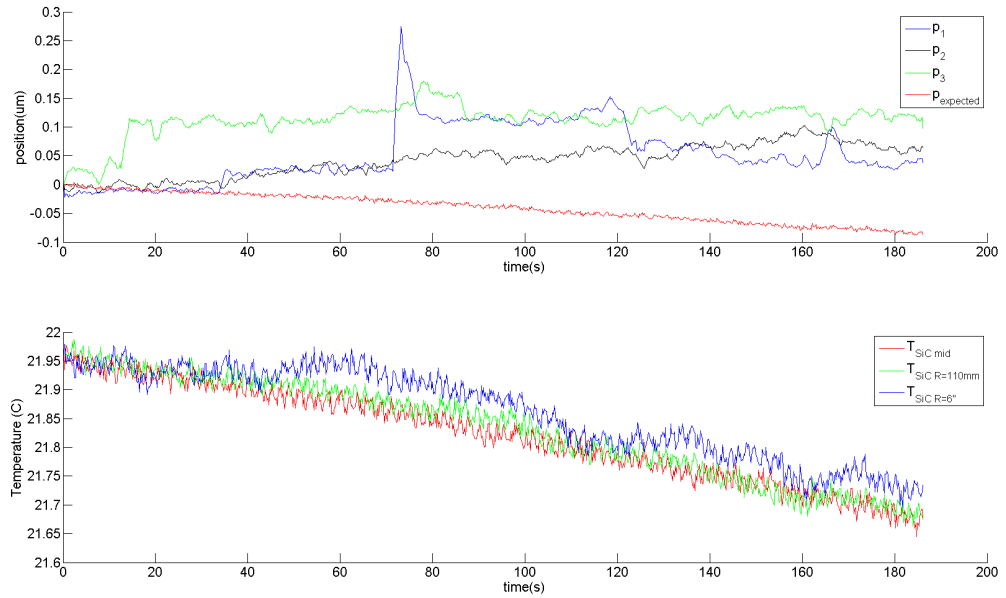

Figure A.11: Multiple jumps of each position, occurring at the same instance with non equal movements.

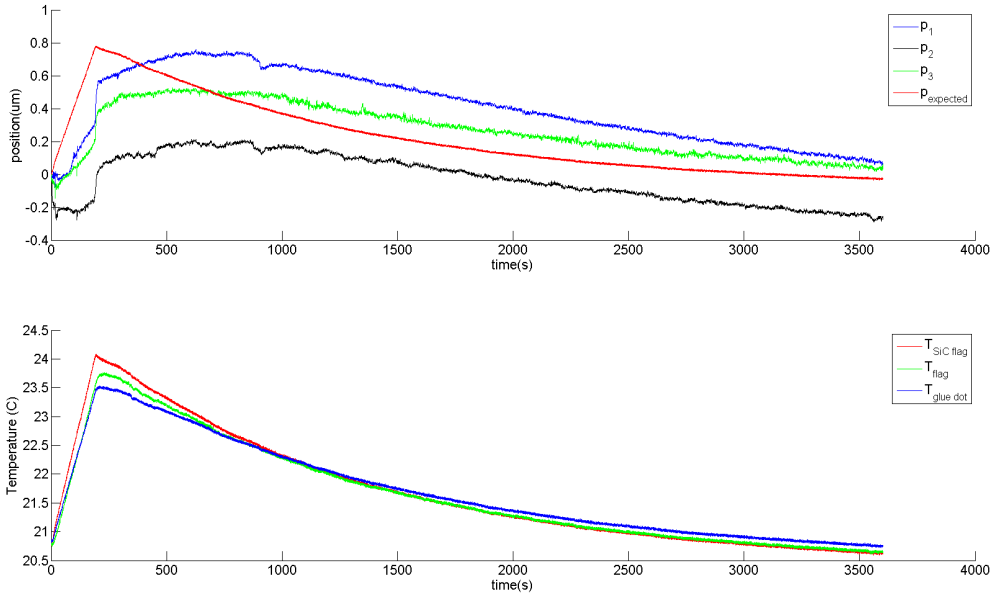

Figure A.12: Single jump occurring together and positions that do not return to the initial position after cooling down.

A.3. Logbook

Meas.	Date	Δt(s)	ΔT(K)	IF release	Comment
t1	30 Sep.	80;170	+5;-1		Cap sensors not fixed in mount
t2	30 Sep.	0;30	0;-0.1		
t3	30 Sep.	100;200	+4;-1		
t4	30 Sep.	400;0	+10;0		
t5	30 Sep.	0;300	0;-1.5		
t6	30 Sep.	200;0	+3;0		
t7	30 Sep.	0;25	0;-0.1		
t8	30 Sep.	450;0	+2+2+2;0		
t12	30 Sep.	70;400	+2;-1		
t13	30 Sep.	0;180	0;-0.3		
1	3 oct.	120;240			Mounted screw and temperature sensor on cap. clamp.
2	3 oct.	120;240			
3	3 oct.	120;240			
4	3 oct.	120;240			
5	4 oct.	120;240			
1	4 oct.	25;250	+0.3;-0.2		T1 on WT at R=110mm
2	4 oct.	200;900	+2;-1		
3	4 oct.	70;130	+1;-0.1	Yes	T1 on WT at R= Rflag
4	4 oct.	80;120	+1;-0.1	Yes	
5	4 oct.	200;100	+3;-0.1	Yes	distance lamp-WT of 10cm
6	4 oct.	200;100	+2;-0.3	No	
8	4 oct.	120;250	+2;-0.5	Yes	All therm. couples at radius of
9	4 oct.	60;120	+1;-0.3		flag T1 on SiC, T2 on flag, T3 on glue dot
1	5 oct.	180 ; 1300	3 ; -2	Yes	distance lamp-WT of 2cm, surrounding vibrations at 980s,1066s ,1088s,1127s, 1215s
2	5 oct.	500 ; 500	0.8 ; -0.4	No	distance lamp-WT of 60cm
3	5 oct.	600 ; 900	0.9 ; -0.6	Yes	distance lamp-WT of 60cm, al. block added.
4	5 oct.				
5	5 oct.		5		
6	5 oct.			Yes	distance lamp-WT is 10cm
7	5 oct.			No	
8	5 oct.			No	at 125s lamp position moved between 2cm and 50 cm several times
9	5 oct.			Yes	Removed the lamp from the setup.
10	5 oct.			No	lamp-WT 30 cm, at 205s lab light off.
1	7 oct.			Yes	T3 is off, each flag grounded
2	7 oct.			Yes	Lamp-WT 10cm
3	7 oct.			Yes	Lamp-WT 2cm
4	7 oct.			No	Lamp-WT 30cm

Table A.1: Logbook of experiment 2

B

Stick slip cancelling mechanism

B.1. Concept development for an anti stick kinematic mount

This section provides a direction in which a solution can be sought for to exclude stick slip. The aim of this section is not to come to a final concept but to provide Mapper with a conceptual framework on stick slip cancelling mechanisms. An anti stick slip kinematic mount should perform two functions:

1. Mount the wafer table with a highly repeatable precision.
2. Exclude stick slip.

Although multiple variations exist, basically two solutions of kinematic mounts exist that could be used to mount the wafer table with a high repeatability: the Maxwell clamp and the Kelvin clamp according to [21]. The Maxwell clamp is used in the present chuck. Many solutions could be thought of to exclude stick slip. For each functionality, different strategies have been designated. The strategies lead to a set of solutions. The section ends with some concepts that have been found.

B.1.1. Mount the wafer table with a highly repeatable precision

A choice can be made out of two solutions, the Kelvin clamp and the Maxwell clamp. The difference in both solutions is that each ball in the Maxwell clamp is constrained in two directions. The balls in a Kelvin clamp are constrained by a 3-2-1 combination by a flat a cone and a groove. Clarifying figures can be found in figure C.1 and C.2.

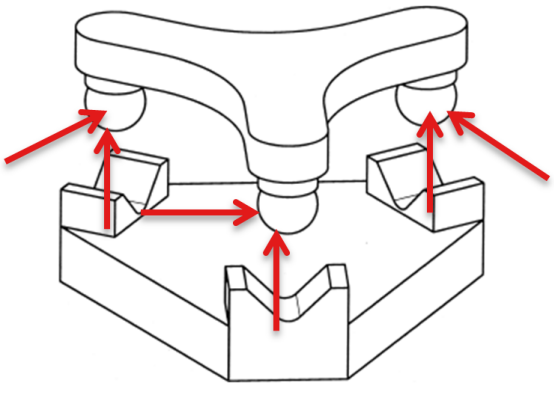

Figure B.1: The Maxwell clamp

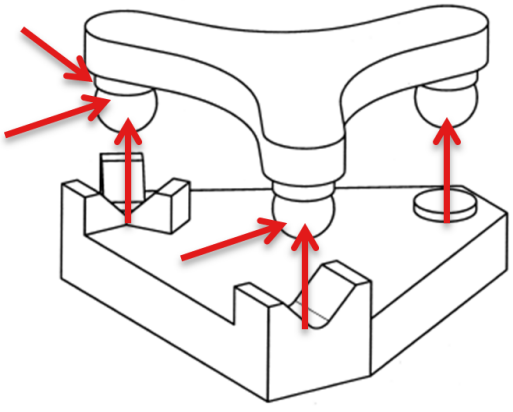

Figure B.2: The Kelvin clamp

B.1.2. Exclude stick slip

6 strategies have been found for the solutions:

1. Exact or over constraint. Note that with this strategy the (non)compliant mechanism is meant. The kinematic mount should always be an exact constraint configuration
2. Monolithic or separate part
3. Compliant non compliant

As in the concept design of the mounting of the mirrors, the strategies are independent and can be put in a 3D space. To visualize solutions, two tables have been made.

Over constraint	Compliant	Non compliant
Monolithic	2,5	
Separate part		4

Exact constraint	Compliant	Non compliant
Monolithic	1,3,6,7	
Separate part		

Table B.1: Solutions located in the strategy space

The solutions that have been found are evaluated in table C.2. The working principle of each solution:

1. A 1 dof stage that makes use of two double flexure mechanisms and 2 intermediate stages. More on this design can be found in [3]
2. A 1 dof over constrained stage by using two leaf springs.
3. A Zerodur platform that which is not prone to expansion so stick slip is not present at all.
4. A 1 dof stage by using double leaf springs. Although over constraint it might work for small movements (see [13]).
5. A 1 dof exact constrained stage by using two leaf springs.
6. A 2 dof exact constrained stage using four double leaf springs mechanisms with 5 intermediate stages (see [3]).

B.2. Minimum compliance

Compliant anti stick slip concepts use the fact that when a spring is connected in series with another spring, the total displacement is larger than the elongation of each separate spring. The stress in each spring becomes lower than when only one spring has been used to get the same total displacement. In an anti stick slip mechanism this can be used as a benefit. When the groove is mounted compliant on for instance a 1dof stage, the total stiffness consists of the contact stiffness and the stiffness of the compliant stage (see figure C.3). This results in a combined stiffness that is lower than the contact stiffness on it's own. The displacement of the ball is now partially covered by a displacement of the compliant stage and partially by the elastic deformation of the contact. The lower the stiffness of the compliant stage becomes, the lower the relative displacement between ball and groove. This means a lower contact stress for the same displacement of the ball. The stiffness of the compliant stage could be tuned in order to keep the contact stress below the static friction level. If this is accomplished, stick slip will not be present at all.
The analytic model that has been derived in chapter 5, resulted in a calculated ball-groove contact stiffness of $0.909 \cdot 10^7$. The related stick displacement is $6.226 \cdot 10^{-8} m$. The displacement of the groove position due to expansion that the contact should "handle" is $\delta = \Delta T L_0 \alpha = 1 \cdot 0.11 \cdot 2 \cdot 10^{-6} = 2.2 \cdot 10^{-7}$. With these results, a minimum compliance or equivalent, a maximum stiffness for the compliant stage can be calculated. This is done as follows:

$$\delta_{\max} = x_2 + x_1 \tag{B.1}$$

$$F_{x_2} = F_{x_1} = F_{\text{static}} \tag{B.2}$$

$$k_{\text{compliant}} x_1 = k_{\text{contact}} \delta_{\max} \tag{B.3}$$

$$k_{\text{compliant}} = \frac{k_{\text{contact}} \delta_{\max}}{x_2 - \delta_{\max}} \tag{B.4}$$

$$k_{\text{compliant}} = \frac{0.909 \cdot 10^7 \cdot 6.226 \cdot 10^{-8}}{(2.2 - 0.6) \cdot 10^{-7}} = 3.54 \cdot 10^6 \text{N/m} \tag{B.5}$$

The calculated maximum stiffness of the compliant stage is $3.54 \cdot 10^6$N/m C.5. When a groove is mounted on a compliant mechanism with this stiffness, the ball will be at the position were it starts to slip. A safety margin needs to be applied because of two reasons (1) The friction force is not constant and (2) The stiffness of the contact might differ from the calculated stiffness. Since the expectation is that the friction force varies by 10 percent and the contact stiffness is lower than calculated, a safety margin of 25 percent will be sufficient not to cause stick slip. Therefore, the compliant stage should have a maximum stiffness of $0.75 \cdot 3.54 \cdot 10^6 = 2.66 \cdot 10^6 N/m$.

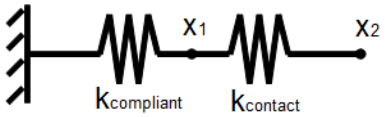

Figure B.3: Equivalent spring model for a compliant groove interface.

B.3. Anti stick slip mechanism concepts

The developed concepts and their evaluation can be found in figure C.3. The first three concepts that have been found make use of grooves that are mounted compliant. The compliant behaviour of the kinematic mount will cause the position of the wafer table to be deterministic. The last concept is a non compliant one.

1. This concept makes use of the Kelvin clamp mount. The 3-2-1 constraints of the clamp have been translated to a fixed cone, a one dof stage and a two dof stage. The stages are made using the over constrained solution 4. The grooves are mounted on top of the stages.

2. This concept uses the same principle as in concept 1 but this time it uses exact constraint stages underneath the grooves.

3. The maxwell clamp configuration is used, under each v-groove a compliant one dof stage is integrated in the SiC chuck which makes it monolithic.

4. A Zerodur platform is mounted to the chuck with rods constraining it in all 6 dof. The thermal stability of Zerodur keeps the grooves at a constant positions relative to each other.

	Solution	Desired (non)compliance	Stiffness in z direction	Simplicity	Dynamic sensitivity	Thermal sensitivity	cost	Overall score
1.	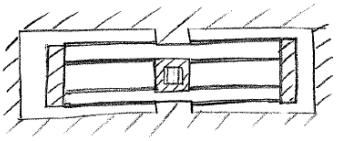	2	1	0	0	1	1	5
2.	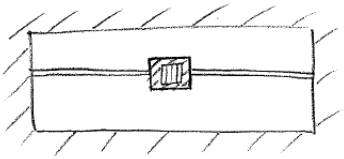	0	0	2	-1	-1	1	1
3.	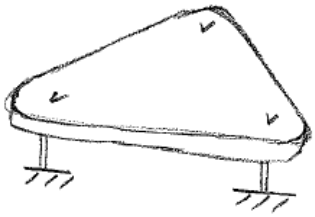	2	2	1	1	2	-2	6
4.	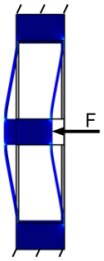	-1	2	2	1	-1	2	5
5.	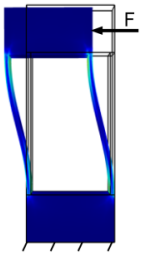	1	2	1	0	1	1	6
6.	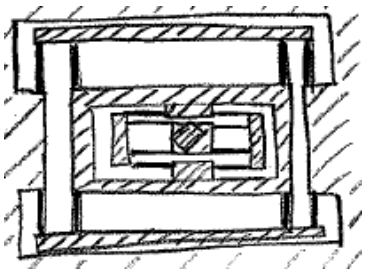	2	1	0	0	1	1	5

Table B.2: Evaluation stick slip excluding solutions

	Solution	Position stab.	Orientation stab.	Dynamic behavior	Stick slip	Simplicity	Overall score
1.	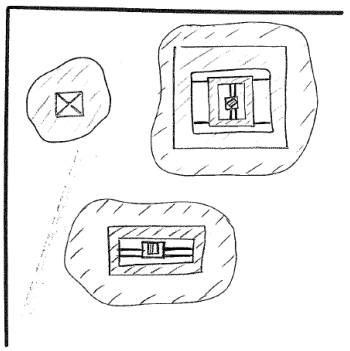	0	0	1	1	-1	1
2.	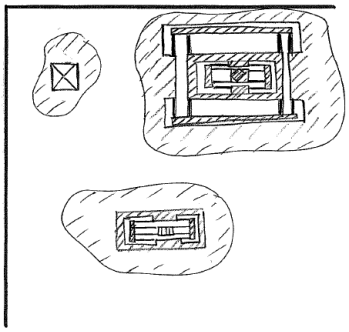	1	1	1	1	-1	3
3.	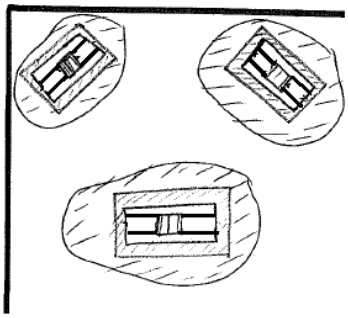	1	1	1	1	1	5
4.	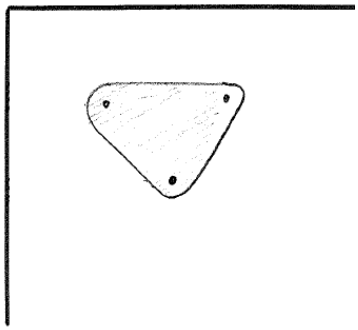	1	1	0	2	-1	3

Table B.3: Evaluation of anti stick slip mechanism concepts

C

Concept trade off

The choice of the most promising concept has been done on an estimated performance evaluation. It is always good to have a second opinion on your work, thoughts about the concepts may come up that might not have taken into account. Therefore all of the developed concepts have been ranked by a team of experts in the field of mechanics and optics. this ranking can be found in figure D.1. The performance evaluation has been done by simple back on the envelope calculations and field experience. The grades that could be given to a concept ranged from 0 to 100. In steps of 0, 0.5, 1, 2, 3, 5, 7, 13, 20, 40, 60, 100. This strange looking set of numbers are close to the set of numbers in the fibonacci sequence. The ranking has been done on feeling, no reference has been used here. Therefore the trade off might not be as representative as the performance evaluations with reference used throughout this thesis. Nevertheless it represents a feeling about which concept will work and which one won't. As it turned out, 2 concepts seem to be promising. The SiC chuck which is also concept of this thesis and coating and polishing the present chuck with a nickel phosphorous layer. Mirrors made in this way seem to have a very low roughness (see [29]. Mapper is currently working on such a solution because it could be implemented on a very short term without many adaptations of the present design. The drawback here is that with this concept, only the optical quality will be improved. No improvements are applied to the rest of the bottlenecks.

Figure C.1: Concept trade off as performed at Mapper lithography.

Bibliography

[1] Print through effect in polishing mirrors. URL `http://www.dreamcellularllc.com/printthrough.htm`.

[2] Michael F Ashby. *Materials Selection in Mechanical Design*. 2004.

[3] Shorya Awtar. *Synthesis and analysis of parallel kinematic XY flexure mechanisms*. PhD thesis, 2003.

[4] Michel Bougoin. Cte homogeneity, isotropy and reproducibility in large parts made of sintered sic. 2012.

[5] Sjef Box. Ontwerp en temperatuurregeling voor nanometerprecisie. 2006.

[6] T.W. Clyne and S.C Gill. Residual stresses in thermal spray coatings and their effect on interfacial adhesion: A review of recent work. 1996.

[7] R. Delfos. Lecture slides on fluid mechanics. 2013.

[8] D.M. Brouwer et al. Freedom and constraint analysis and optimization.

[9] F. Bornebroek et al. Overlay performance in advanced processes. 2000.

[10] Frank M. Anthony et. al. Cryostable lightweight frit bonded silicon mirror. 2002.

[11] H. Kunzmann et al. Scales vs laser iinterferometer performance and comparison of two measuring systems. 1993.

[12] Hagyong Kihm et al. Adjustable bipod fflexure for mounting mirrors in a space telescope. 2012.

[13] Haiyang Li et al. Position-space-based compliant mechanism reconfiguration approach and its application in the reduction of parasitic motion. 2016.

[14] Masao Konaka et al. Ultraprecision polishing of cvd-sic mirrors.

[15] Sanghyuk Kim et al. Fabrication of electroless nickel plated aluminum freeform mirror for an infrared off-axis telescope. *Applied optics*, 2015.

[16] Wen Hwa Chut et al. Analysis of tip deflection and force of a bimetallic cantilever microactuator. 1993.

[17] Yong Shu et al. The ultra precision polishing of large aperture reaction bonded silicon carbide mirror. 2010.

[18] POCO graphite. Properties and characteristics of sic.

[19] E.H. Smith I. Sherrington. Design and performance of a kelvin clamp for use in relocation analysis of surface topography. 1993.

[20] K.L. Johnson. *Contact mechanics*. 1985.

[21] Alexander H. Slocum Layton C. Hale. Optimal design techniques for kinematic couplings. 2000.

[22] A. F. Mills. *Basic Heat & Mass Transfer*. Pearson Education Limited, 3rd edition, 2013.

[23] Donald H. Buckley (NASA). Friction, wear and lubrication in vacuum. 1971.

[24] M. Salmeron R.W. Carpick, D.F. Ogletree. Lateral stiffness: a new nanomechanical measurement for the determination of shear strengths with friction force microscopy. 1997.

[25] M. Spengen. Lecture slides on surface roughness. 2014.

[26] R. Munnig Schmidt; G. Schitter; A. Rankers; J van Eijk. *The design of high performance mechatronics.* IOS Press, 2nd edition, 2014.

[27] Hugo S. Vargas. Sic design guide: Manufacture of silicon carbide products. 2010.

[28] P. R. Y. D. Vukobratovich. *Opto-mechanical system design volume 2.* 2015.

[29] Paul R. Yoder; Daniel Vukobratovich. *Opto-mechanical system design volume 1.* 2015.

[30] Aerotech Inc. William Land. Laser interferometer feedback machine positioning uncertainty. .

[31] Aerotech Inc. William Land. Laser interferometry implementation. .